



UNICAMP

UNIVERSIDADE ESTADUAL DE CAMPINAS

FACULDADE DE ENGENHARIA QUÍMICA

ÁREA DE CONCENTRAÇÃO

DESENVOLVIMENTO DE PROCESSOS QUÍMICOS

**PROCESSO INTENSIFICADO DE HIDRÓLISE ENZIMÁTICA DE
PENICILINA G E PURIFICAÇÃO DOS PRODUTOS EM REATOR
MULTI-ESTÁGIO E CONTRA-CORRENTE**

Doutoranda: Juliana de Souza Ferreira

Orientadora: Telma Teixeira Franco

Co-orientadores: Adrianus Johannes Jozef Straanhof*

Lucas Antonius Maria van der Wielen*

Julho/2004

Campinas – SP

* Department of Biotechnology - Delft University of Technology

**BIBLIOTECA CENTRAL
DESENVOLVIMENTO
COLEÇÃO
UNICAMP**

UNIDADE BC
Nº CHAMADA UNICAMP
F413p
V _____ EX _____
TOMBO BC/ 53734
PROC 06 P.00 123.06
C _____ B _____
PREÇO 11,00
DATA 04/10/06
Nº CPD _____

Bib id 374335

FICHA CATALOGRÁFICA ELABORADA PELA
BIBLIOTECA DA ÁREA DE ENGENHARIA - BAE - UNICAMP

F413p Ferreira, Juliana de Souza
 Processo intensificado de hidrólise enzimática de
 penicilina G e purificação dos produtos em reator multi-
 estágio e contra-corrente / Juliana de Souza Ferreira.--
 Campinas, SP: [s.n.], 2004.

 Orientadores: Telma Teixeira Franco, Lucas Antonius
 Maria van der Wielen e Adrianus Johannes Jozef
 Straanhof.

 Tese (Doutorado) - Universidade Estadual de
 Campinas, Faculdade de Engenharia Química.

 1. Penicilina. 2. Antibióticos beta-lactâmicos. 3.
 Cristalização. 4. Enzimas imobilizadas. I.Franco, Telma
 Teixeira. II. Van der Wielen, Lucas Antonius Maria. III.
 Straanhof, Adrianus Johannes Jozef. IV. Universidade
 Estadual de Campinas. Faculdade de Engenharia
 Química. V. Título.

Título em Inglês: Intensificated process of hydrolysis of penicillin G and purification of the products in a multi-stage counter-current reactor.

Palavras-chave em Inglês: Penicillin, Beta-lactam antibiotics, Immobilized Enzymes e Crystallization.

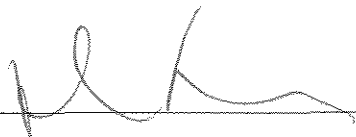
Área de concentração: Desenvolvimento de processos químicos

Titulação: Doutor em Engenharia Química

Banca examinadora: Telma Teixeira Franco, Marco Giulietti, Gustavo Paim Valença, Maria Regina Wolf Maciel, Eliana Kamimura, Heizir Ferreira de Castro

Data da defesa: 16/07/2004

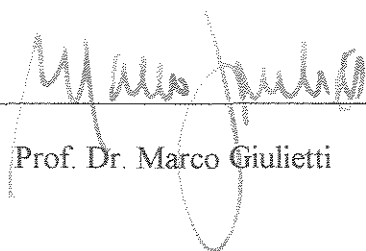
Tese de Doutorado defendida por Juliana de Souza Ferreira e aprovada em 16 de julho de 2004 pela banca examinadora constituída pelos doutores:



Prof.ª. Dr.ª. Telma Teixeira Franco – Orientadora



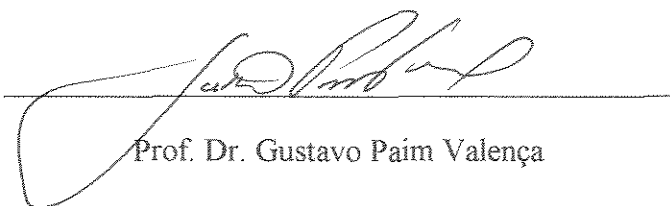
Prof.ª. Dr.ª. Maria Regina Wolf Maciel



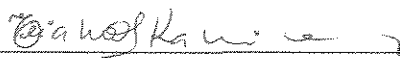
Prof. Dr. Marco Giuliatti



Prof.ª. Dr.ª. Heizer Ferreira de Castro

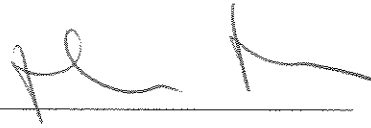


Prof. Dr. Gustavo Paim Valença



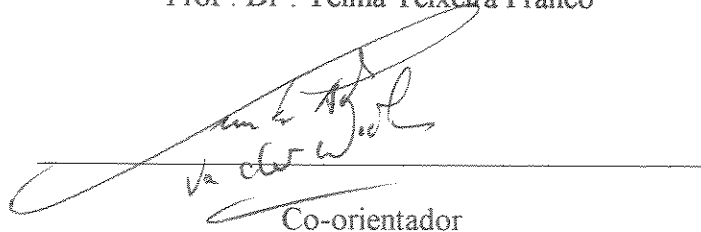
Prof.ª. Dr.ª. Eliana Kamimura

Este exemplar corresponde à versão final da Tese de Doutorado em Engenharia Química



Orientador

Prof.ª Dr.ª Telma Teixeira Franco



Co-orientador

Prof. Dr. Lucas Antonius Maria van der Wielen

Dedico este trabalho às pessoas mais importantes da minha vida: minha família, minha madrinha e meus amigos. Sem o apoio e as palavras de conforto, eu não teria a perseverança em buscar meus objetivos e superar as saudades de vocês.

AGRADECIMENTOS

A Deus pelas oportunidades profissionais, pelas pessoas que me cercam e por ter sempre iluminado meu caminho.

Aos meus pais por terem se esforçado para me proporcionar chances de sempre buscar novas conquistas. Sua dedicação foi e sempre será um grande exemplo para mim. Em especial a minha mãe, pois sei o quanto foi difícil todas as vezes que tivemos que nos despedir e nos manter distantes. Foi sempre compreensiva e suas palavras de apoio e carinho me fortaleceram nos momentos de fraqueza e saudades.

Aos meus irmãos, Regina e Luciano, a minha querida afilhada Bruninha, ao meu cunhado Paulo, e aos meus tios pelo afeto e incentivo ao meu trabalho.

A minha querida madrinha e super amiga, Liliane. Sempre presente em todos os momentos, não bastaram suas palavras de incentivo, me honrou com uma visita em Delft.

À minha orientadora, Telma Teixeira Franco, pela orientação e por ter viabilizado a oportunidade do Doutorado Sanduíche na Holanda na Universidade de Tecnologia de Delft (TUDelft)

Aos meus orientadores, Luuk van der Wielen e Adrie Straathof, do Grupo de Tecnologia de Bioseparação (BST) do Departamento de Biotecnologia da TUDelft. Suas sugestões foram fundamentais para o desenvolvimento deste trabalho. Aliás, ao chegar em Delft na primeira etapa do Doutorado Sanduíche, ainda tinha muitas dificuldades com o idioma. Muito obrigada pela paciência e compreensão durante as reuniões. Foi um prazer trabalhar com vocês. Tenho muita admiração pela organização e disciplina do grupo BST no planejamento de seus projetos. Com certeza, isso contribuirá muito para meu desenvolvimento profissional.

Aos órgãos de fomento, CNPq pela concessão da Bolsa de Doutorado no período em que o trabalho foi desenvolvido na UNICAMP e CAPES pela concessão da Bolsa de Doutorado Sanduíche na TUDelft.

A Marcel Ottens por suas sugestões no trabalho envolvendo cristalização.

Aos técnicos, Lúcio Melo (UNICAMP), Cor Ras, Max Zomerdijk, Stef van Hateren e Angela Proll (TUDelft).

A Jeoren den Hollander (TUDelft) por ter repassado todas as informações necessárias para dar continuidade ao seu trabalho de doutorado, além de ter sido um ótimo colega de sala.

A Xiaonan Li e Minna Vuolanto, pela realização de parte dos experimentos de cristalização, e a Brenda Westerink pela sua contribuição no desenvolvimento da modelagem.

A todos os colegas de trabalho do Laboratório de Engenharia Bioquímica (UNICAMP) e do Grupo de Tecnologia de Bioseparação (TUDelft).

Aos funcionários da AGIF - Instituto UNIEMP e, em especial, ao Prof. Dr. Saul d'Ávila, por permitir que eu trabalhasse período parcial na AGIF, possibilitando à finalização da tese de doutorado.

Aos meus grandes amigos do Brasil e àqueles que conheci durante o Doutorado Sanduíche em Delft (Holanda) por compartilharem tantos momentos inesquecíveis e me confortarem, em especial, nos difíceis momentos de adaptação em um outro país, pela paciência quando tive problemas com o idioma e nos momentos em que a saudade parecia sufocar: Virgínia, Fernanda, Érica (Zac), Lecsi, Wanda, Sérgio, Luciana, Ana Paula, Giselle, Marcos (Kan), Vinícius, Rogério (Baby), Eliana (Lica), Fabiane, Martijn, Zeynep, Aleksandar, Minna, Maria de los Angeles, Maria Claudia, Branko, Edwin, Susana, Beatrix, Patrícia, Xiaonan, Esteban, Desiree, Silvia, Edou, Guo, Marina, Leonardo, Carlota, Beatriz, Fabiana, Oscar, Márcia e Marcos.

Falando em saudades, meus amigos, é impossível deixar esta palavra de lado tendo a experiência de viver em um outro país. Mas isto é sinal de momentos de convivência muito felizes. Faço uso das palavras do compositor Milton Nascimento, “(*...*) *Amigo é coisa pra se guardar no lado esquerdo do peito, mesmo que o tempo e a distância digam não (...)*”.

Enfim, num trabalho de quatro anos, foram tantas as pessoas que conheci e me ajudaram, que é impossível citar todas. Por isso, a todos que contribuíram, direta ou

indiretamente, para este trabalho e para meu aprendizado profissional e pessoal, minhas palavras de agradecimento são eternas.

ACKNOWLEDGEMENTS

The God for the professional chances, for the people who surround me and having always illuminated my way.

To my parents for having worked hard to provide me possibilities to search my conquest. Their devotion was and it will always be a great example for me. In special my mother, because I know how difficult it was all the times that we had to bid farewell and to and keep us apart. She was always comprehensive and her words of support and affection had fortified me at the moments of weakness and homesickness.

To my sister Regina, my brother Luciano, my dear goddaughter Bruninha, to my brother-in-law Paulo, to my uncles and to my aunts for the affection and incentive to my work.

My dear godmother and friend, Liliane. She was always present when I needed. Besides, she honored me with a visit in Delft.

To my supervisor, Telma Teixeira Franco, for the supervision and having made it possible the chance of my “Doctorate Sandwich” in Holland at Delft University of Technology (TUDelft).

To my supervisors, Luuk van der Wielen and Adrie Straathof, of the Group of Bioseparation Technology of the Department of Biotechnology of TUDelft. Their suggestions had been fundamental for the development of this thesis. By the way, when arriving in Delft, at the first stage of my “Doctorate Sandwich”, I still had many difficulties with language (English idiom). I thank you very much for the patience and understanding during the meetings. It was a pleasure to work with you. I have a much admiration for the organization and discipline of the BST group in the planning of its projects. Surely, this will contribute very much for my professional development.

To the financial agencies CNPq for the concession of the scholarship of the doctorate when the work was developed at UNICAMP and CAPES for the concession of the “Doctorate Sandwich” scholarship at TUDelft.

To Marcel Ottens for his suggestions in the work involving crystallization.

To the technicians: Lúcio Melo (UNICAMP), Cor Ras, Max Zomerdijk, Stef van Hateren and Angela Proll (TUDelft).

To Jeoren den Hollander (TUDelft) for having repassed all the information necessary to give continuity to his doctorate work. Besides he was an excellent colleague of room.

To Xiaonan Li and Minna Vuolanto, for the accomplishment of part of the crystallization experiments and to Brenda Westerink for her contribution in the development of the modeling.

To all the colleagues of the Laboratory of Biochemical Engineering at UNICAMP and of the Group of Bioseparation Technology at TUDelft.

To the colleagues of AGIF – UNIEMP Institute, and in special to Prof. Saul d'Ávila for allowing that I worked partial time in AGIF, making it possible the completion of this thesis.

To my great friends of Brazil and to those who I knew during my Doctorate Sandwich in Holland for sharing unforgettable moments and cheering me up, especially at the difficult moments of adaptation in a different country, for the patience when I had problems with the English language and at the moments when the homesickness seemed to suffocate: Virgínia, Fernanda, Érica (Zac), Lecsi, Wanda, Sérgio, Luciana, Ana Paula, Giselle, Marcos (Kan), Vinícius, Rogério (Baby), Eliana (Lica), Fabiane, Martijn, Zeynep, Aleksandar, Minna, Maria de los Angeles, Maria Claudia, Branko, Edwin, Susana, Beatrix, Patrícia, Xiaonan, Esteban, Desiree, Silvia, Edou, Guo, Marina, Leonardo, Carlota, Beatriz, Fabiana, Oscar, Márcia and Marcos.

Speaking about homesickness, my friends, it's impossible to leave this word out having the experience of living in another country. But that is signal of very happy moments of acquaintanceship. I make use of the words of composer Milton Nascimento, “(...) *Friend is a person to keep in one's heart, even if distance or time keeps them apart (...)*”.

At last, in a work of four years, there were so many people who I knew and helped me that it's impossible to mention all of their names. Therefore, for all those who had contributed, directly or indirectly, for this work and for my professional and personal learning, my words of gratefulness are eternal.

*“Só quem toma um sonho como sua forma de viver pode
desvendar o segredo de ser feliz”.*

(Feghali-Nando)

RESUMO

Este trabalho estuda a hidrólise enzimática da penicilina G (PenG) em ácido 6-aminopenicilânico (6-APA) e ácido fenil acético (PAA). Em um reator contra-corrente multi-estágio e em baixos valores de pH, a reação enzimática ocorre na fase aquosa e os produtos são separados entre a fase aquosa e a fase orgânica (acetato de butila). Além disso, em pH baixo, a cristalização do 6-APA ocorre quando concentrações de PenG são altas. Ambos fenômenos deslocam o equilíbrio no sentido de conversão do substrato, promovendo alta produtividade. A primeira etapa deste trabalho refere-se à avaliação da atividade e estabilidade da penicilina amidase a baixo pH e na presença de acetato de butila (BuAc). A enzima apresentou máxima atividade na faixa de pH 8,0 – 9,0 e permaneceu estável mesmo em pHs baixos (3,0 – 6,0) num período de incubação de até 32 dias. Embora a atividade enzimática sofra um decréscimo de aproximadamente 80%, isto não representa empecilho para sua utilização no emprego da hidrólise de PenG em processo contínuo e bifásico (água e BuAc) em pH baixo. O efeito de PenG, PAA e BuAc na cristalização do 6-APA e os parâmetros cinéticos de cristalização também foram avaliados. Os resultados mostraram que as impurezas não exerceram efeito sobre a cristalização de 6-APA, na faixa de pH entre 4 e 5 e nas concentrações de impurezas de 0,55 mM – 3,0 mM. A avaliação da cinética de cristalização possibilitou o uso de um modelo que pode prever as taxas de cristalização de 6-APA. Um modelo quantitativo foi desenvolvido para o cálculo do pH e das concentrações do substrato e dos produtos nos estágios do reator contra-corrente. Os dados fornecidos pelo modelo podem ser utilizados para otimizar as condições de operação como: estágio de alimentação, vazão volumétrica das fases e concentração inicial do substrato. Na última etapa deste trabalho foi feita uma revisão bibliográfica sobre biorreatores extrativos em que são apresentadas as vantagens de cada configuração e as restrições dos processos biocatalíticos. Através desta revisão, foi verificado que o uso de um sistema, formado por agitadores acoplados a hidrociclones em série, pode representar uma opção adequada de reatores multi-estágio contra-corrente para a hidrólise de PenG em escala de laboratório.

Palavras-chave: hidrólise enzimática, Penicilina G, antibióticos semi-sintéticos, processo integrado, cristalização.

ABSTRACT

This work studies the enzymatic hydrolysis of penicillin G (PenG) into 6-aminopenicillanic acid (6-APA) and phenylacetic acid (PAA). In a multi-stage countercurrent reactor and at low pH, the enzymatic reaction takes place in the aqueous phase and the products are separated between the aqueous phase and organic phase (butyl acetate - BuAc). Furthermore, 6-APA crystallization occurs at low pH when PenG concentrations are high. Both phenomena shift the equilibrium towards conversion of substrate, favoring high productivity. The first step of this work, concerns the evaluation of activity and stability of penicillin amidase at low pH and in the presence of butyl acetate (BuAc). The enzyme presented the maximum activity in the pH 8.0 – 9.0 and remained stable at low pHs (3.0 – 6.0) during at least 32 days. Although the enzyme activity decreased by 80%, this does not represent a drawback in the application of a biphasic (water and BuAc) and continuous PenG hydrolysis at low pH. The effect of PenG, PAA and BuAc in APA crystallization and the kinetic parameters were also analyzed. The results showed that impurities have no effect on APA crystallization, in the pH range 4 – 5 and in the impurity concentrations of 0.55 mM – 3.0 mM. The evaluation of crystallization kinetics allowed the use of a model that predicts the APA crystallization rates. A quantitative model was developed in order to calculate the pH and substrates and products concentrations in the countercurrent reactor. The data provided by the model can be used to optimize the operation conditions: stage of feed, flow rate of phases and initial substrate concentration. In the last step of this work, a literature review concerning extractive bioreactor was made. This review presents the advantages of each configuration and the restrictions of the biocatalytic processes. Through this review, a integrated system of mixers and hydrocyclone was suggested as an appropriate option of multi-stage countercurrent reactor for PenG hydrolysis in laboratory scale.

Key-words: enzyme hydrolysis, Penicillin G, semi-synthetic antibiotics, integrated process, crystallization.

SUMÁRIO

Dedicatória	v
Agradecimentos	vi
Acknowledgements	ix
Epígrafe	xii
Resumo	xiii
Abstract	xiv
Nomenclatura	xvii
Capítulo I: Introdução	1
Capítulo II: Revisão Bibliográfica	5
1. Penicilinas	5
2. Antibióticos β -Lactâmicos	6
3. Biocatalisadores	9
4. Remoção do Produto <i>In Situ</i>	11
5. Hidrólise enzimática de PenG em reator multi-estágio e contra-corrente	12
5.1. Aplicação da penicilina amidase em sistema bifásico (água e BuAc) em multi-estágio	15
5.2. Influência de impurezas na cinética de cristalização de APA	16
5.2.1. Solubilidade	18
5.2.2. Nucleação	19
5.2.3. Crescimento dos cristais	21
5.3. Modelo de equilíbrio da hidrólise de PenG em reator multi-estágio e contra-corrente	23

5.3.1. Equilíbrio da hidrólise de PenG em sistema monofásico	26
5.3.2. Partição dos componentes entre as fases aquosa e orgânica	28
5.3.3. Equilíbrio bifásico	29
5.3.4. Equilíbrio da reação trifásico	30
5.4. Bioreatores extrativos	31
6. Referências Bibliográficas	32
Capítulo III: Activity and stability of immobilized penicillin amidase at low pH values	37
Capítulo IV: Crystallization Kinetics of 6-Aminopenicillanic Acid	63
Capítulo V: Modeling of PenG hydrolysis in a counter-current multi-stage reactor	99
Capítulo VI: Extractive Bioreactor Technology	135
Capítulo VII: Conclusões	177
Capítulo VIII: Sugestões para trabalhos futuros	181

NOMENCLATURA

t_{ind} = tempo de indução [min]

J = taxa de nucleação [$\# \cdot m^{-3} \cdot s^{-1}$]

S_0 = razão de supersaturação inicial

S = razão de supersaturação

C = concentração [$mol \cdot L^{-1}$]

C_s = solubilidade

B = constante da inclinação da relação $\ln(t_{ind})$ e $\ln(S_0-1)$

I = fator de medida de detecção do tempo de indução

β = fator de forma

γ = energia superficial [$mJ \cdot m^{-2}$]

v = volume molecular [m^3]

k = constante de Boltzman [$1,38 \cdot 10^{-23} \text{ J/K}$]

T = temperatura [K]

G = taxa de crescimento dos cristais [m/s]

k_g = parâmetro cinético do crescimento de cristais

n = parâmetro cinético do crescimento de cristais

L = tamanho de cristais [μm]

Δt = variação do tempo [min]

S = fator de separação

V = fluxo da fase orgânica

L = fluxo da fase aquosa

K = coeficiente de distribuição

$K_{eq,app}$ = constante de equilíbrio aparente

K_{ref} = constante de equilíbrio da reação de referência

K_a = constante de dissociação

F = Fração da espécie

β = fator de forma

γ = energia interfacial [$\text{mJ}\cdot\text{m}^{-2}$]

v = volume molecular [m^3]

α = razão volumétrica entre as fases aquosa e orgânica

Subscritos

PenG = penicilina G

6-APA = ácido 6-aminopenicilânico

PAA = ácido fenilacético

+ - = estado zwitteriônico de ionização

+ = estado positivo de ionização

- = estado negativo de ionização

0 = estado neutro de ionização

Sobrescritos

aq = fase aquosa

org = fase orgânica

CAPÍTULO I

INTRODUÇÃO

A aplicação de extração contínua de produtos de reação é necessária para aumentar a conversão enzimática por deslocar o equilíbrio termodinâmico; impedir a hidrólise dos produtos; e impedir a inibição enzimática pelos produtos.

As características particulares da hidrólise de penicilina são: conversão limitada pelo equilíbrio, inibição pelo sub-produto (ácido fenilacético), formação de sal devido ao controle de pH e difíceis etapas de separação e purificação devido à semelhança dos compostos. Sistemas líquidos bifásicos (água e solvente orgânico) são uma alternativa para solucionar esses problemas. No entanto, devido à grande semelhança estrutural dos componentes, os coeficientes de partição não são suficientemente diferentes de modo a permitir total conversão em um único estágio, sendo necessário o emprego de um extrator-reator contra-corrente e multi-estágios.

A avaliação da hidrólise de PenG em sistema batelada e bifásico (acetato de butila e água) em valores baixos de pH (3-5), e em um reator em contra-corrente e multi-estágio apresentaram resultados promissores no desenvolvimento e progresso para a produção de 6-APA em sistema intensificado de reação e purificação. Nestas condições, o pH decresce

favorecendo a migração de PAA para a fase orgânica e a cristalização de 6-APA. Ambos fenômenos, separação dos produtos em diferentes fases e cristalização do 6-APA, deslocam o equilíbrio no sentido de conversão do substrato e, conseqüentemente, promovem uma alta produtividade e alta pureza dos produtos. Esses produtos já purificados são utilizados em etapas subseqüentes. O PAA é reciclado e usado na fermentação de PenG e o 6-APA é usado na síntese de antibióticos semi-sintéticos, como amoxicilina e ampicilina.

Os objetivos deste trabalho foram a avaliação da atividade e da estabilidade da penicilina amidase imobilizada a ser usada, e a determinação da cinética de cristalização do produto (6-APA), visto que não se tinha o conhecimento de aplicação desta enzima e de cristalização do 6-APA a baixos valores de pH 3-5 e em sistema bifásico água e acetato de butila. Além dos dados cinéticos de atividade enzimática e de cristalização de 6-APA, foi desenvolvido um modelo no intuito de fornecer as melhores condições de operação do sistema contra-corrente em multi-estágio. Este trabalho ainda incluiu a revisão de bioreatores extrativos como maneira de auxiliar na seleção da melhor configuração de um reator-separador a ser empregado na hidrólise de PenG nas condições desejadas.

As informações obtidas neste trabalho viabiliza a instalação de um reator multi-estágio em contra-corrente para a realização da hidrólise de PenG em 6-APA e PAA em escala de laboratório no intuito de dar prosseguimento aos avanços nos processos de síntese de antibióticos semi-sintéticos.

O conteúdo deste trabalho será apresentado na seguinte forma:

A Revisão Bibliográfica apresentada no Capítulo II engloba informações necessárias para uma melhor compreensão das etapas que foram desenvolvidas.

O estudo da atividade e estabilidade de penicilina amidase (Assemblase®) está apresentado no Capítulo III. As análises foram realizadas a baixos valores de pH, em sistemas tampões de fosfato de potássio saturados com acetato de butila e foram utilizados dois métodos para a determinação de atividade e estabilidade da enzima: titulométrico e

análise por HPLC. Além disso, parâmetros da cinética de degradação de PenG e 6-APA também foram determinados.

A avaliação da cristalização do 6-APA é descrita no Capítulo IV. Os ensaios foram realizados em batelada, a pH 4 e 5 e na presença de impurezas (BuAc, PenG e PAA). A partir desses ensaios, os parâmetros cinéticos da taxa de nucleação e de crescimento dos cristais foram determinados e a influência das impurezas avaliada.

O modelo termodinâmico que descreve as concentrações de equilíbrio dos compostos no sistema bifásico é apresentado no Capítulo V. Este modelo calcula o pH e as concentrações do substrato e produtos nos estágios do reator contra-corrente. Os dados fornecidos pelo modelo podem ser utilizados para otimizar as condições de operação do reator bifásico multi-estágio (ponto de alimentação, vazão volumétrica das fases e concentração inicial do substrato).

O Capítulo VII corresponde a uma revisão da literatura sobre a aplicação de sistemas intensificados em reações enzimáticas de forma a apresentar uma seleção de tipos de biorreatores extrativos de acordo com as diversidades encontradas nas reações biocatalíticas. A apresentação dos tipos de equipamentos foi ilustrada com as vantagens de cada configuração, as com as restrições dos processos biocatalíticos e com os exemplos práticos de aplicação. As informações dos critérios de seleção e dos tipos de biorreatores foram agrupadas em uma tabela de fácil consulta para a escolha do tipo de configuração desejada.

As conclusões e as propostas para trabalhos futuros estão apresentadas nos Capítulos VII e VIII, respectivamente.

CAPÍTULO II

REVISÃO BIBLIOGRÁFICA

1. Penicilinas

As penicilinas possuem um núcleo básico derivado do ácido 6-aminopenicilânico (6-APA), ao qual encontra-se ligado um grupo prostético designado por (R) (Figura 1). O núcleo comum é constituído por um anel tiadiazólico (A) ligado a um anel beta-lactâmico (B). O grupo prostético é o responsável por muitas das características farmacológicas e antibacterianas de cada tipo de penicilina. Das penicilinas obtidas por processos naturais, as únicas empregadas em clínica são a penicilina G (benzilpenicilina) e a penicilina V (fenoximetilpenicilina), esta última também obtida por síntese parcial.

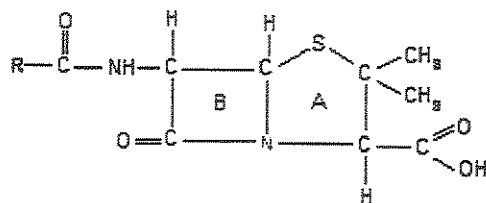


Figura 1: Estrutura molecular da penicilina

A penicilina G é obtida industrialmente por fermentação a partir de cepas de *Penicillium notatum* e *Penicillium chrysogenes*. Apesar de sua enorme utilidade terapêutica, a Penicilina G apresenta três grandes desvantagens:

1. é degradada pelo suco ácido do estômago, o que impede sua utilização por via oral;
2. é destruída pela β -lactamase (penicilinase), o que a torna ineficaz no tratamento de infecções por produtores dessa enzima;
3. seu emprego clínico é freqüentemente acompanhado de manifestações de hipersensibilidade.

Esses três fatores levaram ao desenvolvimento do grupo das penicilinas com modificações estruturais, surgindo, assim, a era das penicilinas semi-sintéticas.

A descoberta das penicilinas semi-sintéticas (penicilinas obtidas pela combinação de processo de fermentação, o qual fornece o 6-APA e o processo químico, com a colocação de radicais a esse núcleo), representou avanço de grande importância na obtenção de derivados com ações específicas, além de permitir sua produção industrial em larga escala. Todavia, faz-se necessário pesquisar novas rotas de produção mais econômicas e que produza menos resíduos (Andersson *et al.*, 2001).

2. Antibióticos β -Lactâmicos

A produção industrial de antibióticos β -lactâmicos e seus intermediários, baseada na estequiometria de conversões químicas tradicionais, está sendo substituída por processos catalisados por enzimas desde que em condições moderadas (meio aquoso, pH neutro e temperatura moderada). No entanto, a maioria dos processos ainda emprega a hidrólise química da Penicilina, sendo todos em meio aquoso e pH 7-8. Apenas recentemente, deu-se início a processos de síntese enzimática para os antibióticos semi-sintéticos. O desenvolvimento de pesquisa nesta área permitiu grande avanço na produção em larga-

escala de antibióticos de alto valor, tais como, amoxicilina, ampicilina, cefaclor, cefadroxila e cefalexina. O esquema de produção de antibióticos derivados da penicilina, denominados Penicilinas Semi-Sintéticas (PSS), como por exemplo, a amoxicilina e a ampicilina, e de antibióticos derivados da cefalosporina, denominados Cefalosporinas Semi-Sintéticas (CSS) está apresentado na Figura 2 (Bruggink *et al.*, 1998, Sodhi *et al.*, 1984).

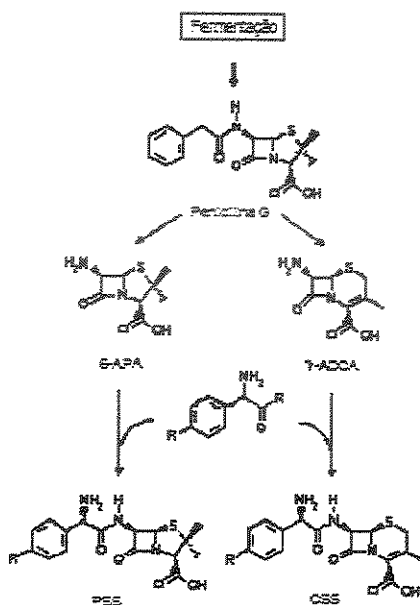


Figura 2: Esquema das reações para produção de antibióticos semi-sintéticos derivados da penicilina e da cefalosporina (Bruggink *et al.*, 1998).

Na abordagem química tradicional, a penicilina G, que é um produto da fermentação, é desacilada a ácido 6-aminopenicilânico (6-APA). Por outro lado, o ácido 7-aminodesacetoxicefalosporânico (7-ADCA), que é um intermediário usado na produção de duas das CSS mais vendidas, pode ser obtido pela expansão oxidativa da PenG seguida por uma desacilação semelhante. Em seguida, o 6-APA e o 7-ADCA são transformados em PSS e CSS, respectivamente, pela condensação com um derivado da D(-) fenilglicina ou da D(-) hidroxifenilglicina (Bruggink *et al.*, 1998, Bailey e Ollis, 1986).

A penicilina G amidase (PGA) é usada para converter a PenG em 6-APA, molécula de caráter anfótero e precursor de penicilinas semi-sintéticas e em ácido fenilacético (PAA), inibidor da hidrólise. Muitas indústrias substituíram a hidrólise química da cadeia lateral, que utilizava produtos químicos prejudiciais e solventes tais como o pentacloreto de fósforo e diclorometano, pela hidrólise catalisada pela penicilina amidase em meio aquoso (Bossi *et al.*, 1999, van der Wielen *et al.*, 1996).

Na produção do antibiótico cefalosporina, utiliza-se não somente a expansão do anel da penicilina G, mas também pode-se obter o núcleo da cefalosporina através da fermentação da cefalosporina C. No entanto, a aplicação da catálise enzimática na hidrólise da cadeia lateral α -aminoadipila na cefalosporina C para produzir o ácido 7-aminocefalosporânico (7-ACA) é menos desenvolvida, pois ainda não foi possível encontrar uma enzima capaz de hidrolisar a cadeia lateral α -aminoadipila.

Devido às peculiaridades de cada antibiótico semi-sintético, a síntese desses compostos catalisada por enzimas, requer um desenvolvimento das técnicas de condensação química e *downstream processing*, empregadas a cada produto, separadamente. Em alguns casos, como os da cefadroxila e do cefaclor, soluções foram encontradas com o uso do agente complexante β -naftol, que protege o produto contra degradação química e enzimática durante o processo de conversão e recuperação.

A Figura 3 representa o esquema das reações de produção dos vários antibióticos semi-sintéticos: ampicilina e amoxicilina, derivados do precursor 6-APA, e cefalexina, cefaclor, e cefadroxila, derivados do precursor 7-ADCA, onde os precursores reagem com fenilglicina modificada por diferentes substituintes químicos (R_1 e R_2).

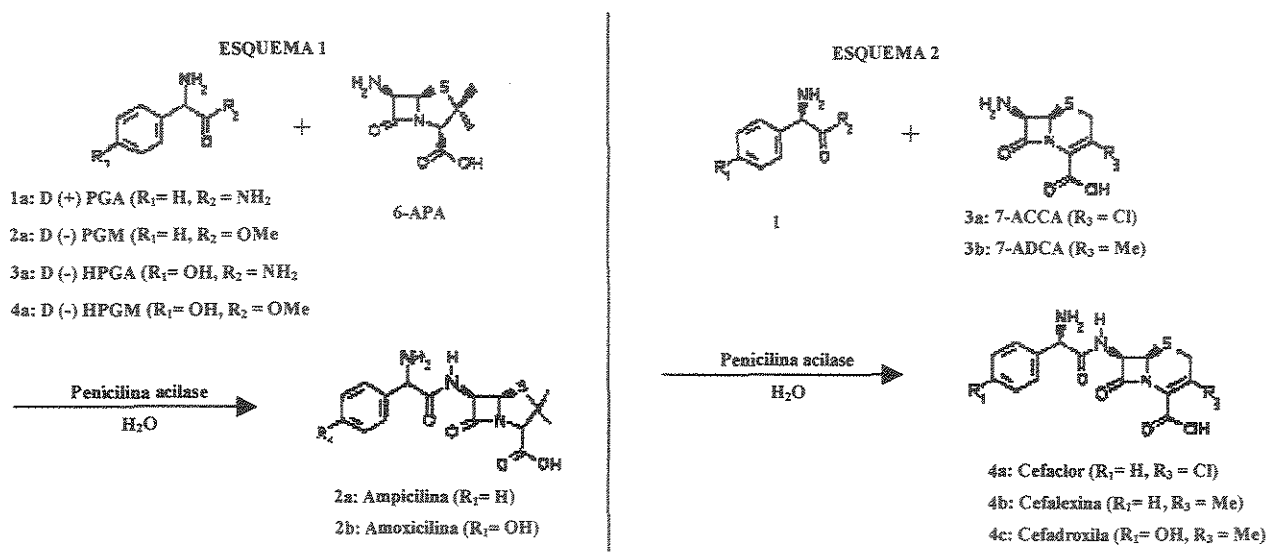


Figura 3: Esquema da reação catalisada por enzima para os antibióticos semi-sintéticos

(Bruggink *et al.*, 1998).

3. Biocatalisadores

As sínteses orgânicas são realizadas de forma que cada ligação é feita individualmente, devido à falta de seletividade e/ou às condições de reações incompatíveis. A alta seletividade de enzimas em condições semelhantes, por exemplo, em sistemas aquosos, permite em princípio o uso de vários biocatalisadores em um único reator (reator batelada, série de colunas, etc), justificando a substituição de sínteses orgânicas por sínteses enzimáticas. Além disso, a aplicação de enzimas como catalisadores em condições moderadas resulta em significativa economia de energia e água, para a indústria e para o meio ambiente (Kirk *et al.*, 2002).

As reações de hidrólise são o uso mais comum de biocatalisadores, mas estudos recentes indicam seu emprego em reações de síntese com várias enzimas e cofatores.

Todavia, várias linhas de pesquisa precisam ser elaboradas para ampliar a utilização de biocatalisadores e biotransformações: técnicas rápidas de análise de grande número de enzimas (naturais ou geneticamente modificadas); métodos rápidos e confiáveis para a preparação de enzimas em batelada; técnicas para a determinação de enzima e de estruturas de sítio ativo assim como das interações com o substrato; métodos de formulação, como por exemplo, a imobilização de enzimas para formar biocatalisadores industriais estáveis. A formulação de biocatalisadores é de fundamental importância, uma vez que a imobilização de enzimas pode influenciar sua seletividade, eficiência e estabilidade (robustez do processo). Assim, ao se melhorar a formulação de enzimas, o número de biocatalisadores disponíveis para aplicação industrial pode ser aumentado para alguns milhares. Além de melhorar os processos de formulação de enzimas, é necessária uma interação mais forte entre a química orgânica e a biologia molecular para que novos biocatalisadores sejam criados (Chaplin e Bucke, 1992)

A integração de biocatalisadores e processo extrativo na síntese de antibióticos semi-sintéticos (ASS) reduz o número de etapas e promove benefícios ao meio ambiente diminuindo o volume de resíduo orgânico. O processo de produção completo, no entanto, é mais complexo devido às várias correntes de reciclo e do grande número de sólidos que devem ser manipulados. Um melhor entendimento da ação enzimática em nível molecular e um projeto racional de catalisadores aperfeiçoados (incluindo imobilização) são necessários para alcançar processos mais ideais nos quais os reciclos são eliminados. Também, *downstream processing* (extração e purificação) mais adequado incluindo, por exemplo, adsorção seletiva dos produtos finais através de técnicas de reconhecimento molecular modernas, é requerido para atingir processos mais viáveis.

4. Remoção do Produto “*In Situ*”

Um dos meios para se promover a extração contínua é a utilização de reações biocatalíticas bifásicas (água e solvente orgânico) que possibilita o aumento da concentração de substratos e produtos no reator; a facilidade de recuperação do biocatalisador e a partição do reagente e do produto entre as fases aquosa e orgânica de forma a facilitar a recuperação dos compostos e minimizar a inibição pelo produto (Lilly, 1982). Esta técnica é denominada Remoção do Produto “*In Situ*”, do inglês *In Situ Product Removal* (ISPR).

A produtividade de processos enzimáticos geralmente é limitada pelo equilíbrio termodinâmico da reação. Isto exige o emprego em excesso de um dos substratos e o reciclo do substrato não convertido, sendo que o último fato caracteriza-se pelo alto custo e consumo excessivo de energia. Portanto, as técnicas de Remoção do Produto/ adotadas no intuito de aumentar a conversão do substrato (e produtividade do processo) e simultaneamente levar a uma corrente de produto com baixa concentração do substrato não convertido e do produto secundário. A técnica de ISPR é baseada na catálise enzimática extrativa, i.e., a integração entre a reação enzimática e a extração do(s) produto(s) em um sistema bifásico (aquosa-orgânica) tendo como finalidade principal deslocar o equilíbrio da reação no sentido de conversão do substrato através da extração de um dos produtos para a fase orgânica. Além disso, a fase orgânica pode também ser um reservatório para substratos de baixa solubilidade em água. Desta maneira, evita-se a inibição por produto ou substrato nos casos em que o inibidor é transferido para a fase orgânica (van der Wielen *et al.*, 2001).

Na aplicação de sistemas bifásicos, o objetivo principal de se utilizar um solvente imiscível em água é de minimizar a exposição do biocatalisador a solventes orgânicos. Deste modo, deve-se levar em consideração a solubilidade do solvente orgânico em água, uma vez que o solvente orgânico pode causar a inibição da reação ou inativar o catalisador (Lilly, 1982).

Na maioria das reações enzimáticas, os reagentes e produtos são estruturalmente semelhantes, o que dificulta encontrar a fase orgânica que os separe completamente. A aplicação de processos de separação em multi-estágios é proposta para promover a purificação de compostos de estruturas semelhantes. A aplicação de catálise enzimática em reação e processos de purificação em multi-estágios promove a conversão completa do reagente e elimina etapas adicionais na purificação de produtos.

5. Hidrólise enzimática de PenG em reator contra-corrente e multi-estágio

O processo convencional de produção de antibióticos semi-sintéticos a partir da PenG é realizado quimicamente, produzindo entre 10 a 100 kg de resíduo por kg de produto. O processo é caracterizado pelo uso de solventes orgânicos halogenados e pela temperatura abaixo de zero, acarretando em um alto consumo de energia. Entretanto, processos biocatalíticos em sistemas aquosos e à temperatura ambiente geram menor quantidade de resíduos em comparação aos processos químicos, havendo uma redução de fator de 5, para a hidrólise de PenG a 6-APA, e de fator de 3, para a síntese de penicilinas semi-sintéticas (Van de Sandt e De Vroom, 2000).

Atualmente, no processo enzimático de produção, por exemplo, da amoxicilina (Amox), a PenG é extraída do caldo de fermentação com um solvente orgânico (acetato de butila) em pH 2.0 - 2.5. Em seguida, PenG é re-extraída para a fase aquosa a pH 6.8 – 8.0 e cristalizada pela adição de acetato de potássio ou acetato de sódio. A PenG cristalina é hidrolisada em ácido 6-aminopenicilânico (6-APA) e ácido fenilacético (PAA) a pH 7-8. O 6-APA é recuperado por cristalização e dissolvido novamente para ser usado como precursor na reação subsequente de síntese da Amox. O processo enzimático (Figura 4), compreende várias etapas e produz uma alta quantidade de resíduos, principalmente pela necessidade de adição de sal ou base que causa a formação de grande quantidade de resíduo (Diender, 2001; den Hollander, 2002).

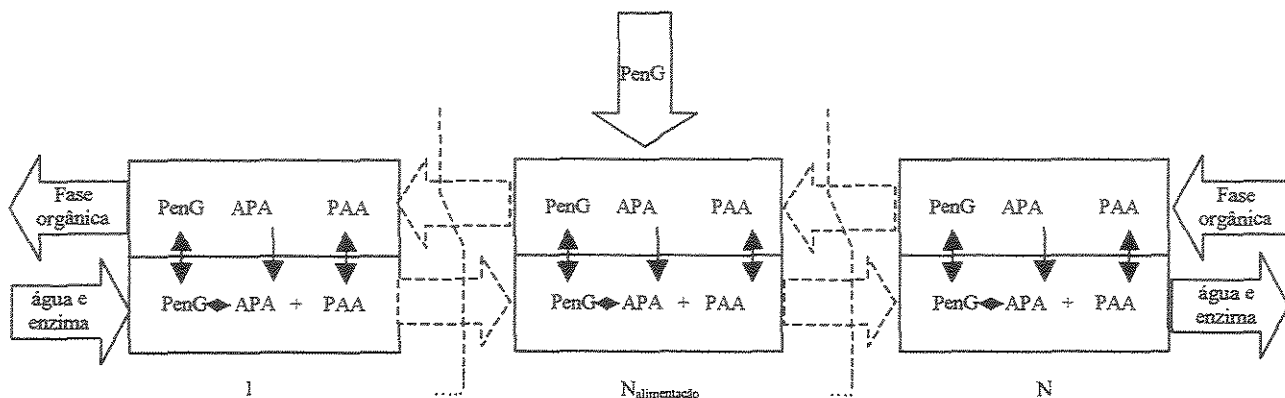


Figura 5: Esquema da hidrólise de PenG em sistema bifásico em multi-estágio (den Hollander, 2002).

Além disso, a formação e recuperação do produto em um reator-separador (reator de fracionamento) apresentam benefícios para sistemas com limitações cinéticas e termodinâmicas simultâneas, demonstrando ser promissora para produtos biotecnológicos instáveis em sistemas biocatalíticos sensíveis ao pH. O processo de hidrólise e purificação integrado é favorável para a desacilação de PenG, na formação do produto principal 6-APA e do produto secundário, PAA. Este processo permite a remoção contínua do PAA que tende diminuir a taxa de reação via inibição (van der Wielen *et al.*, 1996) e dificulta o tratamento com modelos cinéticos, uma vez que a resposta desses modelos se distancia dos dados experimentais na presença de inibidores (Ferreira *et al.*, 2000).

Na ausência de controle de pH, este tende a diminuir favorecendo a cristalização de 6-APA. Nessas condições, a remoção de PAA para o BuAc e a cristalização do 6-APA deslocam o equilíbrio no sentido de conversão da PenG. Além disso, a separação dos produtos em fases diferentes, representa um processo altamente seletivo com alto grau de pureza dos produtos. Sabe-se que PenG sofre decomposição em valores baixos de pH (van der Wielen *et al.*, 1996; Ferreira *et al.*, 2004). No entanto, no sistema proposto, o substrato tende a permanecer em fase orgânica e transferir para a fase aquosa a medida que é

consumido durante a reação. Este fato contribui para que a degradação do substrato não represente empecilho para o sistema proposto, uma vez que a decomposição de PenG ocorre apenas em fase aquosa.

5.1. Aplicação da penicilina amidase no sistema bifásico (água e BuAc) em multi-estágio.

O uso de enzimas solúveis em aplicações industriais apresenta limitações em virtude do custo e das dificuldades técnicas de recuperação e purificação do biocatalisador. Quando enzimas na forma solúvel são utilizadas em processos industriais, elas podem continuar ativas mesmo após o término do processo e em geral não são recicladas e separadas do produto final devido ao custo do processo. A atividade enzimática pode contaminar o produto. Dessa forma, um método de inativação da enzima deve ser aplicado. Estes empecilhos são superados pelo uso de enzimas imobilizadas em matrizes sólidas insolúveis em água, permitindo fácil separação e reutilização do biocatalisador e, geralmente, promovendo o aumento da estabilidade operacional e do tempo de armazenamento, além de favorecer processos mais econômicos e simples. No entanto, a atividade das enzimas imobilizadas pode ser reduzida em relação a enzima solúvel, devido às mudanças conformacionais na estrutura de macromolécula e resistência difusional ao transporte de substratos e produtos no sítio catalítico. Todavia, o uso de enzimas imobilizadas em indústrias químicas, farmacêuticas e de alimentos se encontra em expansão e representa um importante ramo da tecnologia moderna (Travascio *et al.*, 2002; Chaplin e Bucke, 1992).

A penicilina amidase é uma hidrolase N-terminal serine que catalisa a hidrólise de Penicilina G assim como as sínteses de penicilinas e cefalosporinas semi-sintéticas. A penicilina amidase de *Escherichia coli* é a segunda enzima mais usada pela indústria na

forma imobilizada, sendo a hidrólise de penicilina sua aplicação mais importante (Janssen *et al.*, 2002, Cardias *et al.*, 1999, Ferreira *et al.*, 2000).

As propriedades catalíticas da penicilina amidase G e a estereoespecificidade sob condições moderadas de reação (meio aquoso e pH neutro) representam excelentes possibilidades de aplicação desta enzima como catalisador industrial. Todavia, algumas desvantagens operacionais devem ainda ser eliminadas, como: fragilidade e alto custo de recuperação (Cardias *et al.*, 1999, Gonçalves *et al.*, 2003). Estes problemas podem ser diminuídos pela imobilização da enzima (Bruggink *et al.*, 1998, Ferreira *et al.*, 2000). O desenvolvimento das técnicas de imobilização tornou as reações enzimáticas de condensação viáveis economicamente, permitindo reutilização do catalisador inúmeras vezes.

No sistema proposto para a hidrólise de PenG em sistema água e BuAc, o pH tende a diminuir para valores próximos de 3. Por isso, faz-se necessário avaliar a atividade e a estabilidade da penicilina amidase (Assemblase®) em baixos valores de pH e a influência do solvente orgânico. Apesar de vários trabalhos na literatura descreverem a aplicação da penicilina amidase em processos enzimáticos a pH entre 5 e 6 (Topgi *et al.*, 1999; Smijewski *et al.*, 1991; Youshko *et al.*, 2001; Diender *et al.*, 2000; Niertrasz *et al.*, 1999), não há relatos de uso desta enzima a pH's abaixo de 5, em virtude de possíveis danos a estabilidade e atividade da penicilina amidase (Topgi *et al.*, 1999).

5.2. Influência de impurezas na cinética de cristalização de 6-APA.

Na reação de hidrólise de PenG em sistema bifásico, PAA transfere-se para a fase orgânica a medida que é formado; 6-APA, que possui caráter zwitteriônico, permanece na fase aquosa e o pH sofre um decréscimo. Nestas condições, em pH baixo e concentração de equilíbrio superior a sua solubilidade o 6-APA cristaliza-se promovendo o deslocamento do

equilíbrio termodinâmico e, deste modo, um aumento considerável na conversão (Diender *et al.*, 2002).

O 6-APA é um anfólito que pode existir em solução como uma combinação das espécies aniônicas, catiônicas e zwitteriônicas, cujas concentrações relativas são funções da temperatura e pH (Mwangi, 1994). As frações das diferentes espécies de 6-APA em função do pH podem ser observadas na Figura 6.

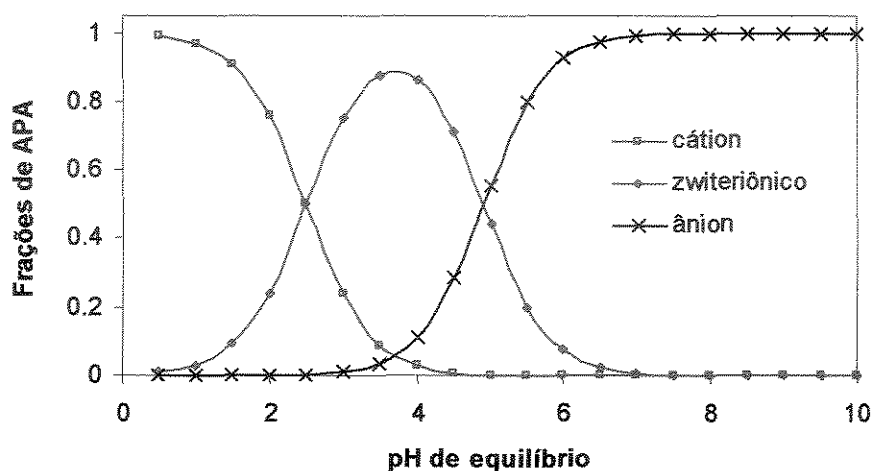


Figura 6: Frações das diferentes espécies de 6-APA em função do pH

A solubilidade do 6-APA é maior em pH's menores ou maiores do que o pH isoeletrico, sendo resultado direto da conversão da espécie zwitteriônica nas espécies catiônicas e aniônicas, respectivamente. O pH isoeletrico corresponde à concentração máxima do zwitterion e mínima solubilidade, pois esta é a espécie mais estável (Mwangi, 1994).

Apesar da importância do 6-APA na produção de antibióticos semi-sintéticos produzidos comercialmente por vários anos, há poucos estudos sobre a cristalização de 6-APA (Mwangi, 1994). Neste trabalho, os parâmetros cinéticos de crescimento dos cristais e de nucleação de 6-APA e a influência das impurezas (PenG, PAA e BuAc) são estudados.

Para melhor compreensão sobre efeito de impurezas na cristalização, alguns conceitos básicos são apresentados a seguir.

5.2.1. Solubilidade

A presença de impurezas pode afetar a solubilidade de um soluto de diferentes maneiras. Raramente, a impureza não altera a solubilidade do soluto. No entanto, casos mais freqüentes de aumento (*salting in*) e diminuição (*salting out*) da solubilidade são registrados, podendo haver a alteração da natureza do sistema nos casos de formação de complexos em virtude de interações entre o soluto e a impureza.

Uma solução saturada é caracterizada pelo estado de equilíbrio termodinâmico. No entanto, é possível obter uma solução, denominada supersaturada, contendo mais sólido dissolvido do que a quantidade representada pela saturação de equilíbrio. No caso do 6-APA, a solução supersaturada é preparada ao diminuir lentamente o pH do sistema de 6-APA concentrado sem agitação. A condição de supersaturação é de fundamental importância para as operações de cristalização (Mullin, 1993).

A Figura 7 representa as diferentes zonas de solubilidade e supersaturação em função da temperatura, onde a cristalização poderá ou não ocorrer espontaneamente.

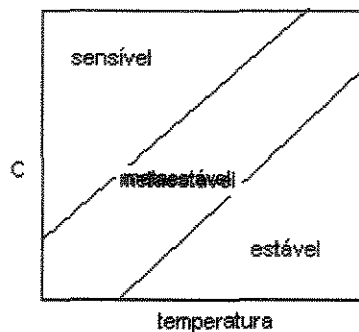


Figure 7: Diagrama de solubilidade-supersaturação (Mullin, 1993)

Na zona estável (não-saturada), onde a concentração é inferior à concentração de saturação, a cristalização é impossível, ao passo que na região sensível (supersaturada), a cristalização ocorre espontaneamente, mas não é inevitável. A região meta-estável é caracterizada por ser supersaturada, no entanto, é improvável a cristalização espontânea, exceto pela adição de sementes.

5.2.2. Nucleação

Um novo cristal pode ser proveniente de diferentes tipos de nucleação, conforme esquema apresentado na Figura 8.

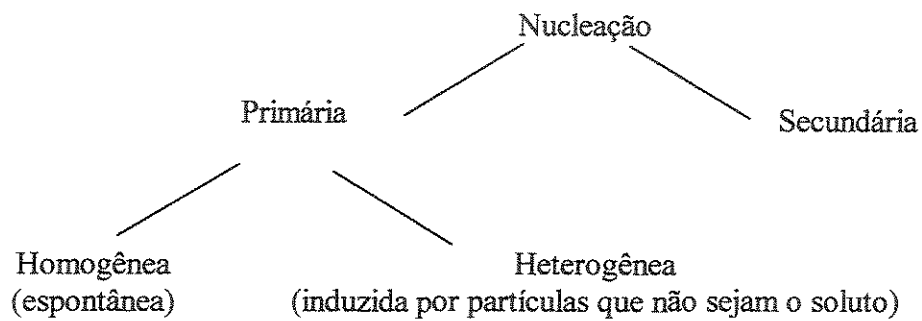


Figura 8: Tipos de nucleação (Mullin, 1993)

A nucleação homogênea é a formação de novos cristais a partir da fase líquida em virtude apenas da supersaturação. A formação de novos cristais na nucleação heterogênea dá-se pela presença de material insolúvel estranho ao sistema que por sua vez apresenta sítios onde os cristais podem ser formados devido à redução da energia necessária para a cristalização. A nucleação induzida pela presença de cristais do próprio soluto denomina-se nucleação secundária e em certo grau é similar a nucleação heterogênea. No caso de

operações de cristalização, deve-se também citar a formação de novos cristais pelo atrito de sólido suspenso na solução.

A avaliação dos parâmetros de nucleação é realizada através da determinação do tempo de indução, definido como o intervalo de tempo em que os primeiros cristais em solução são detectados, de acordo com a Equação 1, sendo que a taxa de nucleação (J) é inversamente proporcional ao tempo de indução (t_{ind}) (Mullin, 1993).

$$t_{ind} \propto J^{-1} \quad (1)$$

A medida do tempo de indução depende da supersaturação inicial da solução e do método de detecção. Nos casos em que o tempo de indução é detectado pela concentração do soluto, a medida dependerá da conversão, enquanto que nos casos em que o tempo de indução for detectado pela reflexão da luz, a medida dependerá da área superficial do cristal. (Ottens *et al.*, 2004). Fazendo-se uso da relação do t_{ind} e a razão de supersaturação $S = C/C_0$, (razão entre a concentração da solução supersaturada e a solubilidade), como na Equação 2

$$t_{ind} \propto \left[(S_0 - 1)^n \right]^{-1} \cdot \exp\left(\frac{B}{(i+1)(\ln(S_0))^2} \right) \quad (2)$$

a relação linear de $\ln t_{ind}$ e $(\ln S_0)^{-2}$ fornece a inclinação $\frac{B}{i+1}$, onde $i=2$ ou 3 caso a medida seja por reflexão ou por concentração, respectivamente. Sendo que o fator B é descrito por:

$$B = \frac{\beta v^2 \gamma^3}{(kT)^3} \quad (3)$$

onde β é o fator de forma (igual a $16\pi/3$ para núcleos esféricos) (Mullin, 1993 e Prasad *et al.*, 2001), γ e a tensão superficial, v é o volume molecular e k é a constante de Boltzman. Deste modo a energia superficial também pode ser estimada.

De acordo com as considerações teóricas acima, a taxa de nucleação deve aumentar com o aumento da supersaturação e diminuir com o aumento da energia superficial.

O grau de supersaturação é um parâmetro crítico no controle da taxa de nucleação, visto que o tamanho do núcleo reduz com o aumento da supersaturação e, conseqüentemente, a probabilidade do núcleo formar cristais é maior (Randolph e Larson, 1971).

A presença de impurezas pode afetar consideravelmente a nucleação. As impurezas solúveis podem inibir a nucleação devido a alterações na solubilidade de equilíbrio ou na estrutura da solução, em virtude da adsorção física ou química da impureza no núcleo ou hetero-núcleo (Prasad *et al.*, 2001). No entanto, a ação de moléculas de alta massa molecular difere da ação dos cátions. No caso de moléculas de alta massa molecular, estas inativam o hetero-núcleo pela adsorção em sua superfície, ao passo que os cátions podem romper a estrutura dos núcleos. A ação das impurezas pode ser verificada por diferentes maneiras. Por exemplo, no caso de cátions, quanto maior a carga maior será o efeito de inibição ($\text{Cr}^{+3} > \text{Fe}^{+3} > \text{Al}^{+3} > \text{Ni}^{+2} > \text{Na}^{+}$). Além disso, existem casos em que a inibição pode ser reduzida quando a concentração da impureza atinge níveis acima de uma concentração limite (Mullin, 1993).

5.2.3. Crescimento dos cristais:

O mecanismo de crescimento do cristal em solução exige o transporte do soluto até a superfície do cristal e, em seguida, a incorporação à rede cristalina. Este transporte é constituído de duas etapas, uma difusional seguida pela etapa de reação de superfície, sendo esta última denominada etapa de integração da partícula. Em sistemas não-agitados, por exemplo, a taxa de crescimento é limitada pela taxa de difusão através de um filme. No entanto, à medida que a agitação aumenta ou a velocidade relativa entre o cristal e o licor-

mãe aumenta, a taxa de crescimento atinge um máximo e a taxa de crescimento passa a ser controlada pela taxa de integração da partícula (ou reação de superfície) (Randolph e Larson, 1971).

Taxa de crescimento do cristal (G) é dada em função da razão de supersaturação (S) como demonstrado na Equação 4 (Tavare, 1995)

$$G = k_g \cdot (S_0 - 1)^n \quad (4)$$

Os parâmetros da cinética de crescimento, k_g e n , são determinados a partir de experimentos de cristalização como sendo os coeficientes linear e angular, respectivamente, dos gráficos de $\ln(G)$ versus $\ln(S-1)$, onde G é obtido pela medida de tamanho dos cristais em função do tempo

$$G = \frac{\Delta L}{\Delta t} \quad (5)$$

e a razão de supersaturação (S) é determinada de acordo com a Equação 6

$$S = \frac{C}{\text{solubilidade}} \quad (6)$$

onde a solubilidade de 6-APA é avaliada usando a Equação 7 (Diender *et al.*, 2000).

$$\text{Solubilidade}_{\text{APA}} = \frac{\text{Solubilidade}_{\text{APA}^{+-}}}{F_{\text{APA}^{+-}}} \quad (7)$$

O efeito de impurezas no crescimento de cristais é amplo, podendo inibir ou acelerar a crescimento. Algumas impurezas ainda podem agir seletivamente, atuando em certas placas cristalográficas, e conseqüentemente, modificando a rede cristalina. Certas impurezas afetam a cristalização estando presentes em concentrações muito baixas (da ordem de 1ppm), enquanto outras apresentam efeitos apenas quando presentes em quantidades consideravelmente elevadas (Mullin, 1993).

O efeito das impurezas de inibição ou de aceleração do crescimento é devido às mudanças de propriedades da solução ou a concentração de equilíbrio. As impurezas podem alterar as características da camada de adsorção na interface solução cristal-solução e influenciar a integração de unidades de crescimento, pois podem estar adsorvidas seletivamente em diferentes placas do cristal, principalmente se há alguma semelhança na estrutura molecular.

5.3. Modelo de equilíbrio da hidrólise de PenG em reator multi-estágio e contra-corrente.

Os reatores em contra-corrente são uma nova classe dos reatores cromatográficos em que duas fases imiscíveis (por exemplo, L/L ou L/S) se movem continuamente em contra-corrente. Tipos convencionais de reatores são operados em batelada porque uma das fases é estacionária. Em reatores enzimáticos em contra-corrente um ou dois substratos são introduzidos e enzimaticamente convertidos em dois produtos, que são separados deslocando o equilíbrio e direcionando as reações para a conversão total.

As vantagens desse sistema são: produção quantitativa em reações limitadas pelo equilíbrio; purificação simplificada do produto e redução do número de operações unitárias, uma vez que pelo menos um dos substratos é convertido totalmente e ambos os produtos são separados um do outro; e o uso de sistema menos diluído ou um menor excesso do segundo substrato. As desvantagens englobam: possibilidade de diluição das correntes do produto; uso relativamente ineficiente da enzima; e projeto e construção relativamente complexos, por ser uma tecnologia recente.

As etapas de separação, em batelada ou contínua, podem levar a separações quase completas quando as diferenças entre os coeficientes de partição dos componentes são elevados. No entanto, no caso de os compostos apresentarem estruturas semelhantes (assim como os ASS em estudo), o parâmetro a ser avaliado na seletividade e recuperação, é o

fator de separação S (Equação 8). Considerando o equilíbrio termodinâmico entre os fluxos de saída de um estágio de equilíbrio simples, o fator de separação S relaciona o desempenho de separação à razão entre o fluxo auxiliar (V) e o fluxo de alimentação (L) e o coeficiente de distribuição do componente (K).

$$S = K \frac{V}{L} \quad (8)$$

Quando a quantidade da fase auxiliar (V) ou o coeficiente de partição (K) aumentam, o fator de separação (S) e o grau de recuperação na fase V também aumentam. Para contato de multi-estágios ou estágio simples com coeficiente de partição constante, pode-se deduzir relações simples, enquanto que para sistemas de multicomponentes com equilíbrio termodinâmico mais complexo, uma descrição adequada exige modelos mais rigorosos com soluções numéricas.

O fator de separação S também pode ser tratado como fator de extração, sendo uma medida para a razão da capacidade dos fluxos de transportar um soluto específico. Quando $S > 1$, uma maior quantidade do composto é transportada com a fase V, e quando $S < 1$, grande parte do composto permanece na fase L.

No modelo de hidrólise de PenG a ser desenvolvido, pretende-se avaliar as diversas situações que levam a melhor separação dos produtos, alterando os estágios de entrada e saída das correntes de alimentação (L - líquida) e auxiliar (V - líquida ou sólida). Operação eficiente e custo adequado podem ser obtidos reduzindo as correntes do processo e otimizando as concentrações, exigindo configurações mais complexas com secções e correntes de refluxo adicionais.

Além disso, o modelo identificará a posição de equilíbrio da hidrólise em sistema bifásico (água e solvente orgânico) contínuo em multi-estágios e em contra-corrente como função do pH, da concentração de PenG na alimentação e razão volumétrica entre as fases aquosa e orgânica. Portanto, o comportamento de partição dos reagentes será também

descrito em função destes parâmetros e combinado com os modelos de cristalização do 6-APA e de equilíbrio da reação.

O processo de modelagem é essencial para a implementação de técnicas para a otimização de custo e do desenvolvimento de estratégia de controle. Técnicas de otimização, baseadas em simulações de modelo cinético, promovem a redução considerável do tempo e do custo. Desta maneira, a viabilidade da hidrólise de PenG em sistema bifásico contínuo pode ser avaliado pela otimização das condições de reação usando este modelo.

Abaixo segue a relação das equações e as considerações teóricas usadas para o desenvolvimento do modelo de hidrólise da PenG. A Figura 9 apresenta o esquema de equilíbrio reação, de partição entre as fases aquosa e orgânica, de dissociação e de cristalização do 6-APA.

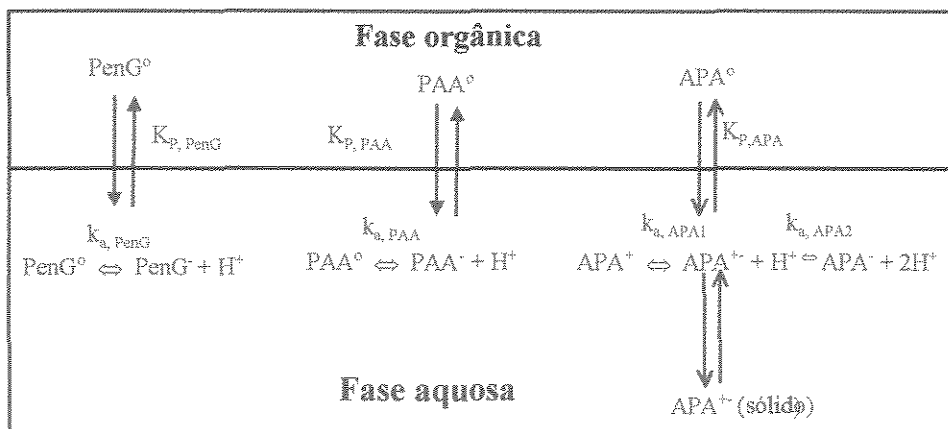


Figure 9: Esquema de equilíbrio da hidrólise de PenG em sistema contra-corrente e cristalização de 6-APA.

Pode-se observar por esse esquema que ao promover a cristalização de 6-APA e a partição de PAA para a fase orgânica, desloca-se o equilíbrio de reação no sentido de formação dos produtos.

5.3.1. Equilíbrio da hidrólise de PenG em sistema monofásico

O equilíbrio da hidrólise de PenG em sistema aquoso pode ser descrito pela constante de equilíbrio aparente ($K_{eq,app}^{aq}$) e pelas concentrações dos reagentes (Equação 9).

$$K_{eq,app}^{aq} = \frac{C_{PAA}^{aq} \cdot C_{APA}^{aq}}{C_{PenG}^{aq}} \quad (9)$$

Este equilíbrio é uma função do pH e a constante de equilíbrio aparente pode ser escrita como função de uma constante da reação de referência e das frações dos reagentes e substratos a um dado pH, sendo a reação de referência dada abaixo (Diender *et al.*, 1998).



Portanto, a constante de reação aparente torna-se:

$$K_{eq,app}^{aq} = K_{ref} \cdot \frac{F_{PenG^-}}{C_{H^+} \cdot F_{PAA^-} \cdot F_{APA^-}} \quad (10)$$

onde K_{ref} é a constante de equilíbrio da reação de referência independente de pH e F_{PenG^-} , F_{PAA^-} e F_{APA^-} são as frações da PenG, PAA e 6-APA no estado aniônico, respectivamente.

As frações F_{PenG^-} , F_{PAA^-} e F_{APA^-} são dadas pelas relações abaixo:

$$F_{PenG^-} = \frac{C_{PenG^-}}{C_{PenG}} \quad (11)$$

$$F_{PAA^-} = \frac{C_{PAA^-}}{C_{PAA}} \quad (12)$$

$$F_{APA^-} = \frac{C_{APA^-}}{C_{APA}} \quad (13)$$

Sabendo que:

$$K_{a, \text{PenG}^-} = \frac{C_{\text{PenG}^-} \cdot C_{\text{H}^+}}{C_{\text{PenG}^-}} \quad (14)$$

$$K_{a, \text{PAA}^-} = \frac{C_{\text{PAA}^-} \cdot C_{\text{H}^+}}{C_{\text{PAA}^-}} \quad (15)$$

$$K_{a, \text{APA}_1} = \frac{C_{\text{APA}^{2-}} \cdot C_{\text{H}^+}}{C_{\text{APA}^-}} \quad (16)$$

$$K_{a, \text{APA}_2} = \frac{C_{\text{APA}^-} \cdot C_{\text{H}^+}}{C_{\text{APA}^{2-}}} \quad (17)$$

onde C_i é a concentração e $K_{a,i}$ é a constante de dissociação do componente i (Tewari e Goldberg, 1988).

E substituindo em (11), (12) e (13), as frações F_{PenG^-} , F_{PAA^-} e F_{APA^-} podem ser calculadas a partir das relações abaixo:

$$F_{\text{PenG}^-} = \frac{1}{1 + \frac{C_{\text{H}^+}}{K_{a, \text{PenG}^-}}} \quad (18)$$

$$F_{\text{PAA}^-} = \frac{1}{1 + \frac{C_{\text{H}^+}}{K_{a, \text{PAA}^-}}} \quad (19)$$

$$F_{\text{APA}^-} = \frac{1}{1 + \frac{C_{\text{H}^+}}{K_{a, \text{APA}_2}} + \frac{(C_{\text{H}^+})^2}{K_{a, \text{APA}_1} \cdot K_{a, \text{APA}_2}}} \quad (20)$$

A Tabela 1 apresenta as reações de dissociação e os respectivos valores $\text{p}K_a$ que ocorrem na faixa de pH entre 3-7 (Diender *et al.*, 2002).

Tabela 1: Reações de dissociação e valores de pK_a (Diender *et al.*, 2002)

Reação de Dissociação	pK _a
$\text{H}_2\text{O} \leftrightarrow \text{OH}^- + \text{H}^+$	14
$\text{PenG}^0 \leftrightarrow \text{PenG}^- + \text{H}^+$	2,5
$\text{APA}^+ \leftrightarrow \text{APA}^{++} + \text{H}^+$	2,5
$\text{APA}^{++} \leftrightarrow \text{APA}^- + \text{H}^+$	4,9
$\text{PAA}^0 \leftrightarrow \text{PAA}^- + \text{H}^+$	4,3

5.3.2. Partição dos componentes entre as fases aquosa e orgânica

Em um sistema bifásico (orgânico – aquoso), os componentes tendem a migrar entre ambas as fases, sendo que os eletrólitos fracos, principalmente espécies eletronicamente neutras migrarão para a fase orgânica (Figura 9).

O coeficiente de partição aparente (global) de um ácido monovalente é dado por:

$$K_{p,i}^{\text{app}} = \frac{C_i^{\text{org}}}{C_i^{\text{aq}}} = \frac{C_{i^0}^{\text{org}}}{C_{i^0}^{\text{aq}} + C_{i^-}^{\text{aq}}} \quad (21)$$

De acordo com as relações indicadas pelas Equações 18 a 20, e substituindo na equação acima, observa-se que o equilíbrio de partição depende do pH e o coeficiente de partição aparente em função do pH pode ser descrito como segue:

$$K_{p,i}^{\text{app}} = K_{p,i}^{\text{ref}} \cdot F_{i^0} \quad (22)$$

onde $K_{p,i}^{ref}$ é o coeficiente de partição intrínseco (pH – independente) e F_{i^0} é a fração da espécie do componente i eletricamente neutra, que são calculadas pelas Equações 18 a 20.

5.3.3. Equilíbrio bifásico

Na hidrólise enzimática de PenG, em sistema bifásico (água e solvente orgânico), considera-se que a reação ocorre apenas na fase aquosa e a medida que PenG é hidrolisada, os componentes migram diferentemente entre as fases aquosa e orgânica até que os equilíbrios de partição e de reação sejam atingidos. Nessa condição de equilíbrio, um balanço de massa para cada componente pode ser formulado para as fases aquosa e orgânica.

$$n_i = (C_{i^0}^{aq} + C_{i^-}^{aq}) \cdot V^{aq} + C_i^{org} \cdot V^{org} \quad (23)$$

onde n é o número de mols e V é o volume das fases aquosa (aq) e orgânica (org), sendo considerado esse volume constante ao longo de todo o processo extrativo. Os balanços estequiométricos para a reação enzimática são dados a seguir:

$$n_{PenG} = n_{PenG^0} - n_{PAA} \quad (24)$$

$$n_{APA} = n_{PAA} \quad (25)$$

A combinação dos coeficientes de partição (Equação 21), dos balanços de massa (Equação 23) e estequiométricos (Equações 24 e 25) dará para cada componente a concentração na fase aquosa como função da concentração de PAA na fase aquosa, dos coeficientes de partição e dos volumes das fases.

Ou seja,

$$C_{PenG}^{aq} = \frac{n_{PenG^0} - C_{PAA}^{aq} \cdot (V^{aq} + V^{org} \cdot K_{p,PAA}^{app})}{(V^{aq} + V^{org} \cdot K_{p,PenG}^{app})} \quad (26)$$

$$C_{PAA}^{aq} = \frac{C_{PAA}^{aq} \cdot (V^{aq} + V^{org} \cdot K_{p,PAA}^{app})}{(V^{aq} + V^{org} \cdot K_{p,APA}^{app})} \quad (27)$$

A substituição das equações acima na Equação 9 e a utilização da Equação 10 fornecerão a concentração aquosa de PAA em função do pH do qual todas as concentrações nas fases orgânicas e aquosas podem ser calculadas. Todavia, em sistemas bifásicos é mais conveniente expressar a constante de equilíbrio de reação em termos de concentração global (bifásico) (Martinek e Semenov, 1981). Estas concentrações bifásicas são dadas pela Equação 28

$$C_i^{bi} = C_i^{aq} \cdot \frac{1 + \alpha \cdot K_{p,i}^{app}}{1 + \alpha} \quad (28)$$

onde α é a razão volumétrica entre as fases aquosa e orgânica $\alpha = \frac{V^{org}}{V^{aq}}$. O equilíbrio de reação bifásico é então expressa como

$$K_{eq,APA}^{bi} = \frac{C_{PAA}^{bi} \cdot C_{APA}^{bi}}{C_{PenG}^{bi}} = K_{eq,APA}^{aq} \cdot \frac{(1 + \alpha \cdot K_{p,PAA}^{app}) \cdot (1 + \alpha \cdot K_{p,APA}^{app})}{(1 + \alpha) \cdot (1 + \alpha \cdot K_{p,PenG}^{app})} \quad (29)$$

Usando as constantes de dissociação dos reagentes representadas na Tabela 2, o valor de K_{ref} de $7,35 \cdot 10^{-8} \pm 1,5 \cdot 10^{-8}$ (Tewari e Goldberg, 1988) e a razão volumétrica α experimental, o valor de $K_{eq,APA}^{bi}$ que pode ser calculado em função do pH.

5.3.4. Equilíbrio da reação trifásico

Se a concentração de equilíbrio de 6-APA em fase aquosa exceder sua solubilidade, 6-APA se cristaliza. A cristalização de 6-APA é favorável à conversão à medida que a hidrólise ocorre, pois o equilíbrio é deslocado (Figura 8). A solubilidade de 6-APA pode ser relacionada como função do pH da seguinte forma (Diender *et al.*, 2000).

$$S_{APA} = \frac{S_{APA^{+-}}}{F_{APA^{+-}}} \quad (30)$$

onde $S_{APA^{+-}}$ é a solubilidade da espécie zwitteriônica de 6-APA. Para o cálculo da constante de equilíbrio bifásico aparente, a solubilidade da 6-APA (S_{APA}) deve ser usada nas Equações 9 e 29 ao invés da C_{APA}^{aq} , simplificando estas equações

5.4. Biorreatores extrativos

Visto a necessidade de encontrar um sistema adequado para realizar a hidrólise de PenG experimentalmente, fez-se uma revisão bibliográfica dos diferentes tipos de reatores e extratores que poderiam ser acoplados e aplicados na hidrólise enzimática de PenG, levando em consideração as condições do modo de operação contínuo, catálise pela penicilina amidase imobilizada e separação dos cristais de 6-APA juntamente com a fase aquosa.

Com base na ampla informação adquirida com relação à diversidade dos tipos de sistemas que podem ser empregados em processos integrados de reação e de extração e as diferentes condições das biocatálises empregando a técnica ISPR, decidiu-se agrupar estas informações em uma revisão sobre biorreatores extrativos e indicar um esquema de escolha do tipo de sistema a ser adotado dependendo das características da reação.

De forma geral, há uma abordagem para a seleção de processos e o *design* de biotransformações. As primeiras etapas envolvem a identificação das restrições e das características dos reagentes, produtos e biocatalisador. A etapa seguinte corresponde à identificação das opções de processo mais adequadas possíveis com base nas restrições já estabelecidas. Diante do número limitado de possibilidades, experimentos devem ser realizados no intuito de aprimorar a seleção e *design* do processo e, finalmente, testar os possíveis efeitos de *scale-up* (Lilly, 1999).

6. Referência Bibliográfica

ANDERSSON, A.C., VAN SCHELTINGA, T., VALEGÅRD, K.. Review: Towards new β -lactam antibiotics. *CMLS Cellular and Molecular Life Sciences*. v. 58, p. 1897-1906. 2001.

BAILEY, J.E., OLLIS, D.F.. *Biochemical Engineering Fundamentals*. 2nd edition. McGraw-Hill Inc. 984 p. 1986.

BOSSI, GUERRERA, S., RIGHETTI, P.G.. Electrically immobilized enzyme reactors: bioconversion of a charged substrate. Hydrolysis of penicillin G by penicillin G acylase. *Biotechnology and Bioengineering*. v. 64, n. 4, p. 383-391, 1999.

BRUGGINK, ROOS, E.C., VROOM, E.. Penicillin acylase in the industrial production of β -lactam antibiotics. *Organic Process Research and Development*. v. 2, n. 2, p. 128-133, 1998.

CARDIAS, H.C.T., GRININGER, C.C., TREVISAN, H.C., GUISAN, J.M., GIORDANO, R.L.C.. Influence of activation on the multipoint immobilization of penicillin G acylase on macroporous silica. *Brazilian Journal Chemical Engineering*. v. 16, n. 2. 141-148. 1999.

CHAPLIN, M.F., BUCKE, C.. Enzyme Technolgy. In: *Future Prospect for Enzyme Technology*. Chapter 8, p. 220-256. Cambridge Press, 1992.

DEN HOLLANDER, J.L., ZOMERDIJK, M., STRAATHOF, A.J.J., VAN DER WIELEN, L.A.M., Continuous penicillin G hydrolysis in countercurrent water - butyl acetate biphasic systems, *Chemical Engineering Science*. v. 57, p. 1591-1598, 2002.

DEN HOLLANDER, J.L.. *Liquid-liquid chromatographic systems for enzymatic reactions*. Tese de doutorado. 2002. 144 p. Tese (Doutorado em Engenharia Química) – Department of Biotechnology. Delft University of Technology, Delft. Holanda..

DIENDER, M.B., STRAATHOF, A.J.J., HEIJNEN, J.J.. Predicting enzyme catalyzed reaction equilibria in cosolvent-water mixtures as a function of pH and solvent composition. *Biocatalysis and Biotransformations*. v. 16, p. 275-289. 1998

DIENDER, M.B., STRAATHOF, A.J.J., VAN DER DOES, T., RAS, C., HEIJNEN, J.J.. Equilibrium modeling of extractive enzymatic hydrolysis of penicillin G with concomitant 6-aminopenicillanic acid precipitation. *Biotechnology and Bioengineering*. v., 78, n. 4, p. 395-402. 2002

DIENDER, M.B., STRAATHOF, A.J.J., VAN DER DOES, T., ZOMERDIJK, M., HEIJNEN, J.J.. Course of pH during the formation of amoxicillin by a suspension-to-suspension reaction. *Enzyme Microb. Technol.* v.27, p. 576. 2000.

DIENDER, M.B.. *New process concepts for the enzymatic synthesis of amoxicillin from penicillin G*. 2001. 128 p. Tese (Doutorado em Engenharia Química) – Department of Biotechnology Delft University of Technology, Delft. Holanda.

FERREIRA, A.L.O., GONÇALVES, L.R.B., GIORDANO, R.C., GIORDANO, R.L.C.. A simplified kinetic model for the side reactions occurring during the enzymatic synthesis of ampicillin. *Brazilian Journal of Chemical Engineering*. v. 17, n. 4-7, p. 835-839, 2000.

FERREIRA, J.S.; STRAATHOF, A.J.J.; FRANCO, T.T.; VAN DER WIELEN, L.A.M. Activity and stability of immobilized penicillin amidase at low pH values. *Journal of Molecular Catalysis B - Enzymatic*. v. 27, p. 29-35, 2004.

GONÇALVES, L.R.B., FERNADEZ-LAFUENTE, R., GUISAN, J.M., GIORDANO, R.L.C., GIORDANO, R.C.. Inhibitory effects in the side reactions occurring during the enzymic synthesis of amoxicillin: p-hydroxyphenylglycine methyl ester and amoxicillin hydrolysis. *Biotechnology and Applied Biochemistry*. v. 38, p. 77-85. 2003.

HERSBACH, G.J.M., VAN DER BEEK, C.P., VAN DIJCK, P.W.M.. The penicillins: properties, biosynthesis and fermentation. In: E.J. Vandamme, editor. *Biotechnology of Industrial Antibiotics*. New York: Marcel Dekker, Inc. p. 45-140, 1984.

- JANSSEN, M.H.A., VAN LANGEN, L.M., PEREIRA, S.R.M., VAN RANTWIJK, F., SHELDON, R.A.. Evaluation of the performance of immobilized penicillin G acylase using active-site titration. *Biotechnology and Bioengineering*. v. 78, n. 4, p. 425-432, 2002.
- KIRK, O., BORCHERT, T.V., FUGLSANG, C.C.. Industrial enzyme applications. *Current Opin in Biotechnology*. v. 13, p. 345-351, 2002.
- LILLY, M.D.. Two-liquid phase biocatalytic reactions. *Journal of Chemical Technology and Biotechnology*. v. 32, p. 162-169, 1982.
- LILLY, M.D.. The development of biochemical engineering science in Europe. *Journal of Biotechnology*. v. 59, p. 11-18. 1999.
- MARTINEK, K., SEMENOV, A.N.. Enzymatic synthesis in biphasic aqueous-organic systems II. Shift of ionic equilibria. *Biochimica et Biophysica Acta*. v. 658, p. 90-101. 1981.
- MULLIN, J.W.. *Crystallization*. 3rd Edition. Butterworth Heinmann. 527 p. 1993.
- MWANGI, S.M.. *Reactive Precipitation of 6-Aminopenicillanic Acid: Application of a Crystallization Methodology*. PhD Thesis. Department of Chemical Engineering. University of Manchester Institute of Science and Technology. 262 p. 1994.
- OTTENS, M., LEBRETON, B., ZOMERDIJK, M., RIJKERS, M.P.W.M., BRUISMA, O.S.L., VAN DER WIELEN, L.A.M.. Impurity effects on the crystallization kinetics of ampicillin. *Submitted IECR 2004*.
- PRASAD, K.V.R., RISTIC, R.I., SHEEN, D.B., SHERWOD, J.N.. Crystallization of paracetamol from solution in the presence and absence of impurity. *International Journal of Pharmaceutics*. v. 215, p. 29-44. 2001.
- RANDOLPH, A.D.; LARSON, M.A.. *Theory of Particulate Processes: Analysis and Techniques for Continuous Crystallization*. Academic Press: New York. 251 p. 1971.

- SMIJEWSKI JR, M.J., BRIGGS, B.S., THOMPSON, A.R., WRIGHT, I.G.. Enantioselective acylation of a beta-lactam intermediate in the synthesis of loracarbef using penicillin G amidase. *Tetrahedron Lett.* v. 32, p. 1621. 1991.
- SODHI, G.S., BAJAJ, R.K., KAUSHIK, N.K.. Semi-synthetic antibiotics: organometallic derivatives of 6-amino penicillin acid. *Inorganic Chimica Acta.* v.92, n. 3, L27-L28, 1984.
- TAVARE, N.S.. *Industrial Crystallization: Process Simulation analysis and Design.* The Plenum Chemical Engineering Series, Plenum Press: New York. 1995.
- TEWARI, Y.B., GOLBERG, R.N.. Thermodynamics of the conversion of penicillin G to phenylacetic acid e 6-aminopenicillanic acid. *Biophysics Chemistry.* v. 29, p. 245-252. 1988.
- TOPGI, R.S., NG, J.S., LANDIS, B., WANG, P., BEHLING, J.R.. Use of enzyme penicillin acylase in selective amidation/amide hydrolysis to resolve ethyl 3-amino-4-pentynoate isomers. *Bioorg. Medic. Chem.* v. 7, p. 22221. 1999.
- TRAVASCIO, P., ZITO, E., DE MAIO, A., SCHRÖEN, C.G.P.H., DURANTE, D., DE LUCA, P., BENCIVENGA, U., MITA, D.G.. Advantages of using non-isothermal bioreactors for the enzymatic synthesis of antibiotics: the penicillin G acylase as enzyme model. *Biotechnology and Bioengineering.* v. 79, n. 3, p. 334-346, 2002.
- VAN DE SANDT, E.J.A.X.; DE VROOM, E.. Innovations in cephalosporin and penicillin production: painting the antibiotics industry green. *Chimica Oggi/Chemistry Today.* v. 18, p. 72-75, 2000.
- VAN DER WIELEN, L. A. M., OTTENS, M., STRAATHOF, A. J. J.. Process technology and process integration in the preparation of penicillins. In: A. Bruggink Synthesis of β -lactam antibiotics. *Chemistry, biocatalysis and process integration.* Dordrecht: Kluwer Academic Publishers. 2001. p. 150.

VAN DER WIELEN, L.A.M, DIEPEN, P.J., HOUWERS, J., LUYBEN, K.C.A. M. A countercurrent adsorptive reactor for acidifying bioconversions. *Chemical Engineering Science*. v. 51, n. 10, p. 2315-2325, 1996.

VAN DER WIELEN, L.A.M., RUDOLPH, S.J.G.. On the generalization of thermodynamics properties for selection of bioseparation processes. *Journal of Chemical and Biochemical Technology*. v. 74, n. 3, p. 275-283, 1999.

YOUSHKO, M.I., VAN LANGEN, L.M., DE VROOM, E., VAN RANTWIJK, F., SHELDON, R.A., ŠVEDAS, V.K.. Highly efficiently synthesis of ampicillin in an "aqueous solution-precipitate" system: repetitive addition of substrates in a semi-continuous process. *Biotechnol. Bioeng.* v. 73, p. 426. 2001.

CAPÍTULO III

A apresentação deste capítulo corresponde ao artigo publicado:

J.S. Ferreira; A.J.J. Straathof; L.A.M. van der Wielen; T.T. Franco. Activity and stability of immobilized penicillin amidase at low pH values. *Journal of Molecular Catalysis B - Enzymatic*. v. 27, p. 29-35, 2004.

Este capítulo corresponde à avaliação da atividade e estabilidade da penicilina amidase (Assemblase®) em condições de baixo pH e soluções tamponadas saturadas com acetato de butila. As análises foram realizadas a baixos valores de pH, em sistemas tampões de fosfato de potássio saturados com acetato de butila e foram utilizados dois métodos para a determinação de atividade e estabilidade da enzima: titulométrico e análise de concentração por HPLC. Além disso, parâmetros da cinética de degradação de PenG e APA também foram determinados.

O método titulométrico se mostrou mais econômico e prático do que as análises de HPLC. No entanto, sua aplicação não é recomendada para pH 4.5 – 5.0, devido a baixa precisão nesta faixa. A máxima atividade enzimática compreendeu a faixa de pH 8.0 – 9.0 e a enzima permaneceu estável mesmo a baixos pH's (3.0 – 6.0). Embora a atividade enzimática sofra um decréscimo de aproximadamente 80%, isto não representa empecilho para sua utilização em processos a baixos pH's, podendo ser perfeitamente viável seu emprego na hidrólise de PenG no processo contínuo bifásico água-acetato de butila.

Activity and stability of immobilized penicillin amidase at low pH values

Juliana S. Ferreira^{a, b}; Adrie J. J. Straathof^a; *Telma T. Franco^b, Luuk A. M. van der Wielen^a

^a *Department of Biotechnology, Delft University of Technology, Julianalaan 67, Delft, The Netherlands*

^b *School of Chemical Engineering, State University of Campinas, P.O. Box 6066, 13081-970 Campinas, SP, Brazil*

* Corresponding address. Tel.: +31-15-278-2330
fax: +31-15-278-2355
E-mail address: a.j.j.straathof@tnw.tudelft.nl

ABSTRACT

Penicillin amidase is being used widely in the production of semi-synthetic β -lactam antibiotics. Usually processes are at pH 7 to 8, but for many new applications the range of pH 3 to 6 is of interest too. Therefore we studied the activity of penicillin amidase at 25° C in potassium phosphate buffer of pH 3.7 to 9, as well as its stability in potassium phosphate buffer of pH 3 to 6. At each pH the enzyme was stable during at least 32 days. On the other hand, immobilized penicillin amidase incubated in butyl acetate lost its stability, showing after 32 days a decrease of 52% in relation to its initial enzymatic activity value. In phosphate buffer, the enzyme showed the highest activity at pH 8 to 9. A gradual decrease to about 20% of this activity occurred when the pH was decreased to 3.7. At even lower pH the enzyme activity could not be determined with the assay that was used due to a very low stability of penicillin G (PenG). The course of penicillin G conversion and 6-aminopenicillanic acid (APA) production, during enzymatic hydrolysis at pH 4, could be quantitatively described by a simple model when the thermodynamic equilibrium of the hydrolysis was taken into account.

Keywords: penicillin amidase; immobilized enzyme; two-phase reaction; penicillin G hydrolysis; pH optimization.

1. Introduction

Enzymes are extensively used in the food, pharmaceutical and chemical industries, as well for analytical purposes. One particularly important enzyme is penicillin amidase (E.C. 3.5.1.11) (Arroyo *et al.*, 2003; Fernández-Lafuente *et al.*, 2003). Enzymatic hydrolysis of penicillins to 6-aminopenicillanic acid (APA) and phenylacetic acid (PAA) by penicillin amidases is used widely in industry. Therefore, much research has been devoted to the study of the kinetics of hydrolysis of penicillin G (PenG) by penicillin amidase as a function of the concentration of substrate and products, pH, temperature, buffer type and concentration, and cosolvent type and concentration (Danzig *et al.*, 1993; Illanes *et al.*, 1996; Azevedo *et al.*, 1999; Erarslan and Güray, 1991; Diender *et al.*, 1998). Most of these works focus on pH 7 to 8, the optimum range for PenG hydrolysis in purely aqueous systems and do not provide systematic studies at lower pH.

Novel reactor configurations are being investigated for enzyme conversions, to enhance their yield and rate, which is in many cases low or even too low for feasible processes. In particular, integrated reactor-separator systems allowing for in situ product removal (ISPR) offer potential improvements, i.e., two-phase reactors (Van Sonsbeek *et al.*, 1993). These systems are tuned at high volumetric capacity and will hence operate under extreme conditions, relative to the 'normal' physiological operation of enzymes (Fernández-Lafuente *et al.*, 1996).

The biphasic system allows the separation of both reaction products due to extraction of PAA to the organic phase and precipitation of APA (Van der Wielen *et al.*, 2001; Chilov and Švedas, 2002). Nevertheless, in a two-phase system, a pH increase above pH 4.4 hampers extraction of phenylacetic acid into organic phase, prevents APA precipitation, and in contrast to the homogeneous reaction, does not improve hydrolysis (Den Hollander *et al.*, 2002).

For penicillin hydrolysis a counter-current multi-stage reactor without pH control is being developed (Diender *et al.*, 2002). In this reactor the pH drops to values as low as 3, depending on the progress of the reaction and concentration of substrate. Therefore it is worthwhile to study enzyme stability and activity under these extreme conditions including pH range 3 to 4. Furthermore, a relatively low pH has been used for many synthesis reactions catalyzed by penicillin amidase for which commercial processes are under development (Smijewski *et al.*, 1991; Diender *et al.*, 2000; Topgi *et al.*, 1999; Schröen *et al.*, 1999; Nierstrasz *et al.*, 1999; Youshko *et al.*, 2001). Such as the syntheses of loracarbef at pH 6, amoxicillin at pH 5.5 – 7, xemilofiban intermediate at pH 5.25 – 6.25, cefamandole at pH 4.25 and ampicillin at pH 6.3. A pH below 5 is believed to have a detrimental effect on penicillin amidase stability and activity (Schröen *et al.*, 1999; Nierstrasz *et al.*).

For an evaluation of enzymatic hydrolysis of PenG at low pH, the stability of PenG and the main product, APA, have to be evaluated. Phenylacetic acid is known to be stable. Penicillin G is unstable in aqueous solution at acid or alkaline conditions (Arnott and Weatherley, 1995; Reschke and Schürigel, 1984; Benedict *et al.*, 1945; Llinás *et al.*, 1998 and 2001; Levine, 1961; Kheirloomoom *et al.*, 1999; Kim and Lee, 1996; Illanes and Fajardo, 2001) and the half-life time may change if the aqueous phase becomes saturated by butyl acetate (Reschke and Schürigel, 1984). The decomposition kinetics is 1st order with maximum stability about pH 6 and the degradation rate of penicillin is much higher at a low pH than at a high pH. There is not much information about degradation of APA in the literature. Studying APA degradation in the pH and temperature ranges of 5.8-6.6 and 35-90° C, respectively, Dennen (1967) showed that the degradation follows pseudo-first order kinetics. At higher pH, higher orders of degradation rates were determined. Furthermore, the author found in all temperature ranges the highest stability at approximately pH 8.

In this work we will only consider a temperature of 25° C, which is used for countercurrent reactor development (Chilov and Švedas, 2002; Diender *et al.*, 2002). In the countercurrent reactor the aqueous phase will be saturated with butyl acetate, and the influence of this solvent will be studied as well.

2. Material and methods

2.1. Materials

Potassium di-hydrogen phosphate (anhydrous extra pure), di-potassium hydrogen phosphate, 85% ortho-phosphoric acid, potassium hydroxide pellets, butyl acetate (BuAc) and acetonitrile were purchased from Merck (Darmstadt, Germany). Phenylacetic acid (PAA) was purchased from Fluka Chemika (Steinheim, Switzerland). All reagents were of analytical grade. Penicillin G potassium salt (PenGK), 6-aminopenicillanic acid (APA) and Assemblase[®] were kindly provided by DSM, Delft, The Netherlands. Assemblase[®] is an immobilized penicillin G amidase from *Escherichia coli*, an in-house enzyme of DSM anti-infectives. The enzyme is supplied in a propylene glycol-water solution. The enzyme was washed with Milli-Q water prior to use and filtered to dryness.

2.2. Standard enzyme assay

The standard assay was performed at pH 8.0 in a magnetically stirred glass reactor, at 25° C. PenGK salt (1.00 g) was dissolved in 50 mL potassium phosphate buffer (40 mM) saturated with butyl acetate (BuAc). The reaction was started by the addition of 450 – 500 mg of enzyme. The pH was kept constant, using 0.250 M KOH in a digital burette.

During the initial part of the reaction (5 min), the burette reading was recorded. At pH 8.0, the number of the moles of KOH addition corresponds to the number of moles of PenG (n_{PenG}) converted into APA and PAA. These assays were carried out in duplicate. The initial reaction rate was determined from linear regression of time-course profile and the enzyme activity (A) was calculated from:

$$A = \frac{(n_{\text{PenG0}} - n_{\text{PenG}})}{m_{\text{enz}} \times \text{time}} \quad (1)$$

2.3. Degradation of penicillin G and 6-aminopenicillanic acid

The degradation of PenG was evaluated at pH 3.0, 3.5, 4.0 and 4.5, in a magnetically stirred glass reactor at 25° C. PenGK salt (1.00 g) was dissolved in 50 mL potassium buffer (40 mM) saturated with BuAc. The pH was controlled using a pH stat system with H₃PO₄ (40 mM) as titrant. To prevent significant dilution the pH control procedure was preceded by a pH adjustment with some drops of H₃PO₄ (85%) for pH 3.0, H₃PO₄ (0.5 M) for pH 3.5 and H₃PO₄ (0.1 M) for pH 4.5 and 4.0.

Samples were withdrawn, filtered (Millex by Millipore, 0.45 µm pore size), and added to Eppendorf tubes filled with 1.5 mL of cold (4° C) KOH solution, in a way to adjust the pH of the sample to approximately 6.5 - 7.5. The samples were analyzed for PenG in duplicate by HPLC.

For the degradation of APA, experiments were carried out at pH 3.5, 4.0, 4.5 and 5.0 in similar procedure. However, after samples were withdrawn and filtered, 1 mL was diluted into 25 mL before HPLC analysis for APA.

2.4. Influence of pH on enzyme activity

Reactions at pH 4.0, 4.5, 5.0, 6.0, 7.0, 8.0 and 9.0 were carried out to determine the enzyme activity. The standard assays were allowed to take place in 40 mM potassium phosphate buffers saturated with BuAc. The buffers were prepared by mixing different volumes of aqueous solutions of K₂HPO₄, KH₂PO₄ and H₃PO₄. The titration solutions were

KOH (0.25 M) for pH 5.0, 6.0, 7.0, 8.0 and 9.0 and H₃PO₄ (40 mM) for pH 4.0 and 4.5. Especially for 4.0, and 4.5, the pH of the reaction medium had to be corrected with H₃PO₄ solution (0.1 M) right after adding PenGK salt, since the pH increased as soon as PenGK was added.

At pH values below 7.0, the number of moles of acid or base added in the titration method does not correspond to the number of moles of PenGK transformed in products. The dissociation state of the reactants should be taken into account. As the pH decreases the fractions of the negative forms decrease ($F_{\text{PenGminus}}$, F_{PAAminus} and F_{APAminus}) while fractions of the positive (F_{APAplus}), zwitterionic ($F_{\text{APAminus/plus}}$) or uncharged ($F_{\text{PenGuncharged}}$, $F_{\text{PAAuncharged}}$ and $F_{\text{APAuncharged}}$) forms start to be produced (Chilov and Švedas, 2002). Therefore, at low pH the reaction is not acidifying anymore but producing base. The net charged fractions of each component are shown in Figure 1.

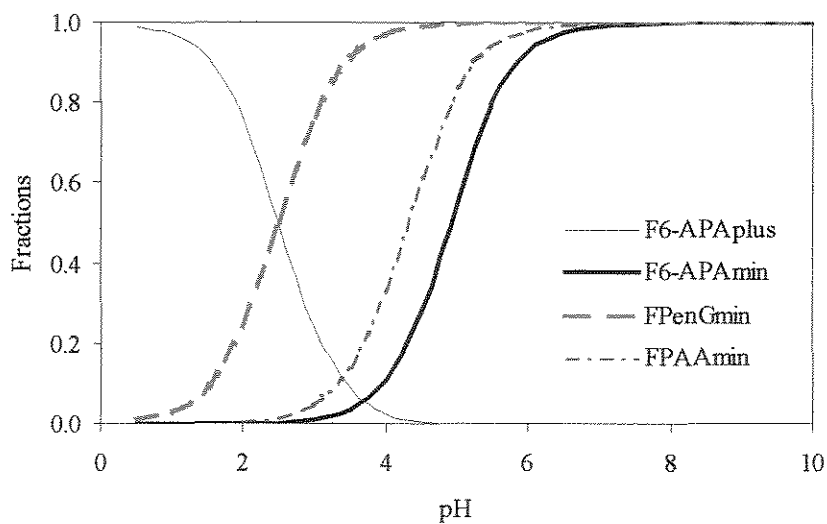


Figure 1: Fraction of the charged species of the reactants as part of each reactant's total concentration. Calculation performed with the dissociation constants in Diender *et al.* (2000).

For these species, the charged amounts are related to the overall amounts as follows:

$$n_{\text{APAplus}} = F_{\text{APAplus}} \times n_{\text{APA}} \quad (2)$$

$$n_{\text{APAminus}} = F_{\text{APAminus}} \times n_{\text{APA}} \quad (3)$$

$$n_{\text{PenGminus}} = F_{\text{PenGminus}} \times n_{\text{PenG}} \quad (4)$$

$$n_{\text{PAAminus}} = F_{\text{PAAminus}} \times n_{\text{PAA}} \quad (5)$$

These charged amounts can be substituted in the charge balance:

$$n_{\text{Kplus}} + n_{\text{APAplus}} + n_{\text{Hplus}} = n_{\text{H2PO4minus}} + 2 \times n_{\text{HPO4minus2}} + n_{\text{PenGminus}} + n_{\text{APAminus}} + n_{\text{PAAminus}} + n_{\text{OHminus}} \quad (6)$$

After eliminating n_{APA} and n_{PAA} using the stoichiometric balances,

$$n_{\text{PenG0}} = n_{\text{PenG}} + n_{\text{APA}} = n_{\text{PenG}} + n_{\text{PAA}} \quad (7)$$

Equation 8 is obtained.

$$n_{\text{PenG}} = \frac{-n_{\text{Kplus}} + (-F_{\text{APAplus}} + F_{\text{APAminus}} + F_{\text{PAAminus}}) \times n_{\text{PenG0}} - n_{\text{Hplus}} + n_{\text{H2PO4minus}} + 2 \times n_{\text{HPO4minus2}} + n_{\text{OHminus}}}{-F_{\text{APAplus}} - F_{\text{PenGminus}} + F_{\text{APAminus}} + F_{\text{PAAminus}}} \quad (8)$$

knowing the values of the added amounts of potassium, phosphate and penicillin, the activity can be calculated.

Besides the recording of the burette reading, in one of the duplicate series of experiments, four to six samples (500 μL) were withdrawn from the reaction mixture after the start of the reaction with 1 minute intervals and filtered (Millex by Millipore, 0.45 μm pore size) to remove the enzyme and stop the reaction. As the reaction occurred, APA and PAA were formed and they were detected by HPLC. The initial reaction rate was determined based on the amount of APA produced. For the assays at pH 4.0 and 4.5, the

filtrate was collected in Eppendorf tubes filled with 1.5 mL of cold (4° C) KOH, in order to correct the pH to 6.5 – 7.5 and avoid decomposition of the compounds.

2.5. Influence of pH on enzyme stability

Potassium phosphate buffer (40 mM) at pH 3.0, 4.0, 5.0 and 6.0, was mixed with BuAc. The saturated phases were separated with a separation funnel. After washing with water and filtration to dryness, the enzyme (450 – 500 mg) was incubated in 1 mL of five different solutions, namely the four potassium phosphate buffers of pH 3.0, 4.0, 5.0 and 6.0 saturated with BuAc and with BuAc solution saturated with potassium phosphate buffer of pH 6.0. The incubation was performed in closed Eppendorf tubes at 25° C, for different intervals. After this interval, the remaining activity was measured. The content of the Eppendorf tube was transferred to the reaction vessel, mixed with 49 mL of potassium phosphate buffer of pH 8.0 saturated with BuAc, and the standard enzyme assay was performed.

2.6. HPLC analysis

The samples were analyzed by HPLC (Waters), using a C18 - Delta Pak column (particle size - 5 µm, Pore size - 300 Å, column size – 3.9 X 150 mm), and C18 – Platinum EPS column (particle size - 5 µm, Pore size - 100 Å, column size – 4.6 X 250 mm), and UV detector. The mobile phase was 28:72 (v/v) of acetonitrile and 0.64 g L⁻¹ KH₂PO₄ aqueous solution, the pH was adjusted to 2.75 with H₃PO₄. The flow was 0.7 mL min⁻¹, in the Delta Pak column and 1.0 mL min⁻¹ in the Platinum EPS column. The elution times of APA, PAA and PenG were 2.2, 5.3 and 9.0 min, respectively, when analyzed in the Delta Pak column and 3.3 min, 7.7 min and 13.9 min in the Platinum EPS column.

3. Results and discussion

3.1. Influence of pH on degradation of penicillin G and 6-aminopenicillanic acid

During enzymatic activity assays at low pH the chromatograms showed peaks not identified as APA, PAA or PenG, indicating that spontaneous degradation of some of the reactants occurred. Therefore, this background of degradation of PenG and APA was investigated.

At pH 4.5 in the absence of enzyme, there was no degradation of PenG within 5 min of reaction, the duration of the enzymatic assay. However, a peak with retention time of 4.8 – 5.0 min was present in the chromatograms of pH 3.0 - 4.0. No APA or PAA was formed.

Logarithmic plots of PenG concentration against time were linear for both pH values indicating first order degradation. The degradation rate constants were determined from the slope of these graphs. The values of the degradation rate constants (see Table 1) correspond to half-life times of 21 min, 210 min and 780 min at pH 3.0, 3.5 and 4.0, respectively. Table 1 also presents the data reported in the literature. The results are within a wide range of values, probably due to the different methods employed to determine the concentration of PenG, such as colorimetric, NMR, and HPLC. We assume that the HPLC method used by us is the most accurate method. According to the last two data in Table 1, butyl acetate does not influence the PenG degradation.

Table 1: Values of degradation rate constant of PenG in aqueous solution.

pH	T ($^{\circ}\text{C}$)	k_d (h^{-1})	$t_{\text{half-life}}$ (h)	Reference
3.0	25	1.932	0.35	This work*
3.0	25	1.002	0.68	Kheirilomoom <i>et al.</i> (1999)
3.0	35	1.140	0.60	Llinás <i>et al.</i> (1998)
3.0	24	0.294	2.33	Benedict <i>et al.</i> (1945)
3.5	25	0.198	3.50	This work*
3.5	25	0.252	2.75	Kheirilomoom <i>et al.</i> (1999)
3.5	35	0.450	1.53	Llinás <i>et al.</i> (1998)
4.0	25	0.053	13	This work*
5.0	25	0.0108	64.2	Reschke and Schürgel (1984)
5.0	25	0.0096	72.2	Reschke and Schürgel (1984)*

* aqueous solution saturated with BuAc

Degradation of APA was determined at pH 3.5, 4.0, 4.5 and 5.0 and it turned out to be much slower than degradation of PenG. The values of first order degradation rate constants are shown in Table 2.

Table 2: Values of degradation rate constant of APA at $T = 25^{\circ} \text{C}$.

PH	$k_d \text{ (h}^{-1}\text{)}$	$t_{\text{half-life}} \text{ (h)}$
3.5	0.0085	82
4.0	0.0058	120
4.5	0.0053	131
5.0	0.0036	192

3.2. *Influence of pH on enzyme activity*

In order to check the reliability of reaction set up, some preliminary assays were carried out in aqueous and in phosphate buffer solution (results not shown). The most reliable results were obtained with phosphate buffer solution, since the variation of pH is large in unbuffered aqueous solution and the accuracy of the results was low.

No difference was found between the data obtained from preliminary assays involving potassium phosphate buffer and from assays involving potassium phosphate buffer saturated with BuAc. This is in agreement with previous results on the influence of organic solvents on penicillin amidase (Kim and Lee, 1996; Illanes and Fajardo, 2001).

The influence of pH on penicillin amidase activity is shown in Figure 2, which presents results from both the titration method and HPLC analysis. The highest activity is about $280 \mu\text{mol g}_{\text{enz}}^{-1} \text{min}^{-1}$ and occurs in the range of pH 8.0 and 9.0. It is worth to point out that enzyme activity is still about $50 \mu\text{mol g}_{\text{enz}}^{-1} \text{min}^{-1}$ at pH 3.7. At even lower pH, the enzyme activity could not be determined due to the instability of PenG. For pH above 5.0, the data obtained from both methods were similar (Figure 2), although the HPLC results showed higher errors taking into account a 95% confidence limit. Nevertheless, the

application of the titration method is not recommended for pH's close to pK_a of APA. Like in earlier work (Diender *et al.*, 1998 and 2002; Chilov and Švedas, 2002), the value used to calculate the fraction of the Equation 3 was 4.9, however the literature also reports values from 4.6 to 5.4 (Švedas *et al.*, 1980; Tewari and Goldberg, 1988). As this value is not precisely known, an error can occur in the calculation of the APA fractions and consequently, in the determination of enzyme activity by Equation 1 and 8.

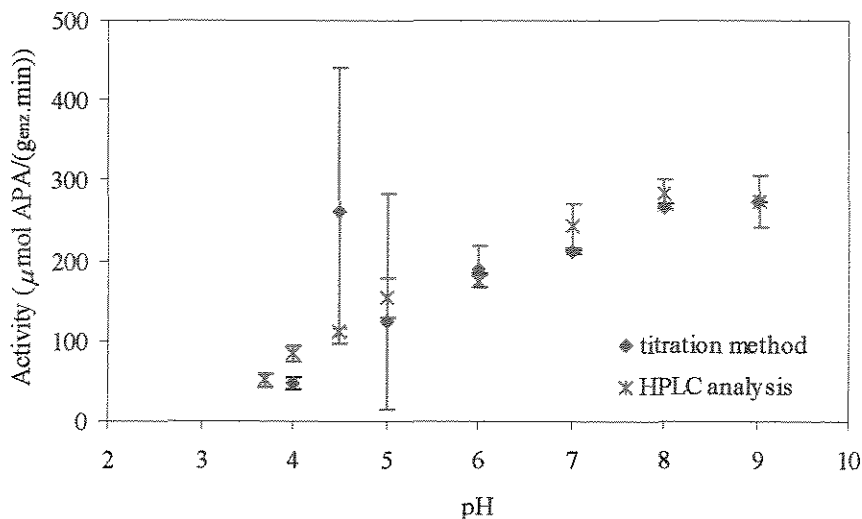


Figure 2: Enzymatic activity of penicillin amidase including 95% confidence range.

In order to determine if diffusion limitation of PenG in the immobilization matrix might have influenced the data, the efficiency was calculated. By assuming that the average diameter was 0.42 mm and the diffusion coefficient of PenG into the catalyst was $0.2 \cdot 10^{-9} \text{ m}^2 \text{ s}^{-1}$ (Van der Wielen, 1996), the characteristic time for diffusion was calculated to be 222 s. At the highest initial reaction rate, the first order reaction characteristic time was 22 min. The ratio of these values provided a Damköhler_(II) number of 0.18, which means that the efficiency was 100%. The buffer concentration was approximately equal to the reactant concentration so that pH gradients in the particles were absent (Van der Wielen, 1996).

3.3. *Stability of penicillin amidase*

Figure 3 presents the results of residual activity of penicillin amidase after incubation in phosphate buffer solution saturated with BuAc at pH's 3.0, 4.0, 5.0 and 6.0 and incubation in BuAc saturated with potassium phosphate buffer of pH 6.0. The plot shows that the enzyme remained stable in aqueous solution at each pH during at least 32 days, despite of the presence of BuAc. This provides large opportunities for developing a counter-current enzymatic hydrolysis of PenG in a two-phase system of BuAc and water (Diender *et al.*, 2002). The incubation would have to be extended or carried out under more stressing conditions to determine at which pH the enzyme would show maximum activity, but this was beyond the scope of this study. However, a 58% decrease of the enzyme activity in the standard assay at pH 8.0 ($280 \mu\text{mol g}_{\text{enz}}^{-1} \text{min}^{-1}$) occurred upon incubation in BuAc saturated with potassium phosphate buffer of pH 6.0 during 32 days corresponding to enzyme activity of $117 \mu\text{mol g}_{\text{enz}}^{-1} \text{min}^{-1}$. This may be explained by denaturation. The literature (Klibanov, 1997; Ebert *et al.*, 1998; Fernandez-Lafuente *et al.*, 1999) reports inactivation of most of the industrial enzymes (free or immobilized) when they are incubated in organic solvents with the same polarity of butyl acetate.

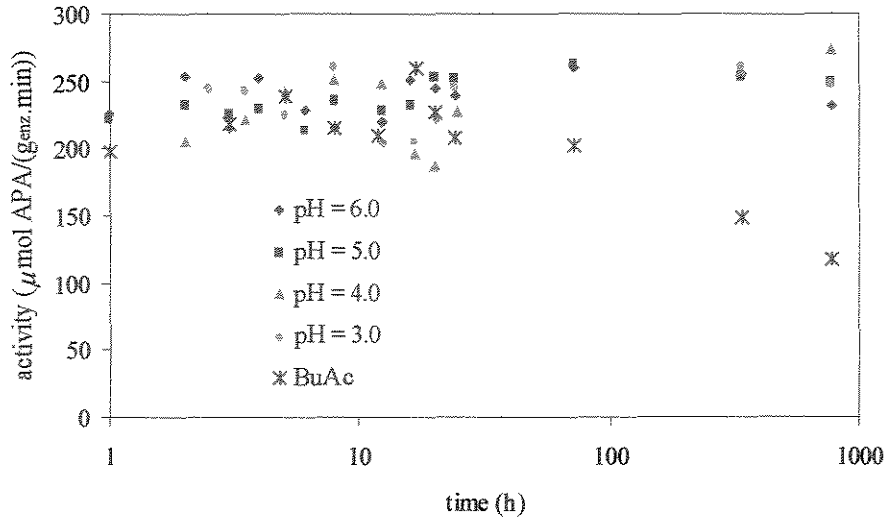


Figure 3: Stability of penicillin amidase incubated in buffer solution saturated with BuAc at pH's 3.0, 4.0, 5.0 and 6.0 and in BuAc saturated with potassium phosphate buffer for 32 days. The data were determined by titration method. Similar results were obtained by HPLC analysis.

3.4. Hydrolysis of PenG by penicillin amidase at pH 4.0

The rate equation that is obtained when considering the mechanism of the (Van der Wielen *et al.*, 1997) contains many kinetic parameters that are unknown. For simplicity, it was assumed that the substrate and product concentrations would be much lower than the Michaelis and inhibition constants. The result is Equation 9

$$r_{\text{enz}} = k_{\text{enz}} \times C_{\text{enz}} \times \left(C_{\text{PenG}} - \frac{C_{\text{PAA}} \cdot C_{\text{APA}}}{K_{\text{app}}} \right) \quad (9)$$

The apparent equilibrium constant, K_{app} , can be calculated at pH 4.0 using Equation 10

$$K_{app} = \frac{K_{eq} \times F_{PenGminus}}{F_{APAminus} \times F_{PAAminus} \times C_{Hplus}} \quad (10)$$

according to the reference reaction with equilibrium constant K_{eq} :



The value of equilibrium constant adopted was $7.35 \cdot 10^{-8} \cdot \text{mol L}^{-1}$, given by Tewari and Goldberg (1988).

Knowing the initial enzymatic reaction rate and using the degradation rate constants for PenG and APA, results obtained from a long term experiment for hydrolysis of PenG at pH 4.0 were compared with a simple model simulation in which the enzymatic reaction rate was assumed to follow Equation 9.

Figure 4 shows that the model, which contains no adjustable parameters, agrees with the experimental data that are presented in Table 3. Although the literature (Danzig *et al.*, 1993; Van der Wielen *et al.*, 1997; Duan and Chen, 1996) reports that inhibition occurs, and mainly due to PAA as a competitive inhibitor, our results show that PenG hydrolysis at pH 4.0 is limited exclusively by the thermodynamic equilibrium. After equilibration, degradation of PenG occurs, and to a smaller extent, of APA. It should be pointed out that the pH values reported in the literature were higher and the product concentration was different.

Table 3: Experimental data of PenG hydrolysis at pH 4.0 and T = 25° C.

Time (min)	C _{6-APA} (mM)	C _{PAA} (mM)	C _{PenG} (mM)
0.5	0.87	0.54	51.83
1.6	2.44	1.96	49.13
3.2	4.31	2.99	47.48
5.8	7.22	5.48	44.65
54	21.56	16.00	29.56
83	22.67	16.88	27.76
132	23.11	20.73	27.08
175	22.20	***	26.31
240	21.81	****	25.59
1186	14.74	16.34	12.75
1232	14.52	16.44	12.59
1282	13.29	14.36	11.93
1360	13.65	18.76	11.69
1541	12.98	17.33	10.62
1649	12.68	16.30	11.11
2526	10.56	16.52	8.21
2560	10.18	15.68	8.16
4309	5.55	17.50	4.32
4380	6.29	17.19	4.22
5807	5.65	22.33	0.85
5865	5.41	19.64	2.92

In Figure (4), the enzymatic reaction rapidly proceeds towards equilibrium, but degradation occurs of PenG, and to a smaller extent, of APA. This leads to a reversal of the enzymatic hydrolysis equilibrium and consequently to a decrease in PAA concentration.

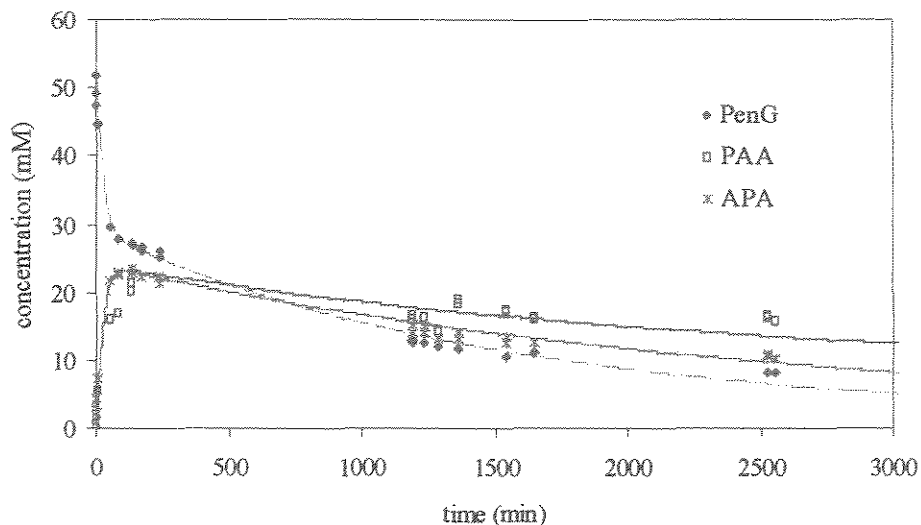


Figure 4: Hydrolysis of PenG by penicillin amidase at pH 4.0. Markers are experimental data, lines are simulations using $k_{dpenG} = 0.053 \text{ h}^{-1}$, $k_{dAPA} = 0.0058 \text{ h}^{-1}$, $k_{enz} = 1.5575 \cdot 10^{-3} \text{ L g}_{enz}^{-1} \text{ min}^{-1}$, $C_{PenG0} = 54 \text{ mM}$, $C_{enz} = 9.47 \text{ g L}^{-1}$

4. Conclusions

This work allowed the determination of the optimum pH and stability of penicillin amidase in PenG hydrolysis by a titration method as well as HPLC analysis. The data were in agreement with each other. The titration method was more economical and practical, but its application is not recommended for pH 4.5 - 5.0, because of a low accuracy in this range. The enzyme presented maximum activity in the pH range 8.0 - 9.0. In contrast to the common belief, penicillin amidase does not show decreased stability if the pH is decreased from 8.0 to 3.0. Although the enzyme activity decreased by about 80%, this does not

confine processes to high pH values. The major limitation at low pH seems to be the low chemical stability of PenG and, to a less extent, of APA. Based on this information, conditions can be found that will be suitable for the hydrolysis of PenG in a butyl acetate – water continuous process.

Acknowledgements

The authors gratefully acknowledge Brazilian government (CNPq and CAPES), for the financial support and DSM – Delft, The Netherlands for donating the enzyme and reactants.

Nomenclature

A = enzyme activity ($\mu\text{mol g}_{\text{enz}}^{-1} \text{min}^{-1}$)

C = concentration of PenG (mM)

C_{enz} = concentration of enzyme (g L^{-1})

F = fraction of the specie

K_{app} = apparent equilibrium constant (mol L^{-1})

k_{d} = degradation rate constant (h^{-1})

k_{enz} = enzymatic rate constant ($\text{L g}^{-1} \text{min}^{-1}$)

K_{eq} = equilibrium constant (mol L^{-1})

m_{enz} = mass of enzyme (g)

n = amount (mol)

r_{enz} = enzymatic reaction rate ($\text{mol L}^{-1} \text{min}^{-1}$)

T = temperature ($^{\circ}\text{C}$)

$t_{\text{half-time}}$ = half-life time (h)

Subscripts

0 = initial situation

APA = 6-aminopenicillanic acid

minus = negative state of ionization

minus/plus = zwitterionic state of ionization

PAA = phenylacetic acid

PenG = penicillin G

plus = positive state of ionization

uncharged = neutral state of ionization

References

- ARNOTT, I.A.; WEATHERLEY, L.R.. The stability of penicillin G during recovery by electrically enhanced extraction. *Proc. Biochem.* 30 (1995) 447.
- ARROYO, M.; DE LA MATA, I.; ACEBAL, C.; CASTILLÓN, M. P.. Biotechnological applications of penicillin acylases: state-of-the-art. *Appl Microbiol Biotechnol.* 60 (2003) 507.
- AZEVEDO, A.M.; FONSECA, L.P.; PRAZERES, D.M.F.. Stability and stabilisation of penicillin acylase. *J. Chem. Technol. Biotechnol.* 74 (1999) 1110.
- BENEDICT, R.G.; SCHMIDT, W. H.; COGHILL, R.D.; OLESON; A.P.. Penicillin. III. The stability of penicillin in aqueous solution. *J. Bacteriol.* 49 (1945) 85.
- CHILOV, G. G.; ŠVEDAS, V.. Enzymatic hydrolysis of β -lactam antibiotics at low pH in a two-phase "aqueous solution-water-immiscible organic solvent" system. *Can. J. Chem.* 80 (2002) 699.
- DANZIG, J.; TISCHER, W.; WANDREY, C.. Bioreaction engineering for improved 6-APA production. *Indian J. Chem.* 32B (1993) 40.
- DEN HOLLANDER, J.L.; ZOMERDIJK, M.; STRAATHOF, A.J.J.; VAN DER WIELEN, L.A.M.. Continuous enzymatic penicillin G hydrolysis in countercurrent water-butyl acetate biphasic systems. *Chem. Eng. Sci.* 57 (2002) 1591.
- DENNEN, D.W.. Degradation kinetics of 6-aminopenicillanic acid. *J. Pharm. Sci.* 56 (1967) 1273.
- DIENDER, M.B.; STRAATHOF A.J.J.; HEIJNEN, J.J.. Predicting enzyme catalyzed reaction equilibria in cosolvent-water mixtures as a function of pH and solvent composition. *Biocat. Biotransform.* 16 (1998) 275.

DIENDER, M.B.; STRAATHOF, A.J.J.; VAN DER DOES, T.; RAS, C.; HEIJNEN, J.J.. Equilibrium modelling of extractive enzymatic hydrolysis of penicillin G with concomitant 6-aminopenicillanic acid crystallization. *Biotechnol. Bioeng.* 78 (2002) 395.

DIENDER, M.B.; STRAATHOF, A.J.J.; VAN DER DOES, T.; ZOMERDIJK, M.; HEIJNEN, J.J.. Course of pH during the formation of amoxicillin by a suspension-to-suspension reaction. *Enzyme Microb. Technol.* 27 (2000) 576.

DUAN, G.; CHEN, J.Y.. Kinetics analysis of the effects of products removal on the hydrolysis of penicillin G by immobilised penicillin acylase. *Proc. Biochem.* 31 (1996) 27.

EBERT, C.; GARDOSSI, L.; LINDA, P.. Activity of immobilised penicillin amidase in toluene at controlled water activity. *J. Mol. Catal. B: Enzym.* 5 (1998) 241.

ERARSLAN, A.; GÜRAY, A.. Kinetic investigation of penicillin acylase from a mutant strain of *Escherichia coli* ATCC 11105 immobilised on oxirane-acrylic beads. *J. Chem. Tech. Biotechnol.* 51 (1991) 181.

FERNANDEZ-LAFUENTE, R.; ROSELL, C.M.; CAANAN-HADEN, L.; RODES, L.; GUISÁN, J.M.. Facile synthesis of artificial enzyme nano-environments via solid-phase chemistry of immobilized derivatives: Dramatic stabilization of penicillin acylase versus organic solvents. *Enzyme Microb. Technol.* 24 (1999) 96.

FERNÁNDEZ-LAFUENTE, R.; ROSELL, C. M.; PIATKOWSKA, B.; GUISÁN, J. M.. Synthesis of antibiotics (cephaloglycin) catalyzed by penicillin G acylase: Evaluation and optimization of different synthetic approaches. *Enzyme Microb. Technol.* 19 (1996) 9.

ILLANES, A.; ALTAMIRANO, C.; ZÚÑIGA, M.E.. Thermal inactivation of immobilised penicillin acylase in the presence of substrate and products. *Biotechnol. Bioeng.* 50 (1996) 609.

ILLANES, A.; FAJARDO, A.. Kinetically controlled synthesis of ampicillin with immobilized penicillin acylase in the presence of organic cosolvents. *J. Mol. Catal. B: Enzym.* 11 (2001) 587.

KHEIROLOMOOM, A.; KAZEMI-VAYSARI, A.; ARDJMAND, M.; BARADAR-KHOSHFETRAT, A.. The combined effects of pH and temperature on penicillin G decomposition and its stability modelling. *Proc. Biochem.* 35 (1999) 205.

KIM, M.G.; LEE, S.B.. Penicillin acylase-catalyzed synthesis of pivampicillin: Effect of reaction variables and organic cosolvents. *J. Mol. Catal. B: Enzym.* 1 (1996) 71

KLIBANOV, A.M.. Why are enzymes less active in organic solvents than in water? *Trends Biotechnol.* 15 (1997) 97.

LEVINE, B. B.. Studies on the formation of the penicillin antigen. II. Some reactions of D-benzylpenicillenic acid in aqueous solution at pH 7.5. *Arch. Biochem. Biophys.* 93 (1961) 50.

LLINÁS, A.; VILANOVA, B.; FRAU, J.; MUÑOZ, F.; DONOSO, J.; PAGE, M.I.. Chemical reactivity of penicillins and cephalosporins. Intramolecular involvement of the acyl-amido side chain. *J. Org. Chem.* 63 (1998) 9052.

LLINÁS, A.; VILANOVA, B.; MUÑOZ, F.; DONOSO, J.. The role of a β -proton transfer donor in the degradation of benzylpenicillin. *J. Mol. Catal. A: Chem.* 175 (2001) 3.

NIERSTRASZ, V.A.; SCHRÖEN, C.G.P.H.; BOSMA, R.; KROON, P.J.; BEEFTINK, H.H.; JANSSEN, A.E.M.; TRAMPER, J.. Thermodynamically controlled synthesis of cefamandole. *Biocatal. Biotransform.* 17 (1999) 209.

RESCHKE, M.; SCHÜGERL, K.. Reactive extraction of penicillin I: Stability of penicillin G in the presence of carriers and relationships for distribution coefficients and degrees of extraction. *Chem. Eng. J.* 28 (1984) B1.

SCHRÖEN, C. G. P. H.; NIERSTRASZ, V. A.; KROON, P. J.; BOSMA, R.; JANSSEN, A. E. M.; BEEFTINK, H. H.; TRAMPER, J.. Thermodynamically controlled synthesis of β -lactam antibiotics. Equilibrium concentrations and side-chain properties. *Enzyme Microb. Technol.* 24 (1999) 498.

SMIJEWSKI, JR, M.J.; BRIGGS, B.S.; THOMPSON, A.R.; WRIGHT, I.G.. Enantioselective acylation of a beta-lactam intermediate in the synthesis of loracarbef using penicillin G amidase. *Tetrahedron Lett.* 32 (1991) 1621.

ŠVEDAS, V.K.; MARGOLIN, A.L.; BEREZIN, I.V.. Enzymatic synthesis of β -lactam antibiotics: a thermodynamic background. *Enzyme Microb. Technol.* 2 (1980) 138.

TEWARI, Y.B.; GOLDBERG, R.N.. Thermodynamics of the conversion of penicillin G to phenylacetic acid and 6-aminopenicillanic acid. *Biophys. Chem.* 29 (1988) 245.

TOPGI, R.S.; NG, J.S.; LANDIS, B.; WANG, P.; BEHLING, J.R.. Use of enzyme penicillin acylase in selective amidation/amide hydrolysis to resolve ethyl 3-amino-4-pentynoate isomers. *Bioorg. Medic. Chem.* 7 (1999) 2221.

VAN DER WIELEN, L. A. M.; OTTENS, M.; STRAATHOF, A. J. J.. Process technology and process integration in the preparation of penicillins. In: A. Bruggink (Ed.), Synthesis of β -lactam antibiotics. Chemistry, biocatalysis and process integration. Kluwer Academic Publishers. Dordrecht, 2001. p. 150.

VAN DER WIELEN, L.A.M.. A countercurrent adsorptive fluidized bed reactor for heterogeneous bioconversions. Ph.D. Thesis, Delft University of Technology, Delft, The Netherlands (1996).

VAN DER WIELEN, L.A.M.; BUEL, M.J.; STRAATHOF, A.J.J.; LUYBEN, K.CH.A.M.. Modeling of the enzymatic deacylation of Penicillin G: equilibrium and kinetic considerations. *Biocatal. Biotransform.* 15, (1997) 121.

VAN SONSBEEK, H.M.; BEEFTINK, H.H.; TRAMPER, J.. Two-liquid phase bioreactors. *Enzyme Microb. Technol.* 15 (1993) 722.

YOUSKO, M.I.; VAN LANGEN, L.M.; DE VROOM, E.; VAN RANTWIJK, F.; SHELDON, R.A.; ŠVEDAS, V.K.. Highly efficiently synthesis of ampicillin in an "aqueous solution-precipitate" system: repetitive addition of substrates in a semi-continuous process. *Biotechnol. Bioeng.* 73 (2001) 426.

CAPÍTULO IV

A avaliação da cristalização do APA é descrita no Capítulo IV.

A determinação dos parâmetros cinéticos da cristalização de APA é fundamental para dar continuidade ao estudo de implantação de um reator multi-estágio e contracorrente, destinado à hidrólise de PenG em sistema bifásico água e acetato de butila. Os ensaios foram realizados em batelada, a pH 4 e 5 e na presença de impurezas (BuAc, PenG e PAA). As análises foram baseadas na avaliação da análise de tempo de indução, taxa de supersaturação, taxa de crescimento e distribuição do tamanho de cristais, possibilitando uma análise da influência das impurezas na cristalização do APA. Os resultados mostraram que as impurezas não exerceram efeito sobre a cristalização de APA, na faixa de pH e de concentrações avaliadas.

Este trabalho possibilitou a obtenção de um modelo que pode prever as taxas de cristalização de APA nas mesmas condições que serão empregadas na hidrólise de PenG em reator multi-estágio e bifásico, água e acetato de butila.

Crystallization Kinetics of 6-Aminopenicillanic Acid

Juliana S. Ferreira^{a, b}, Xiaonan Li^a, Adrie J. J. Straathof^{a, *}, M. Ottens^a, Telma T. Franco^b,
Luuk A. M. van der Wielen^a

^a *Department of Biotechnology, Delft University of Technology, Julianalaan 6, Delft, The Netherlands*

^b *School of Chemical Engineering, State University of Campinas. P.O. Box 6066, 13081-970 Campinas. SP, Brazil*

* Corresponding address. Tel.: +31-15-278-2330
fax: +31-15-278-2355
E-mail address: a.j.j.straathof@tnw.tudelft.nl

ABSTRACT

The semi-synthetic penicillins, derived from 6-aminopenicillanic acid (APA), constitute an important group of antibiotics. APA is produced by Penicillin G (PenG) hydrolysis. Improvements of APA production can be achieved by carrying out the reaction in a multi-stage water and butyl acetate (BuAc) reactor, without pH control. Under these conditions, the pH drops as the reaction occurs and APA crystallizes. Crystallization is a complex process in which nucleation, crystal growth, and sometimes, attrition and agglomeration can interact. Normally, large crystals and a narrow size distribution are desired for crystallization to take place, for which the downstream processes are facilitated. This study concerns on the determination of crystallization kinetics of APA in the presence of other components found in the PenG hydrolysis, i.e., the PenG, the by-product phenylacetic acid (PAA) and the solvent BuAc. This evaluation was based on the analyses of induction time, growth rate and crystal size distribution, at pH 4 and 5. A mathematical model based on the population balance was used as well. The results showed that the impurities have no influence on the APA crystallization, within the pH range and impurity concentrations evaluated. This work provides enough information about APA crystallization to be used in the design of a multi-stage counter-current reactor for PenG hydrolysis.

Keywords: crystallization, 6-aminopenicillanic acid, antibiotics, impurities, crystal size distribution.

1. Introduction

Biotechnological operations, such as enzymatic reactions used in aqueous-organic environments, are becoming increasingly important for the production of pharmaceutical products such as penicillin derivatives. Improvements on the synthesis of semi-synthetic antibiotics are obtained by the integration of reaction and purification systems (Chilov and Švedas, 2002; van der Wielen *et al.*, 2001). In particular, a multi-stage counter-current reactor for penicillin G (PenG) hydrolysis without pH control has been developed (den Hollander *et al.*, 2002). The biphasic system is formed by water and butyl acetate (BuAc) and the pH is not controlled. Under these conditions, the pH drops as the reaction occurs. At low pH, both, the transfer of PAA to the organic phase and crystallization of APA, are favorable. Thus, the equilibrium is shifted towards PenG conversion and hydrolysis products are obtained in different streams (Diender *et al.*, 2002).

Therefore, APA crystallization takes place in a multicomponent system where the presence of other solutes than the target product might significantly influence the kinetics of crystallization (Ottens *et al.*, 2001, 2004). Reactive crystallization usually produces sparingly soluble small crystals, which often causes problems in downstream processing, especially in filtration, but also in the treatment of the mother liquor as well in the drying and packing of the crystalline product (Yang *et al.*, 2002).

Usually crystal growth rates are reduced by impurities. The retarding effect of an impurity, however, is affected by the solution supersaturation, the higher the supersaturation, the weaker the retardation (Mullin, 1993; Chianese *et al.*, 1995; Klug, 1993). Nevertheless, there are few examples of increase in growth rate with increasing impurity concentration in the existing literature (Sangwal, 1993; Sangwal, 1996; Sangwal and Mielniczek-Brózska, 2001].

Although the goal of future steps is the crystallization of APA in continuous system, the data obtained in batch provides enough information. According to Gutwald and

Mersmann (1994), the growth and nucleation rates should not depend on the operation mode of the crystallizers but more or less on supersaturation, the type of crystallizers (stirred vessel, fluidized bed, forced circulation) and the mean specific power input. As a result, these authors concluded that the seeded batch experiments are subject to the same secondary nucleation mechanisms that are important in continuous crystallizers.

The current work focuses on the determination of kinetic parameters of APA crystallization as well as the influence of PenG, PAA and the organic solvent, BuAc in order to obtain enough information to be used in design of countercurrent multi-stage reactor. Therefore, the experimental conditions were restricted to the same pH range that the reactor will be operated. Furthermore, a mathematical model will be used based on a population balance for crystals in a specific size class in order to simulate the solute concentration in the liquid phase as a function of time (the so-called desupersaturation curve) and the crystal size distribution (CSD) (Ottens *et al.*, 2001).

2. Theory

2.1. Induction time and interfacial energy

Induction time is referred to the period of time at which crystals are first detected in the system, and is considerably influenced by the level of supersaturation, state of agitation, presence of impurities, and viscosity. Despite its complexity and uncertain composition, the induction period has frequently been used as a measure of the nucleation event, making the simplifying assumption that it can be considered to be inversely proportional to the rate of nucleation (Mullin, 1993):

$$t_{\text{ind}} \propto J^{-1} \quad (1)$$

The induction time not only depends on the initial supersaturation but also on the detection method. If for instance a concentration measurement is used, the induction time depends on the conversion, whereas for light reflection, the detection depends on the crystal surface area produced.

$$t_{\text{ind}} \propto \left[(S_0 - 1)^n \right]^{\frac{-1}{i+1}} \cdot \exp\left(\frac{B}{(i+1)(\ln(S_0))^2} \right) \quad (2)$$

The linear dependence of $\ln(t_{\text{ind}})$ and $(\ln S)^{-2}$ gives the slope $\frac{B}{i+1}$, where $i = 2$ or 3 if the detection was made by light reflection or concentration measurement, respectively (Ottens *et al.*, 2001).

The factor B is described as

$$B = \frac{\beta v^2 \gamma^3}{(kT)^3} \quad (3)$$

Where β is the shape factor (equal to $16\pi/3$ for a spherical nucleus) (Prasad *et al.*, 2001), γ is the interfacial energy, v is the molecular volume and k is the Boltzman constant. So, from the equation above, the interfacial energy can be estimated. These parameters are used in the model to simulate the solute concentration and the crystal size distribution.

2.2. Crystallization rates and Crystal Size Distribution (CSD)

A model based on a population base balance for crystals in a specific size class is used to simulate the solute concentration in the liquid phase as function of time and the Crystal Size Distribution (CSD) (Randolph and Larson, 1971).

$$\frac{\partial Vn(t, x)}{\partial t} = -\frac{\partial Vn(t, x) \partial G(t, x)}{\partial x} + Vb(t, x) - Vd(t, x) - \sum_k \Phi_k n_k(t, x) \quad (4)$$

where V is the compartment volume in m^3 , n is the number of particles per volume per size class in $\# \cdot m^{-4}$, t is the time in s , x is the length coordinate in m , G is the growth rate in $m \cdot s^{-1}$, b is the birth function in a certain crystal size class in $\# \cdot m^{-4} \cdot s^{-1}$, d is the death function in a certain crystal size in $\# \cdot m^{-4} \cdot s^{-1}$, Φ_k is the flow rate of the k^{th} stream containing crystals entering or leaving the compartment in $m^3 \cdot s^{-1}$.

Equation 1 reduces under the constraints of a constant volume batch operation (no input and output) and under the assumptions of no agglomeration, no breakage, and no death; birth only in the lowest particle class; the size-independent growth to the following hyperbolic partial differential equation (PDE)

$$\frac{\partial n(t, x)}{\partial t} = - \frac{\partial [n(t, x) \partial G(t)]}{\partial x} \quad (5)$$

To solve this PDE, boundary and initial conditions are required. The boundary condition at $x = 0$ is given by the commonly applied equation

$$n(t, 0) = \frac{J(t)}{G(t)} \quad (6)$$

where J is the nucleation rate in $\# \cdot m^{-3} \cdot s^{-1}$. The initial condition at $t = 0$ is given by

$$n(0, x) = 0 \quad (7)$$

The desupersaturation is obtained by solving the following component mass balance

$$M_w V \frac{\partial C(t)}{\partial t} + \frac{\partial M(t)}{\partial x} = 0 \quad (8)$$

where M_w is the molar mass of the crystallizing component. The mass of crystals formed (M) is given by integration over all crystal size classes

$$M(t) = \int k_v \rho_v n(t, x) x^3 dx \quad (9)$$

where k_v is the crystal shape factor and ρ_v is the crystal density in $\text{kg}\cdot\text{m}^{-3}$. The nucleation rate is described by (Tavare, 1995).

$$J(t) = J_0 \exp\left(-\frac{B}{\ln(S(t))^2}\right) \quad (10)$$

The growth rate is given by (Tavare, 1995).

$$G(t) = k_g (S(t) - 1)^n \quad (11)$$

Both nucleation rate and the growth rate are dependent on the supersaturation ratio of the crystallization component

$$S(t) = \frac{C(t)}{C_s} \quad (12)$$

The parameters presented in Equations 9 to 12, i.e., k_v , B , k_g , n , C_s , are unknown and it is necessary to determine them in order to get a complete model. The procedure to obtain experimentally these parameters is described in the Materials and Method.

Parameter J_0 is determined by carrying out simulations with the overall model and fitting J_0 to the experimental data.

3. Material and methods

3.1. Materials

Potassium di-hydrogen phosphate (anhydrous extra pure), 85% ortho-phosphoric acid, 36-38% hydrochloric acid, 25% ammonium hydroxide were purchased from J.T.Baker, and acetonitrile was purchased from Merck (Darmstadt, Germany). Phenylacetic acid (PAA) butyl acetate (BuAc) and were purchased from Fluka Chemika (Steinheim,

Switzerland). All reagents were of analytical grade. Penicillin G potassium salt (PenGK), 6-aminopenicillanic acid (APA) were kindly provided by DSM, Delft, The Netherlands.

3.2. Determination of the solubility of APA

An aqueous solution saturated with butyl acetate (BuAc) was prepared by mixing Milli Q water and BuAc in a ratio of 0.3 (BuAc: water; w/w) with a magnetic stirrer and separating both phases using separation funnel. The pH of this aqueous solution was corrected to 4.0 with HCl (5.0 M) and aliquots of 100 mL were transferred to an Erlenmeyer flask, and approximately 5.40 g of 6-aminopenicillanic acid (APA) was added. The flask was closed to avoid evaporation and the suspension was magnetically agitated at 25° C for 30 min and left to settle for 30 min. The interval of 30 min for agitation and for settlement was used after testing the minimum period of time adequate to achieve the equilibrium without causing degradation of APA.

This was the minimum time necessary to reach the equilibrium and avoid APA degradation. This procedure was followed to determine APA solubility within pH range of 4.0 and 5.0 with or without impurities. A solution of NH₄OH (2M) was used to correct the pH to the aimed value after addition of APA. The impurities evaluated were penicillin G (PenG) and phenylacetic acid (PAA). The concentrations of PenG were 1 mM, and 10 mM, and of PAA 1mM, 5 mM and 10 mM.

Liquid samples were filtered through a 0.2 µm cellulose nitrate membrane syringe filter. Subsequently 4 mL of filtered solution was diluted in 25 mL with Milli Q water. The concentration of APA was determined by HPLC analysis.

3.3 Crystallization experiments

The growth rate and induction time of APA were determined in a batch crystallizer. The scheme of the equipment is shown in Figure 1. The crystallizer itself consisted of a 2 L cylindrical glass jacketed vessel, stirred by a 4 bladed turbine impeller, and provided with 3 baffles. The refrigeration/heating system kept the temperature constant at 25°C. The laser probe provided reflection signals that were registered in the computer by LabView software. The HPLC was used to determine the concentration of APA and the CSD was determined by the analysis in a microscopic.

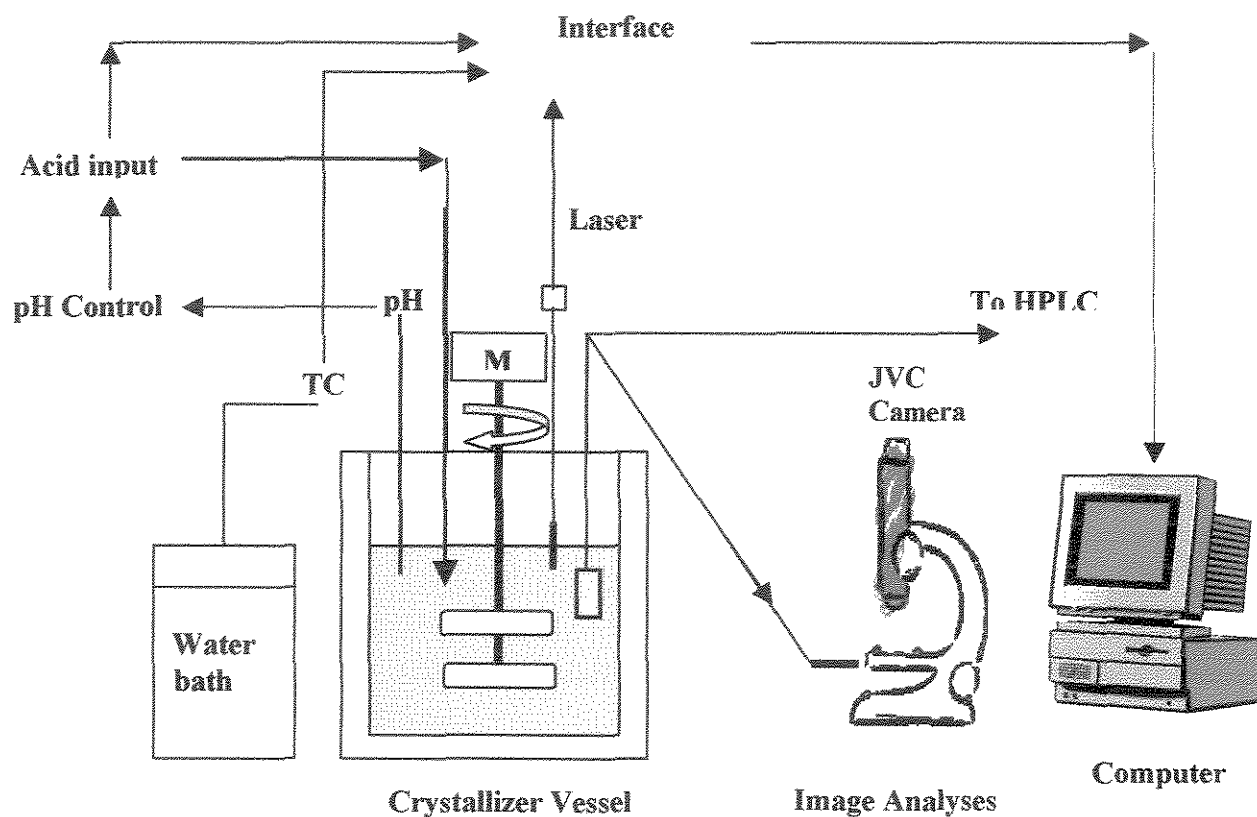


Figure 1: Batch experimental system (Ottens *et al.*, 2001).

Supersaturated solutions were prepared by dissolving a previously measured amount of APA in 600 mL Milli Q water saturated with BuAc (0.03 w/w; BuAc: water) at room temperature. All APA crystals were dissolved thoroughly by addition of 25% aqueous ammonium hydroxide and the pH was adjusted to about 6.0 with 37% aqueous hydrochloric acid. The solution was then made up to 2 liters and filtered through 0.2 μm cellulose nitrate membrane filters. The solution was transferred to a 2 liter jacketed vessel at 25⁰C under agitation of 200 rpm. The pH was corrected to pH 4.0 or 5.0, according to the assay by adding HCl (5 M). The crystallization assays started by the addition of 1.0 g of seeds.

In assays that were carried out in the presence of PenG, crystals of the impurity were added simultaneously with the seeds, giving a concentration range that varied from 0.55 mM to 1.13 mM. In the case of PAA, the assay was carried out by dissolving it in water before adding it to the crystallizer, since takes PAA some time to dissolve completely.

For the assay containing 20% (v/v) of BuAc, APA solution was prepared as aforementioned and 1600 mL of APA solution was mixed with 400 mL of BuAc.

Every 30 min a 15 mL sample was taken from the crystallizer using a syringe. Half of the sample was filtered initially through a 0.2 μm cellulose nitrate membrane syringe filter. Subsequently 4 mL of filtered solution was diluted in 25 mL with water. The concentration of APA was determined by HPLC analysis. The remaining end of the sample was used for image analysis.

3.4 Image Analysis

Sample was taken from the syringe and introduced into a glass cell, the time recorded and three pictures of crystals in solution were taken for future analyses of size and

amount of crystals applying the program Leica Qwin. This procedure was done 3 times, i.e., for each sample, three mean times (t_{mean}) and three corresponding mean lengths (L_{mean}) of the crystals were obtained. In the end of the assay (about 9 hours), a last sample was withdrawn and several images were saved to determine the crystal size distribution of APA (CSD).

Figure 2 presents some pictures of the crystals that were taken for analyses of size and amount of crystals.

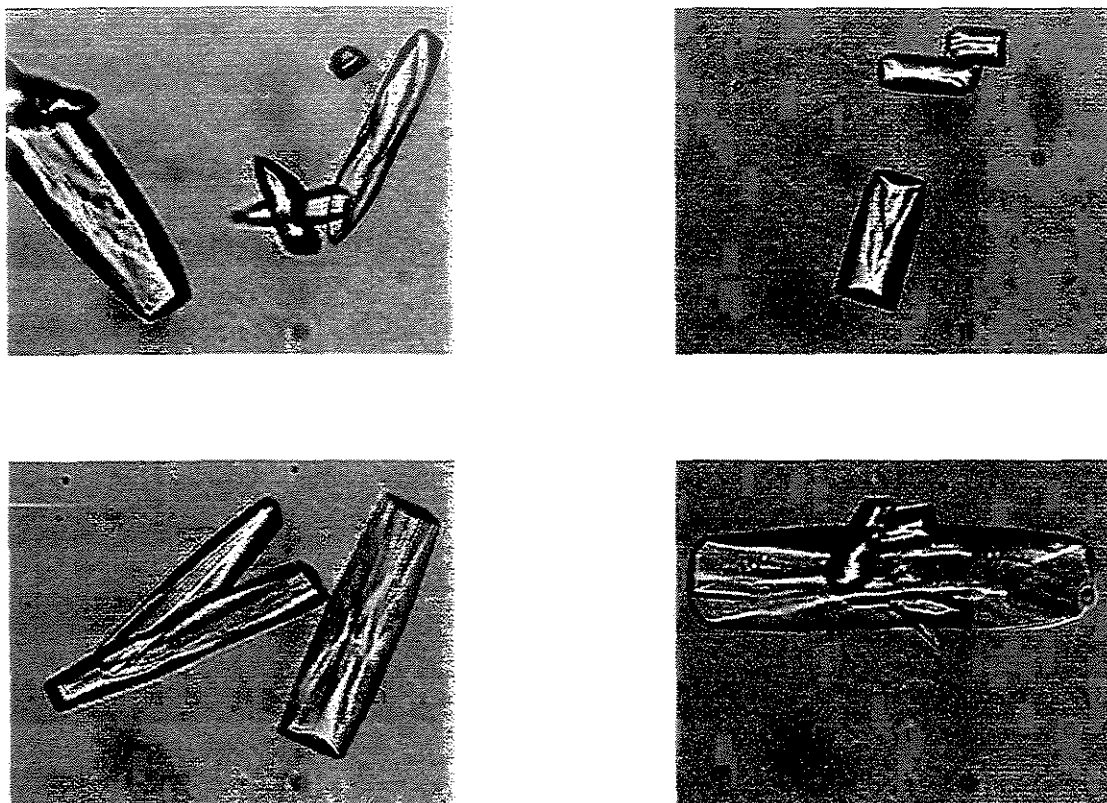


Figure 2: Pictures of APA crystals. Assay at $\text{pH} = 4.0$ and $C_{\text{PAA}} = 1.13\text{mM}$.

3.5 Growth rate determination

The growth rate (G) Equation 13 given:

$$G = \frac{\Delta L}{\Delta t} \quad (13)$$

is determined using L_{mean} and t_{mean} obtained as shown in Scheme 1.

The supersaturation ratio (S) was determined according to the Equation 12 where concentration is determined by HPLC analysis and solubility of APA was evaluated using Equation 14.

$$\text{Solubility}_{\text{APA}} = \frac{\text{Solubility}_{\text{APA}^{++}}}{F_{\text{APA}^{++}}} \quad (14)$$

The parameters in this equation will be given in the Results and Discussion Section.

Finally, the growth rate (G) equation as a function of supersaturation ratio (S) can be obtained as indicated in Equation 11 or Equation 15

$$\ln G = \ln k_g + n \times \ln(S-1) \quad (15)$$

3.6 Determination of Induction time and interfacial energy

The assays to determine the induction time followed the same procedure used in growth rate, except that in this case, seeds were not added to the crystals. The impurities were added to the crystallizer at time $t = 0$, and assays were carried out adding the impurity. PenG was dissolved before addition and PAA was added in solid state or dissolved before addition. For induction time assays, the presence of BuAc was not tested. Aqueous solution saturated with BuAc (0.03% w/w, BuAc, water) was used in all experiments.

The induction time values were plotted as function of supersaturation ratio and the data were fit by linear regression. The nucleation coefficient is calculated through the slope of this regression, according to Equation 16

$$B = \text{slope} \times (1+i) \quad (16)$$

In our case where $i = 3$, because the induction time is detected by concentration (Ottens *et al.*, 2001). When induction time is detected by light detection, $i = 2$.

Consequently, the interfacial energy ($J m^{-2}$) is determine by using Equation 3 where k is Boltzman constant ($1.38 \cdot 10^{-23} J K^{-1}$), T is temperature (298.15 K), v is the molar volume ($2.5658 \cdot 10^{-28} m^3$), calculated by Equation 17

$$v = \frac{M_w}{\rho \cdot A} \quad (17)$$

where M_w is the molar weight of APA ($0.216 kg mol^{-1}$), ρ is the density ($1.4 \cdot 10^3 kg m^{-3}$) and A is Avogrado's number ($6.02 \cdot 10^{23}$).

3.7 HPLC analysis

The samples were analyzed by HPLC (Waters), using a C18 – Platinum EPS column (particle size - 5 μm , Pore size - 100 Å, column size – 4.6 X 250 mm), and UV detection. The mobile phase was 28:72 (v/v) of acetonitrile and 0.64 g L⁻¹ KH₂PO₄ aqueous solution, the pH was adjusted to 2.75 with H₃PO₄. The flow was 1.0 mL min⁻¹. The elution times of APA, PAA and PenG were 3.3 min, 7.7 min and 13.9 min.

4 Results and Discussion

4.1 Influence of impurities on the solubility of APA

The solubility data of pure APA within pH range of 4.0 and 5.0 are shown in Figure 3. From these data the intrinsic solubility of the zwitterionic, corresponding to 12.02 mM, could be obtained according to the Equation 18

$$S_{\text{APA}^{+-}} = S_{\text{APA}} \times F_{\text{APA}^{+-}} \quad (18)$$

where $F_{\text{APA}^{+-}}$ is the fraction of the zwitterionic and given by the equation below.

$$F_{\text{APA}^{+-}} = \frac{\frac{10^{-\text{pKa}_1}}{10^{-\text{pH}}}}{1 + \frac{10^{-\text{pKa}_1}}{10^{-\text{pH}}} + \frac{10^{-\text{pKa}_1} \times 10^{-\text{pKa}_2}}{(10^{-\text{pH}})^2}} \quad (19)$$

pKa_1 and pKa_2 are the dissociation constant, of APA, 2.5 and 4.9, respectively (Diender *et al.*, 1998).

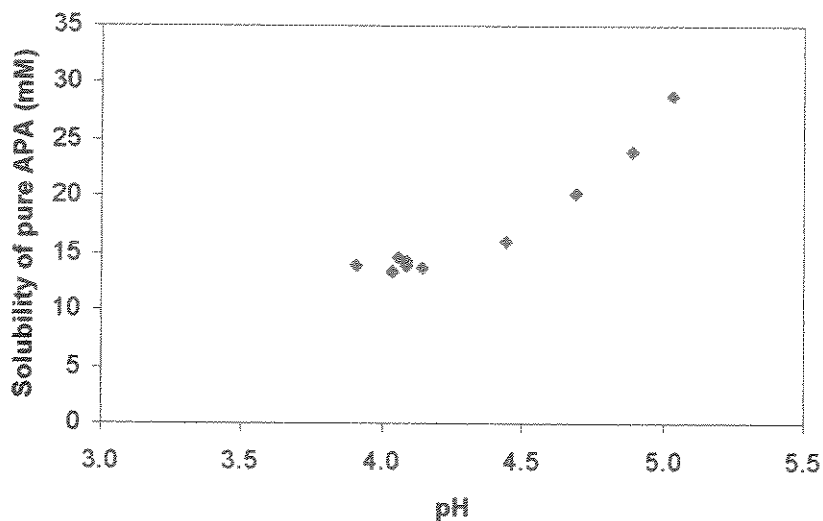


Figure 3: Solubility of pure APA at 25° C.

The solubility values of APA found in the literature are different. Mwangi (1994) reported a value of 16.18 mM as the minimum solubility, and Tavare and Jadhav (1996) found a value of 12.02 mM (25° C). The value obtained in this work for pH 3.91 to 4.09 and corresponding to 14.09 mM agrees with the data of 13.83 mM at the isoelectric point at 25° C reported by ZareNezhad (2002).

Figure 4 and 5 show the solubility of APA in the pH range of 4 to 5 and in the presence either of PenG or PAA, respectively. The corresponding experimental data of these assays are presented in Tables 1 and 2.

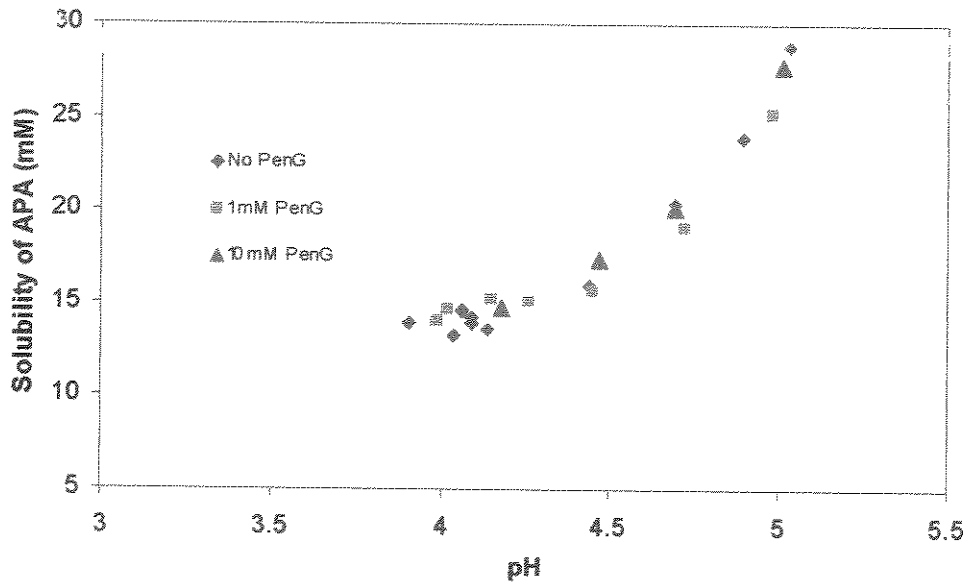


Figure 4: Solubility of impure APA at 25° C ($C_{\text{PenG}} = 0, 1.0$ and 10 mM).

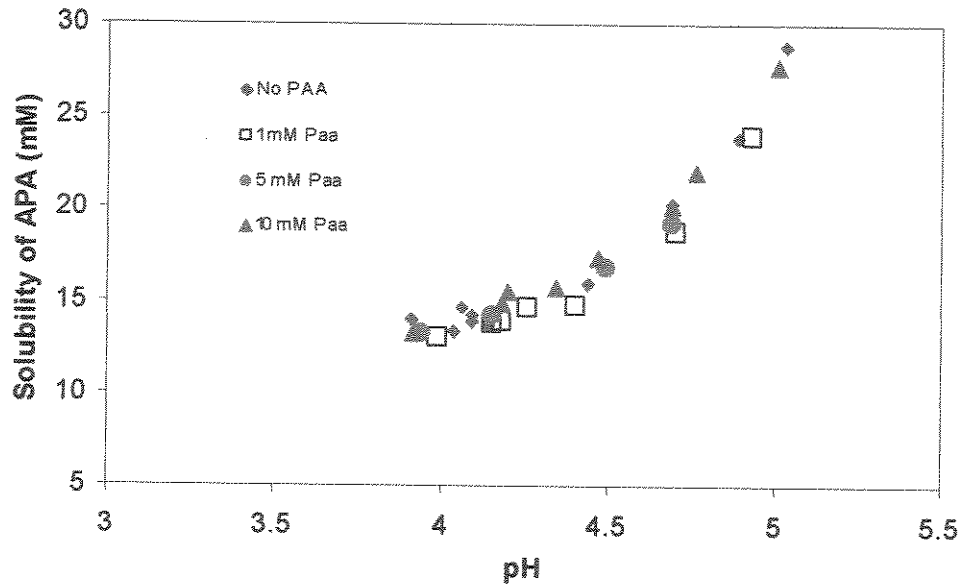


Figure 5: Solubility of impure APA at 25°C ($C_{\text{PAA}} = 0, 1.0, 5.0$ and 10 mM).

Table 1: Solubility of impure APA at 25° C ($C_{\text{PenG}} = 0, 1.0$ and 10 mM).

pH	No PenG	$C_{\text{PenG}} = 1\text{mM}$	$C_{\text{PenG}} = 10\text{mM}$	Solubility Eq 18	Error (%)
3.91	13.94			13.72	-1.6
3.99		14.05		13.89	-1.2
4.02		14.66		13.97	-4.9
4.04	13.30			14.03	5.2
4.06	14.60			14.09	-3.6
4.06	14.66			14.09	-4.1
4.09	13.86			14.19	2.4
4.09	14.19			14.19	0.0
4.14	13.63			14.39	5.2
4.15		15.24		14.43	-5.6
4.18			14.81	14.56	-1.7
4.26		15.08		14.98	-0.6
4.44	15.93			16.33	2.5
4.45		15.67		16.42	4.6
4.47			17.32	16.62	-4.2
4.69	20.31			19.51	-4.1
4.69			20.12	19.51	-3.1
4.72		19.08		20.04	4.8
4.89	23.84			23.82	-0.1
4.98		25.16		26.51	5.1
5.01			27.77	27.55	-0.8
5.03	28.78			28.27	-1.8

Table 2: Solubility of impure APA at 25°C ($C_{PAA} = 0, 1.0, 5.0$ and 10 mM).

pH	No PAA	$C_{PAA} = 1\text{mM}$	$C_{PAA} = 5\text{mM}$	$C_{PAA} = 10\text{mM}$	Solubility _{Eq 18}	Error(%)
3.91	13.94				13.72	-1.6
3.92				13.18	13.74	4.0
3.94			13.24		13.78	3.9
3.99		13.04			13.89	6.1
4.04	13.30				14.03	5.2
4.06	14.60				14.09	-3.6
4.06	14.66				14.09	-4.1
4.09	13.86				14.19	2.4
4.09	14.19				14.19	0.0
4.14	13.63				14.39	5.2
4.15		13.79			14.43	4.4
4.15			14.23		14.43	1.3
4.18		13.93			14.56	4.4
4.18				14.81	14.56	-1.7
4.20				15.44	14.66	-5.3
4.26		14.62			14.98	2.4
4.34				15.67	15.51	-1.0
4.40		14.72			15.97	7.9
4.44	15.93				16.33	2.5
4.47				17.32	16.62	-4.2
4.49			16.78		16.82	0.2
4.69	20.31				19.51	-4.1
4.69			19.18		19.51	1.7
4.69				20.12	19.51	-3.1
4.70		18.71			19.68	4.9
4.76				21.96	20.80	-5.6
4.89	23.84				23.82	-0.1
4.93		23.98			24.95	3.9
5.01				27.77	27.55	-0.8
5.03	28.78				28.27	-1.8

The error when comparing the experimental data and the solubility given by Equation 18 is less than 10% for all assays. This proves that the effect of the impurities, at least in the concentration and pH range evaluated, is negligible. This is in agreement with Sangwal (1993) who assesses that at low concentrations, the effect of impurities on solubility is usually negligible.

4.2 Induction time and interfacial energy

The results of induction time presented in this section were detected by concentration determining when the desupersaturation curve of APA starts. The determination of induction time is not very precise, independently on the method used. It's possible to check in the study developed by Pino-Garcia and Rasmuson (2003) that even obtaining 1,350 results, the data are very scattered. Figure 6 presents the graph in which APA concentration is plotted against time for different initial supersaturation ratios, at pH 5.0. The graph shown in Figure 6 indicates how difficult the detection of induction time is, namely, where exactly the time when the concentration starts to decrease. For instance, the assay of initial supersaturation ratio 2.87 was the only that provided a curve that presents a sharp decrease of APA concentration, that is, making possible an easy identification of the induction time.

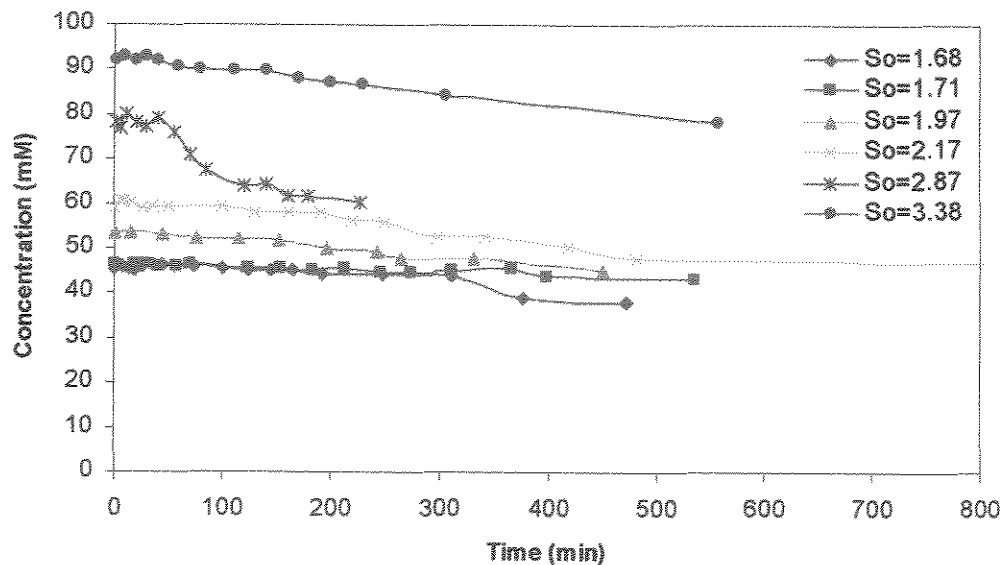


Figure 6: Desupersaturation curves of APA for various initial supersaturation ratios at pH 5.0.

Graphs of induction time as function of initial supersaturation ratio (S_0) were plotted separately for each situation, namely, for each impurity at different concentrations and at different pH. Nevertheless, assuming a confidence limit of 95%, the regression curves for pure or impure systems were comprehended in the same range of values, i.e., no statistically significant difference was detected. Therefore, one graph combining all data of pure and impure assays at pH 4 and 5 is shown in Figure 7 according to Equation 2.

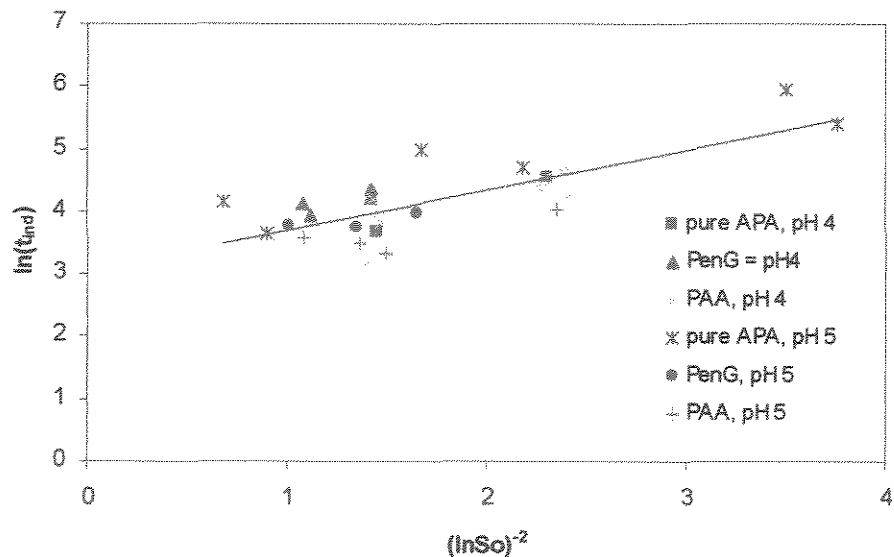


Figure 7: Induction time in minutes as function of supersaturation ratio, for pure and impure APA, at pH 4 and pH 5. The impurity concentrations are 0.55 mM and 1.13 mM of PenG or PAA

Higher concentration of impurities was tested at pH 5.0. Nevertheless, the impurities presented no effect on the APA nucleation, even when increasing the concentration of PAA or PenG to 3.0 mM.

No nucleation was observed in the assay in the presence of PenG (0.55 mM) at S_0 1.9 within 17 h of experiment. Probably, this inhibition was caused by the presence of further impurities, e.g, impurities that come from the air, since care was taken in cleaning the pieces of equipment, namely, crystallizer, impeller, blades and laser probe and in preparing the sample for analysis. Therefore, this effect was not taken into account and the conclusion that impurities have no impact on the induction time was based on the analysis of all data at once, as discussed above.

The data of induction time detected by reflection was also analyzed. The regression lines obtained by plots of induction time as a function of initial supersaturation ratio for both types of data, determined by APA concentration or reflection, provided the slope B and, consequently, the interfacial energy (γ), given by Equations 16 and 3, respectively. The values of B and γ and respective standard error are presented in Table 3.

Table 3: Values of B and γ using data determined by APA concentration or reflection by laser probe.

Group of Data	Data determined by APA concentration			Data determined by reflection		
	B	γ (10^{-3}J/m^2)	SE_{γ}	B	$\gamma(10^{-3}\text{J/m}^2)$	SE_{γ}
Only at pH 4.0	2.094	5.095	0.553	1.273	4.316	23.30
Only at pH 5.0	2.749	5.578	0.404	2.536	5.431	81.58
At 4.0 and 5.0	2.586	5.466	0.297	1.889	4.923	37.95

In Table 3, SE_{γ} , the standard error in the estimation of interfacial energy, is calculated according to Pino-Garcia and Rasmuson (2003) as a propagation of the uncertainty in the estimated slopes, and given by Equation 20:

$$SE_{\gamma} = \frac{\gamma}{3} \cdot \frac{SE_{\text{slope}}}{\text{slope}} \quad (20)$$

where SE_{slope} is the standard error in estimation of the slope of the linear regression and given by Equation 21

$$SE_{\text{slope}} = SE_{yx} \times \sqrt{\frac{1}{SS_{xx}}} \quad (21)$$

where SE_{yx} is the standard error in the prediction of Y values ($\ln(t_{ind})$) for each X $\left(\frac{1}{(\ln So)^2} \right)$ in the linear regression and SS_{xx} is the sum of squares of deviations from the mean for each X.

Analyzing Table 3 above, we observe that the standard errors provided by results detected by reflection are considerable higher than those provided by results detected by APA concentration. This large difference may be explained due to the fact that the laser probe was not installed in all assays. Consequently, the amount of data is not statistically significant for a good fit. Furthermore, the variation of the reflection signal is not so sharp. Probably, increasing the scale of reflection signal we could improve the accuracy of this method that presents advantages of being practical, fast and economical.

The results obtained by concentration of APA for data for each value of pH (4.0 or 5.0) showed that the values of interfacial energy did not present significant difference (Table 3). The lowest standard error obtained when data for pH 4.0 and 5.0 are analyzed at same linear regression, proved that γ equal 5.466 J m^{-2} should be used for determination of nucleation rate constant.

Other common result with the research by Ottens *et. al.* (2004) is that the value of interfacial energy (γ) in the presence of PG was practically the same as for the pure AMPI system.

In order to obtain a complete idea of the effect of impurities on APA crystallization, different experimental conditions, especially higher C_{PenG} at pH lower than 4.0 and higher than 5.0 should be tested. Nevertheless, such detailed study is beyond of the scope of this current work.

4.3 APA growth rate

The assays of growth rate of APA crystals at pH 5.0 were carried out at different supersaturation levels, in pure aqueous phase and one assay in aqueous phase saturated with BuAc and without impurities. The assays at pH 4.0 were carried out in aqueous phase saturated with BuAc and only one assay in biphasic system (20% v/v; BuAc: Aqueous phase saturated with BuAc). Furthermore, at pH 4.0, the assays were characterized by the presence of impurities (PenG and/or PAA). The presence of PAA as impurity was evaluated by adding it as solid and dissolving it before addition to crystallizer. This was done after realizing that it takes time for PAA to dissolve completely and PAA particles could affect the crystallization of APA. Furthermore, one assay at pH 5.0 in the presence of PenG was carried out as well.

The analysis of data for APA growth rate resulted in the graph shown in Figure 8 and the rate constant shown in Table 4.

Before analyzing all data of growth as function of initial supersaturation ratio for pH 4.0 and 5.0 and for all concentrations of impurities (C_{PenG} , C_{PAA} and C_{BuAc}), relations of growth rate were obtained as function of pH or impurity concentration. However, the results showed no statistical difference between the impure and pure systems, except for the assay characterized by the presence of both PenG and PAA as impurities. Therefore, the experimental data were grouped in order to obtain two regressions as shown in Figure 8.

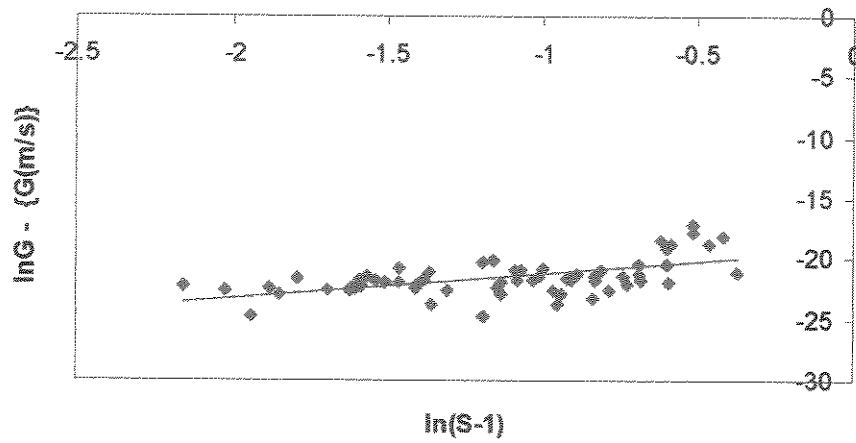


Figure 8: APA growth rate for pure and impure systems at pH 4.0 and 5.0.

From the analysis of growth rate, the kinetic rate constants were determined according to Table 4, based on the Equation 15.

Table 4: Kinetic rate constants of APA growth rate at pH 4.0 and 5.0

Assay	$\ln k_g$	$SE_{\ln k_g}$	n	SE_n	$SE_{\ln G}$
Pure and impure systems at pH 4.0 and 5.0	-19.275	0.429	1.992	0.355	1.243

Where $SE_{\ln k_g}$ and SE_n are the standard errors for the constants $\ln k_g$, and n, respectively, and $SE_{\ln G}$ is the standard error in the prediction of $\ln G$.

Therefore, from the data determined by growth rate experiments, the equation of growth rate (22) is determined:

$$G = 4.256 \times 10^{-9} \times (S - 1)^{1.992} \quad (22)$$

Concerning on the influence of impurities, inhibition of the growth rate has often reported in the literature (Rauls *et al.*, 2000; Chianese *et al.*, 1995; Klug, 1993). According to Mullin (1993), impurities can affect growth rate in different ways. Some impurities suppress growth entirely; some may enhance growth. Some impurities can exert an influence at very low concentrations, less than 1 part per million, whereas others need to be present in fairly large amounts before having any effect, similarly to the case of this current research. Yang *et al.* (2002) investigated the effect of different immiscible additives on the reactive crystallization of a benzoic acid derivative and found that aliphatic hexane had no effect.

With respect to the specific effect of solvent on the growth rate were found a few references (Lahav and Leiserowitz, 2001). Lahav and Leiserowitz (2001) presented an approach that can lead to fast growth by a “relay” mechanism and can suit the case of APA crystallization, since the compounds evaluated by these authors present zwitterionic character as in APA. In this example, the zwitterionic molecules are aligned so as to expose CO₂ groups at one end of the polar c-axis and NH₃⁺ groups at the opposite end. They propose the water molecules may be strongly bound by hydrogen bonds to the outermost layer (00-1) of CO₂ groups. In contrast, the pockets act as proton acceptors for the NH₃⁺ moiety by solvent water within the pockets yields repulsive or, at best, weakly attractive interactions. The pockets will, therefore, be weakly hydrated and so relatively easily accessible to approaching solute molecules. There is, however, an alternative mechanism which may account for the faster growth.

In order to obtain a thorough idea of the influence of the impurities investigated in this research on the reactive crystallization of APA, a wide investigation including higher concentrations of impurities, especially PenG and BuAc. The former was expected to present an inhibition effect due to the similarities between the molecular structures. The

latter should be evaluated since only few references about influence of organic solvent were found in the literature. Nevertheless, the results determined in this work provided enough information that will be used in the future design of a multi-stage countercurrent reactor for PenG hydrolysis.

4.4 Evaluation of model for APA crystallization

The evaluation of the results allowed to determine the parameters of crystals dimensions like length, width, and the amount of particles that are presented in Table 5.

Table 5: Parameters of crystal dimensions of APA.

Assay	C_{PenG} (mM)	C_{PAA} (mM)	So	AR	Dp (μ m)	SD _{Dp}	k_v
1	0	0	1.99	1.901	12.739	9.816	0.415
2	0 ^a	0 ^a	1.91	1.924	13.667	9.681	0.405
3	0.55	0	1.88	2.089	13.496	8.161	0.344
4	0	0.55 ^b	1.85	1.765	14.323	9.454	0.481
5	1.13	0	1.79	2.052	13.042	10.589	0.356
6	1.13 ^c	0	1.89	1.798	10.492	8.276	0.464
7	0	1.13 ^b	1.93	1.866	15.116	14.375	0.431
8	0	1.13	1.95	1.87	12.625	15.773	0.429
Mean			1.90	1.908	13.188	-----	0.416

^a with 20% BuAc

^b not dissolved but added as solid

^c pH 5.0

Where:

D_p is the average size taking into account the number of particles of each size class of crystals, according to the (24)

$$D_p = \frac{\sum n_i \cdot L_i}{\sum n_i} \quad (24)$$

SD_{D_p} is the standard deviation obtained as:

$$SD_{D_p} = \sqrt{(SD_{\text{length}})^2 + (SD_{\text{width}})^2} \quad (25)$$

AR is the aspect ratio of the crystal:

$$AR = \frac{\text{length}}{\text{width}} \quad (26)$$

k_v is the volume factor calculated by the Equation 27

$$k_v = \frac{3}{2} \times \frac{1}{(AR)^2} \quad (27)$$

The mean size of APA crystals were within the same range, whether PAA was added in a solid state or dissolved.

The kinetic rate constants of nucleation ($\gamma = 5.466 \text{ mJ m}^{-2}$) and growth ($n = 2.0$, $k_g = 4.26 \cdot 10^{-9} \text{ m s}^{-1}$) rates and the parameter of crystal dimension ($k_v = 0.42$) presented in Tables 3, 4 and 5, respectively, were used in simulations based on Equations 4 to 12. The best agreement with the de-supersaturation curve and the CSD was obtained when the initial nucleation rate constant (J_0) was $4.5 \cdot 10^9 \text{ \# m}^{-3} \text{ s}^{-1}$. Figure 9 shows the graphs obtained by using the model, including the CSD, the mass distribution, desupersaturation, nucleation and growth curves.

These kinetic parameters will be used to design the multi-stage countercurrent reactor

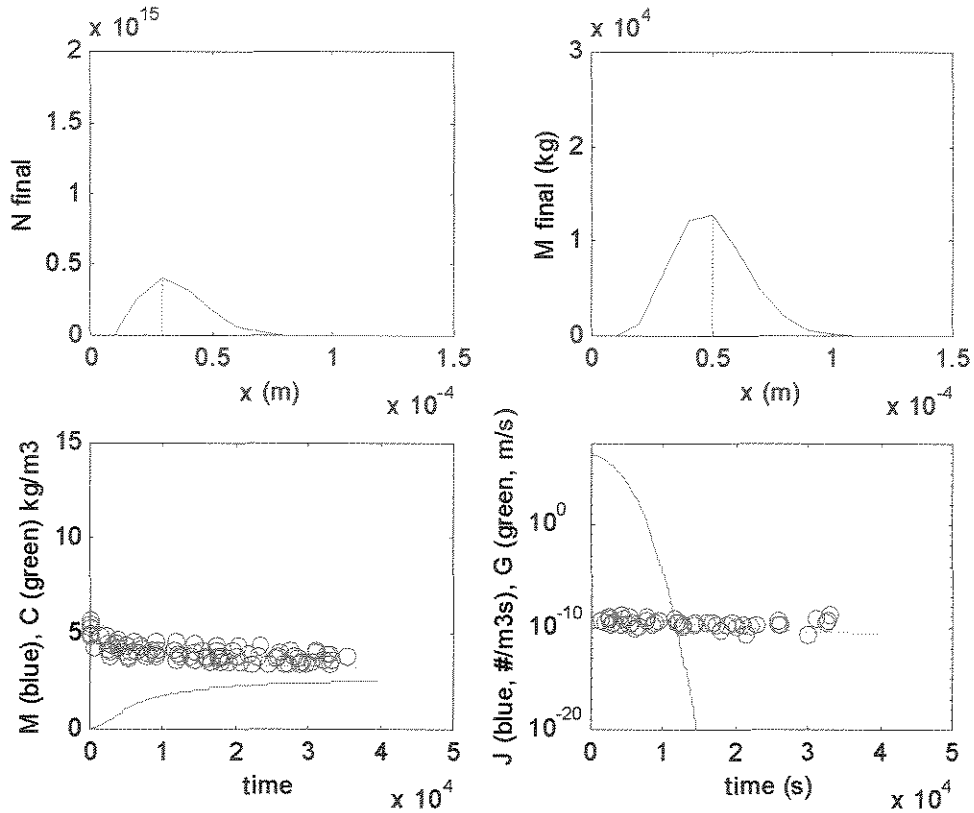


Figure 9: Plots of CSD, mass distribution, de-supersaturation, nucleation and growth rate.

$$J_0 = 4.50 \cdot 10^9 \# \text{ m}^{-3} \text{ s}^{-1}; B = 2.59; \gamma = 5.47 \cdot 10^{-3} \text{ J m}^{-2}; S_0 = 1.90; k_v = 0.42; k_g = 4.26 \cdot 10^{-9} \text{ m s}^{-1}; n = 2.0; AR = 1.91.$$

5 Conclusion

This work allowed to determine the kinetic parameters of APA crystallization at pH 4 and 5. The results indicate that the impurities studied did not affect APA crystallization, at least within the situations analyzed, namely, PenG and PAA concentrations of 0.55 mM and 1.13 mM and BuAc in 20% (v/v) in a biphasic system, and pH 4.0 and 5.0. Other experimental conditions should be verified for a complete conclusion concerning on the influence of impurities on APA crystallization. However, this approach is out of the scope of this current work. The information provided by this research was enough to obtain a model that reasonably predicts APA crystallization rates in the same conditions that that the multi-stage counter-current reactor for PenG hydrolysis will be operated.

6 Acknowledgement

The authors gratefully acknowledge Brazilian government (CNPq and CAPES), for financial support and DSM – Delft, The Netherlands for donating the chemicals. They are also grateful for the skillful assistance of Minna Vuolanto from University of Jyväskylä of Finland by carrying out the induction assays as part of her Training Period at the Delft University of Technology.

7 Nomenclature

ΔC Concentration driving force

B Nucleation factor

B	Birth function	$\#. \text{ m}^{-3} \text{ s}^{-1}$
C	Concentration	mM
C _s	Solubility	mM
D	Death function	$\#. \text{ m}^{-3} \text{ s}^{-1}$
G	growth rate	m s^{-1}
J	nucleation rate	$\#. \text{ m}^{-3} \text{ s}^{-1}$
K	Boltzmann constant	J K^{-1}
k _g	growth rate constant	
M	Mass of crystals formed	
M _w	Molar mass of APA	
N	Number of particles per volume per size class	$\#. \text{ m}^{-4} \text{ s}^{-1}$
N	Kinetic parameter of growth rate	
S	super-saturation ratio	
T	Temperature	K
t _{ind}	Induction time	S
V	compartment volume	m^3

Greek symbols

γ	interfacial energy	J m^{-2}
β	shape factor	
v	molecular volume	M^3
Φ_k	Flow rate of the kth stream containing crystal entering or leaving the compartment	$\text{m}^3 \text{s}^{-1}$

Subscripts

APA	Aminopenicillanic Acid
PAA	Phenylacetic Acid
PenG	Penicillin G
IMP	Impurity
0	Initial

8 Reference

- CHIANESE, A., KAREL, M., MAZZAROTTA, B.. Crystal growth kinetics of pentaerythritol. *The Chemical Engineering Journal*. 1995. 58. 215-221.
- CHILOV, G. G., ŠVEDAS, V.. Enzymatic hydrolysis of β -lactam antibiotics at low pH in a two-phase "aqueous solution-water-immiscible organic solvent" system. *Can. J. Chem.* 80 (2002) 699

- DIENDER, M.B., STRAATHOF, A.J.J., HEIJNEN, J.J.. Predicting enzyme catalyzed reaction equilibria in cosolvent-water mixtures as a function of pH and solvent composition. *Biocatalysis and Biotransformations*. v. 16, p. 275-289. 1998
- DIENDER, M.B., STRAATHOF, A.J.J., VAN DER DOES, T., RAS., HEIJNEN, J.J.. Equilibrium modeling of extractive enzymatic hydrolysis of penicillin G with concomitant 6-aminopenicillanic acid precipitation. *Biotech. Bioeng.* 2002.78 (4). 395-402.
- KLUG, D.L.. IN: MYERSON, A.S. (Ed.) *Handbook of Industrial Crystallization*. Butterworth-Heinemann. London. 1993. p. 65.
- LAHAV, M., LEISEROWITZ, L.. The effect of solvent on crystal growth and morphology. *Chem. Eng. Sci.* 2001. 56. 2245-2253.
- MULLIN, J.W.. *Crystallization*. Third Edition. Butterworth-Heinemann. 1993. 527 p.
- MWANGI, S.M.. *Reactive precipitation of 6-aminopenicillanic acid: Application of a crystallization methodology*. 1994. PhD thesis. The Victoria University of Manchester Faculty of Technology.
- OTTENS, M.; LEBRETON, B.; ZOMERDIJK, M.; RIJKERS, M.P.W.M.; BRUINSMA, O.S.L.; VAN DER WIELEN, L.A.M.. Impurity effects on the crystallization kinetics of Ampicillin. Submitted to IECR 2004.
- PINO-GARCIA, O.; RASMUSON, Å. C.. Primary nucleation of vanillin explored by a novel multicell device. *Ind. Eng. Chem. Res.* 2003. 42. 4899-4900.
- PRASAD, K.V.R., RISTIC, R. I., SHEEN, D.B., SHERWOOD, J.N.. Crystallization of paracetamol from solution in the presence and absence of impurity. *Int. J. Pharmaceutics*.2001. 215. 29-44.
- RANDOLPH, A.D., LARSON, M.A.. *Theory of particulate processes: Analysis and techniques of continuous crystallization*. Academic Press. 1971. 251 p.

- RAUL, M.; BARTOSCH, K.; KIND, M.; KUCH, ST.; LACMANN, R.; MERSMANN, A.. The influence of impurities on crystallization kinetics – a case study on ammonium sulfate. *Journal of Crystal Growth*. 2000. 213. 116-128.
- SANGWAL, K.. Effect of impurities on the crystal growth processes. *Prog. Crystal Growth and Charact.* 1996. 32. 3-43.
- SANGWAL, K.. Effect of impurities on the processes of crystal growth. *Journal of Crystal Growth*. 1993. 128. (1-4). 1236-1244.
- SANGWAL, K.; MIELNICZEK-BRZÓSKA, E.. Effect of Fe(III) ions on the growth kinetics of ammonium oxalate monohydrate crystals from aqueous solutions. *Journal of Crystal Growth*. 2001. 233. 343-354.
- TAVARE, N.S., JADHAV, V.K.. Solubilities of 6-aminopenicillanic acid and phenoxyacetic acid in hydrotope solutions. *J. Chem. Eng. Data*. 1996. 41. 1196-1202.
- TAVARE, N.S.. *Industrial Crystallization: Process Simulation Analysis and Design*. The Plenum Chemical Series: Plenum Press: New York. 1995.
- VAN DER WIELEN, L. A. M., OTTENS, M., STRAATHOF, A. J. J.. Process technology and process integration in the preparation of penicillins. In: A. Bruggink Synthesis of β -lactam antibiotics. *Chemistry, biocatalysis and process integration*. Dordrecht: Kluwer Academic Publishers. 2001. p. 150.
- YANG, G., LOUHI-KULTANEN, M., OINAS, P., SHA, Z., KALLAS, J.. The effect of immiscible additives on the batch reactive crystallization of a benzoic acid derivative. *J. Chem. Eng. Japan*. 2002. 35 (11). 1140-1145.
- ZARENEZHAD, B.. Prediction of the solubility of 6APA in aqueous phase and optimum control scheme for batch crystallization process through pH variation. *Korean J. Chem. Eng.* 2002. 19 (6). 992-995.

CAPÍTULO V

Neste Capítulo é apresentado o modelo termodinâmico que descreve as concentrações de equilíbrio dos compostos no sistema bifásico. O principal propósito de se utilizar a modelagem do reator multi-estágio e contra-corrente é a obtenção de informações prévias para a instalação do reator e realização de experimentos, no intuito de reduzir significativamente o volume de materiais, além de contribuir para otimização do tempo empregado no projeto do reator.

O modelo calcula o pH e as concentrações do substrato e produtos nos estágios do reator contra-corrente. Os dados fornecidos pelo modelo podem ser utilizados para otimizar as condições de operação do reator bifásico multi-estágio (ponto de alimentação, vazão volumétrica das fases e concentração inicial do substrato).

Modeling of PenG hydrolysis in a counter-current multi-stage reactor.

Juliana S. Ferreira^{a, b}, Brenda H. Westerink^a, Adrie J. J. Straathof^{a*}, M. Ottens^a, Telma T. Franco^b, Luuk A. M. van der Wielen^a

^a *Department of Biotechnology, Delft University of Technology, Julianalaan 67, Delft, The Netherlands*

^b *School of Chemical Engineering, State University of Campinas, P.O. Box 6066, 13081-970 Campinas, SP, Brazil*

* Corresponding address. Tel.: +31-15-278-2330
fax: +31-15-278-2355
E-mail address: a.j.j.straathof@tnw.tudelft.nl

ABSTRACT

6-Aminopenicillanic acid (APA) is the building block for the synthesis of semi-synthetic antibiotics (SSA's). It is produced by the enzymatic hydrolysis of Penicillin G (PenG) in a production volume of around 10,000 tons. Current research aims at *process integration* of different steps in the production of those semi-synthetic antibiotics. This is achieved by combining different unit operations. The heart of this process design is a series of continuous stirred tank reactors. In these reactors the PenG is extracted from an organic phase to an aqueous phase, where it is hydrolyzed by immobilized amygdase to APA and phenylacetic acid (PAA). The PAA prefers the organic phase and is extracted from the aqueous phase. When APA exceeds its solubility it crystallizes. The three-phase system that leaves the reactor is separated into an aqueous crystal phase and an organic phase. Therefore, in this system, the extraction, the reaction and the crystallization are combined. The advantages of this set-up are: almost complete conversion of substrate by equilibrium limited reaction, separation of products, less unit operation necessary compared to the existing process and less waste produced. The process design results depend strongly on the used assumptions for crystal growth rate, APA solubility and enzyme stability. To increase the validity of the conceptual process design these assumptions should be verified carefully.

Keywords: Downstream Processing, Penicillin G hydrolysis, Modelling, Multiphase Reactors, Simulation, Crystallization.

1. Introduction

The fractionating counter-current extractive enzymatic reactor is a good option for short cutting the current APA production process and maybe eventually for the production of semi-synthetic antibiotics (SSA's). It can give a high conversion as the reaction equilibrium is shifted to the product side. Products are separated and APA is obtained relatively pure. Furthermore, no addition of base is needed. A truly integrated process is obtained as reaction and separation take place in one system.

The aim of this work is the development of a mathematical model of a counter-current fractionating reactor for the hydrolysis of penicillin G.

A set of mixer-settlers is used to establish counter-current contact of the two immiscible liquid phases. Immobilized penicillin amidase, which is kept in the mixer, catalyses the hydrolysis reaction of PenG into APA and PAA. PenG is fed in an intermediate stage with the organic phase. Subsequently it is extracted to the aqueous phase. The enzymatic hydrolysis of PenG is assumed to take place only in the aqueous phase. As the reaction takes place, the reactants establish a partitioning equilibrium between the organic phase and the aqueous phase. When the equilibrium concentration of APA in the aqueous phase exceeds the maximum solubility, it crystallizes. This will shift the yield towards the product side (Diender *et al.*, 2002). The block scheme of this process is shown in Figure 1.

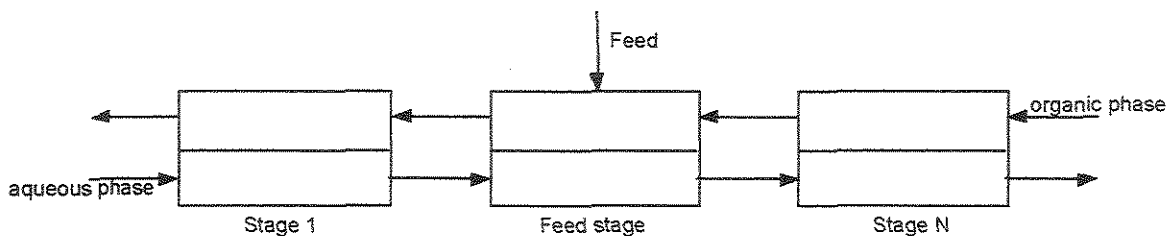


Figure 1: Block scheme of counter-current enzymatic reactor

The mixture of the aqueous phase together with APA crystals and the organic phase is fed into a phase separator, where the two liquids have to be separated. The crystals should be transported with the aqueous phase to prevent backmixing of APA. In Figure 2 a single stage of the counter-current enzymatic reactor is shown.

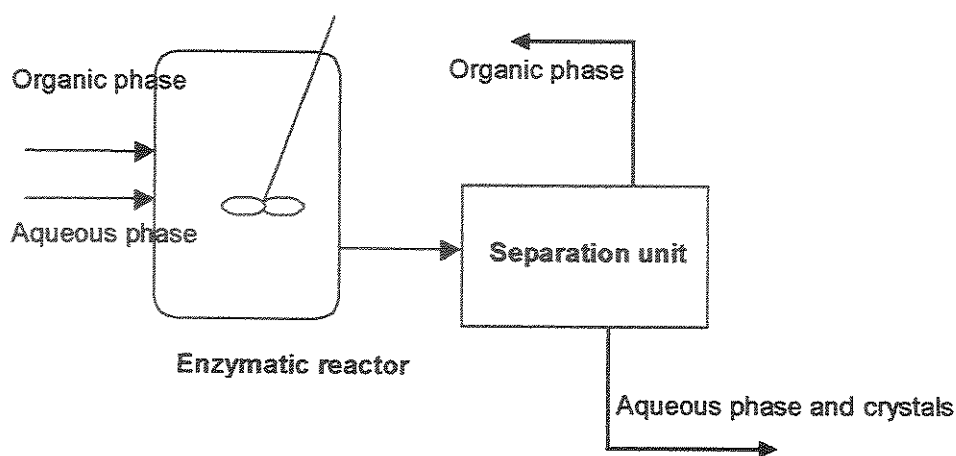


Figure 2: Single stage of counter-current enzymatic reactor.

Diender *et al.* (2002) presented a mathematical model for the prediction of the hydrolysis equilibrium as a function of pH, initial PenG concentration and phase volume ratio in a batch two-phase system. Crystallization of APA was included in this model. Den Hollander *et al.* (2002) presented a mathematical model, which was used to predict the concentrations and pH along a counter-current reactor. The latter model did not include crystallization of APA. The results of the model are only valid when the concentration of APA is lower than the solubility. This means that the concentration of PenG in the feed should be low. For full-scale process this will not be the case. Furthermore, the crystallization of APA will shift the reaction equilibrium to the product side which is beneficial for the yield of the process.

The model developed in this work includes the crystallization of APA. Moreover, it is included the effect of backmixing, which is caused by inefficient phase disengagement in the settler, such that a fraction of the appropriate phase flow leaving the settler is entrained and actually carried back, in the reverse direction along the cascade, by entrainment in the other phase that might lead to a decrease in conversion (Ingham and Dunn, 1994). It is possible to predict the conversion of PenG and the purity of the product streams and the average size of the formed APA crystals with this model.

2. Theory

The models presented by Diender *et al.* (2002) and Den Hollander *et al.* (2002) are both based on equilibrium stages. The streams leaving the reactor are assumed to be in equilibrium with each other. Non-equilibrium models are rate based and include mass transfer. This work is developed based in a transient model, since solving a set of non-linear algebraic equations needs good initial guesses and may give multiple steady-state solutions (Van der Wielen *et al.*, 1996).

2.1. Development of the three phase model

Figure 3 schematically shows extraction, hydrolysis and crystallization in one stage of the counter-current fractionating reactor.

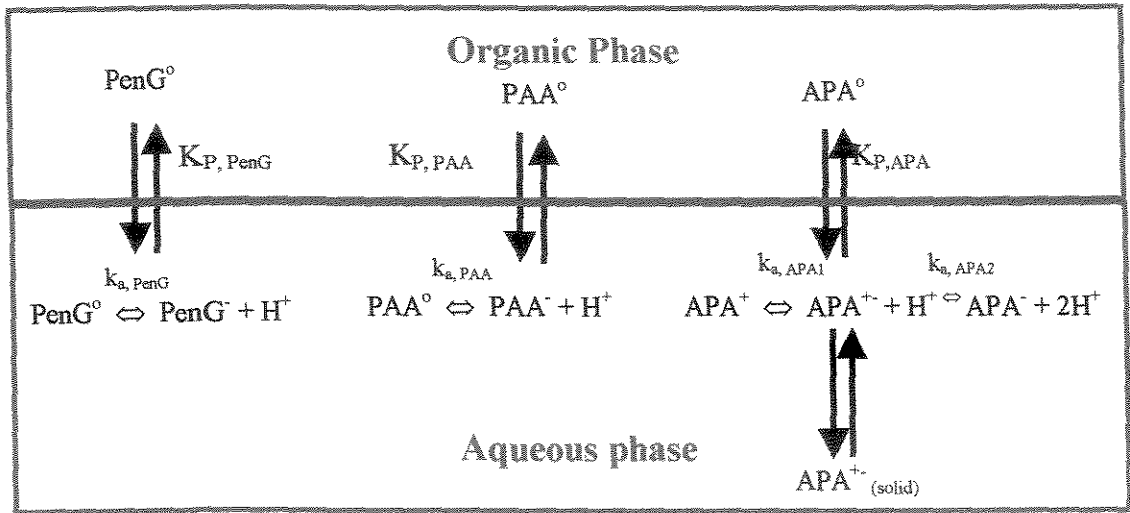


Figure 3: Schematic representation of one stage of counter-current reactor (not shown is inflow from other stages)

For every component i in every stage j a continuity equation is set up. For components in the aqueous phase this is given by:

$$(1 - \varepsilon_j)M_j \left(\frac{dC_{i,j}}{dt} \right) = L_{j-1}C_{i,j-1} - L_jC_{i,j} + (1 - \varepsilon_j)M_j \sum r_{i,j} \quad (1)$$

For components in the auxiliary phase this is given by:

$$\varepsilon_j M_j \left(\frac{dq_{i,j}}{dt} \right) = V_{j+1}q_{i,j+1} - V_j q_{i,j} - \varepsilon_j M_j \sum r_{i,j} + F_j z_{i,j} \quad (2)$$

where M_j is the mass in stage j in kg, ε_j is the auxiliary hold-up in stage j in kg·kg⁻¹, $C_{i,j}$ is the concentration of component i in stage j in the aqueous phase in mol kg⁻¹, $q_{i,j}$ is the

concentration of component i in stage j in the solvent phase in mol kg^{-1} , L_j is the aqueous flow rate from stage j in $\text{kg}\cdot\text{s}^{-1}$, V_j is the solvent flow rate from stage j in $\text{kg}\cdot\text{s}^{-1}$, $r_{i,j}$ is the extraction, reaction, dissociation or crystallization rate in $\text{mol kg}^{-1}\cdot\text{s}^{-1}$, F_j is the feed flow rate to stage j in $\text{kg}\cdot\text{s}^{-1}$ and $z_{i,j}$ is the concentration of component i in that feed in mol kg^{-1} .

The reactor is made of N counter-current CSTR's. A set of 13 non-linear, stiff, ordinary differential equations are obtained which are solved in Matlab with a variable step size solver (ode15s). The following assumptions are made to simplify the model (Ingham and Dunn, 1994): all reactors are ideally mixed; the whole process is isothermic and isobaric; and the mode is limited to two completely immiscible liquid phases, the aqueous phase and the organic phase. Although one of the phases, the dispersed phase, is in the form of droplets, dispersed in a continuum of the other, this is neglected and each liquid phase is assumed to consist of separate, well-mixed stage volumes. In fact, water and butyl acetate are almost immiscible.

The structure of the Matlab model together with the names of the different files is shown in Figure 4.

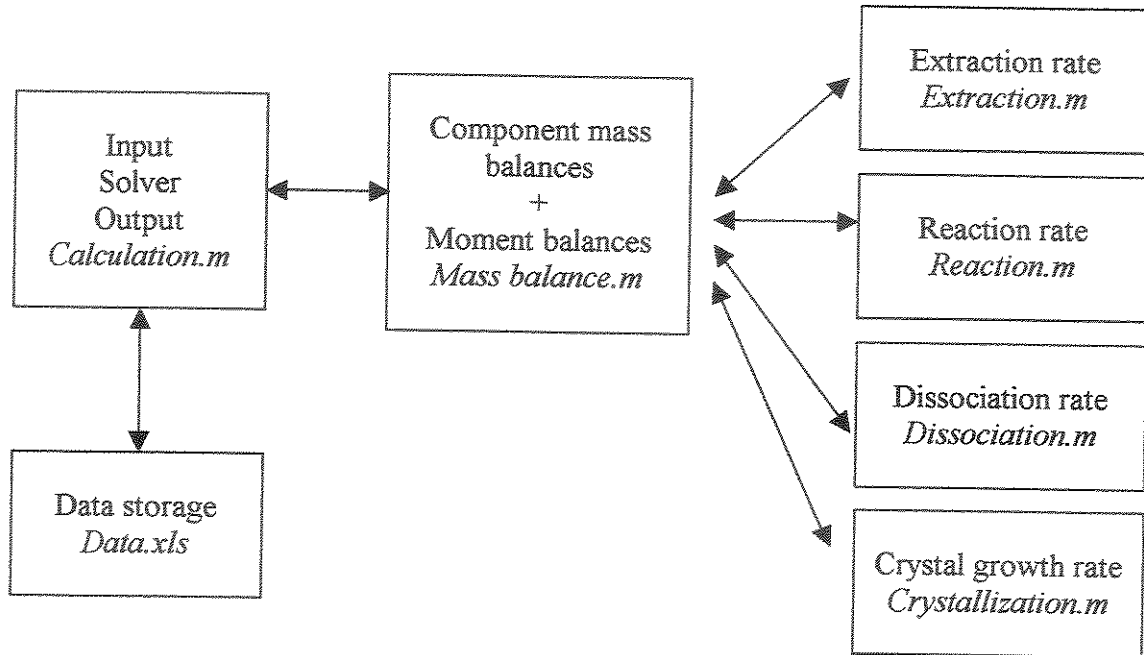


Figure 4: Model structure

The input data for the model are: number of stages, feed stage, aqueous and organic flow rate, feed rate, concentration of HPenG in the feed, volume of the reactor and amount of backmixing.

With this model the concentration of every component in every stage in time is calculated. From these data the conversion of steady state is calculated by:

$$\xi = 1 - \frac{V_1 \cdot q_{HPenG,1} + L_N \cdot C_{HPenG,N} + L_N \cdot C_{PenG-,N}}{F_{NF} \cdot z_{HPenG,NF}} \quad (3)$$

where F_{NF} is the feed flow rate in the feed stage in $\text{kg} \cdot \text{s}^{-1}$ and $z_{i,NF}$ is the concentration of component i in the feed in mol kg^{-1} .

The purity of the products in the exit stream is given by:

$$P_{PAA,1} = \frac{q_{PAA,1}}{q_{PAA,1} + q_{HPenG,1} + q_{APA,1}} \quad (4)$$

$$P_{APA,N} = \frac{C_{APA,N}}{C_{APA,N} + C_{HPenG,N} + C_{PAA,N}} \quad (5)$$

2.1.1. Modelling PenG hydrolyses

For the conversion of PenG to PAA and APA the following reference reaction is presented:



The equilibrium of PenG hydrolysis in aqueous system can be described by the equilibrium constant as defined by Tewari and Goldberg (1988):

$$K_{eq} = \frac{\gamma_{APA^-} C_{APA^-} \cdot \gamma_{paa^-} C_{paa^-} \cdot \gamma_{H^+} C_{H^+}}{\gamma_{PenG^-} C_{PenG^-} \cdot \gamma_{H_2O} C_{H_2O}} \quad (6)$$

With γ_i being the activity coefficient. Effects of non-ideality introduced by ionic strength can be accounted for by using the extended Debye-Hückel equations. This will certainly be the case with high feed concentrations of PenG. So far, the activity coefficient of the components are set to unity. The concentration of water is assumed constant and taken out the equation, which will then be:

$$K_{eq} = \frac{C_{APA^-} \cdot C_{paa^-} \cdot C_{H^+}}{C_{PenG^-}} \quad (7)$$

Tewari and Golberg (1988) found a value of $7.35 \cdot 10^{-8}$ mol kg⁻¹ for the equilibrium constant at 298.15 K.

The reaction rate is dependent on pH due to combination of the influence of the pH on the reaction equilibrium and the reaction rate of the enzyme (Van der Wielen *et al.*, 1996). This last dependency is neglected and a concentration-based model is used to describe the pseudohomogeneous reaction rate (Minotti *et al.*, 1998):

$$r_r = k_r \left(C_{PenG^-} - \frac{C_{PAA} C_{APA^-} C_{H^+}}{K_{eq}} \right) \quad (8)$$

where r_r is the reaction rate for the forward reaction in mol kg⁻¹·s⁻¹, k_r is the forward reaction rate constant in s⁻¹, K_{eq} is the reaction equilibrium constant in mol kg⁻¹ and C_i the concentration of species i in the aqueous phase in mol kg⁻¹. The influence of k_r on the conversion is examined as well.

As the catalyst is immobilized in gel beads transport of substrate to and products out of the beads occurs. It is assumed that there is no mass limitation and that the reaction is the limiting step (Ferreira *et al.*, 2004). Furthermore it is assumed that the presence of organic solvent has no influence on the enzyme activity (Ferreira, *et al.*, 2004) and that the reaction takes place only in the aqueous phase.

2.1.2. Modeling PenG partitioning

The partition coefficient of a component is defined as:

$$K_i = \frac{q_i}{C_i} \quad (9)$$

where q_i is the concentration of species i in the solvent phase in mol kg⁻¹ and C_i is the concentration of species i in the aqueous phase.

It is assumed that only the net uncharged component partition between the aqueous and organic phase. The partition coefficients of the net uncharged components in a water-butyl acetate biphasic system are given at 25 °C (Diender *et al.*, 2000) and described in Table 1.

Table 1: Partition coefficients of PenG, APA and PAA at 25° C (Diender *et al.*, 2000).

Component	K _P [-]
PenG(org)/PenG(aq)	69
PAA(org)/PAA(aq)	29
APA ⁺ (org)/APA ⁺ (aq)	0.001

The extraction rate is given by:

$$r_e = k_l a \left(\frac{q_i}{K_i} - C_i \right) \quad (10)$$

where r_e is the extraction rate in $\text{mol kg}^{-1} \cdot \text{s}^{-1}$ and $k_l a$ is the mass transfer coefficient in s^{-1} . The influence of $k_l a$ on the conversion is examined as well.

It is assumed that k_L is constant. Otherwise, the result is that the overall coefficient k_L varies with the concentration, and therefore in modeling the case of a non-linear equilibrium extraction, further functional relationships relating the mass transfer coefficient to concentration would be required, such as $k_L = f(C_i)$ (Ingham and Dunn, 1994).

2.1.3. Modeling dissociation kinetics

Immediate dissociation is assumed. For simplicity reasons this is modeled based with a high dissociation rate constant of 100 s^{-1} . Dissociation constants are given in Table 2.

$$r_d = k_d \left(C_{HA} - \frac{C_{H^+} \cdot C_{A^-}}{K_a} \right) \quad (11)$$

where r_d is the dissociation rate in $\text{mol kg}^{-1} \cdot \text{s}^{-1}$, k_d is the dissociation rate constant in s^{-1} and K_a is the dissociation constant in mol kg^{-1} .

Table 2: Dissociation constants (Diender *et al.*, 2000)

Component	pKa
PenG	2.5
PAA	4.3
APA [±]	4.9
APA ⁺	2.5
H ₂ O	14

2.1.4. Modeling crystallization kinetics

When the concentration of APA exceeds solubility, crystals of APA[±] are formed.

To calculate the amount of crystals formed the method of moments as described by Van Rosmalen (1994) is used. The method of moments represents the Crystal Size Distribution (CSD) in its first four moments m_0 to m_3 , related to the total number, N_T , total length, L_T , total surface area, A_T , and total volume, V_T , of the crystals, all expressed per kg aqueous phase. The balance of the moments is shown in Table 3. These balances can be solved in time together with the component balances aforementioned.

Table 3: Moments balance

Moments	Name	Moment balance	
m_0	N_T	$(1 - \varepsilon_j)M_j \left(\frac{dN_{T,j}}{dt} \right) = L_{j-1}N_{T,j-1} - L_jN_{T,j} + (1 - \varepsilon_j)M_j(J + B_0)$	(12)
m_1	L_T	$(1 - \varepsilon_j)M_j \left(\frac{dL_{T,j}}{dt} \right) = L_{j-1}L_{T,j-1} - L_jL_{T,j} + (1 - \varepsilon_j)M_j(N_T G)$	(13)
m_2	A_T	$(1 - \varepsilon_j)M_j \left(\frac{dA_{T,j}}{dt} \right) = L_{j-1}A_{T,j-1} - L_jA_{T,j} + (1 - \varepsilon_j)M_j(2k_o L_T G)$	(14)
m_3	V_T	$(1 - \varepsilon_j)M_j \left(\frac{dV_{T,j}}{dt} \right) = L_{j-1}V_{T,j-1} - L_jV_{T,j} + (1 - \varepsilon_j)M_j \left(3 \frac{k_v}{k_a} A_T G \right)$	(15)

where M_j is the mass in stage j in kg, ε_j is the auxiliary hold-up in stage j in $\text{kg} \cdot \text{kg}^{-1}$, L_j is the aqueous flow rate from stage j in $\text{kg} \cdot \text{s}^{-1}$, J is the primary nucleation rate in $\# \cdot \text{kg}^{-1} \cdot \text{s}^{-1}$, B_0 is the secondary nucleation rate in $\# \cdot \text{kg}^{-1} \cdot \text{s}^{-1}$, G is the crystal growth rate in $\text{m} \cdot \text{s}^{-1}$, k_a is the surface area shape factor [-] and k_v is the volumetric shape factor [-].

This method only holds if the crystallization process does not show size-dependent processes. Furthermore it cannot reconstruct the population density from the different moments.

The APA crystallization rate in $\text{mol} \cdot \text{kg}^{-1} \cdot \text{s}^{-1}$ is given by (Mullin, 1993):

$$r_c = 3 \left(\frac{k_v}{k_a} \right) A_T G \frac{\rho_c}{M_w} \quad (16)$$

where G is growth rate in $\text{m}\cdot\text{s}^{-1}$, A is surface area of the crystals in $\text{m}^2\cdot\text{kg}^{-1}$, ρ_c is the density of APA crystals in $\text{kg}\cdot\text{m}^{-3}$ and M_w is the molar weight of APA in $\text{kg}\cdot\text{mol}^{-1}$.

In a continuous crystallizer the main phenomena causing nucleation is secondary nucleation, for which lower saturation is needed than for primary nucleation. The secondary nucleation rate is a function of the supersaturation, the power input and the total crystal mass in the crystallizer. As the exact dependency is not known and also the process variable power input is unknown the number of crystals is assumed constant. This is selected from the supersaturation that will be obtained from simulation. The supersaturation in continuous crystallizers will be very low.

The surface area shape factor k_a and the volumetric shape factor k_v are assumed to be one as no other information is available.

The growth rate of APA crystals in $\text{m}\cdot\text{s}^{-1}$ is given in equation to the supersaturation ratio of APA presented in Chapter IV

$$G = 4.256 \times 10^{-9} (S - 1)^{1.992} \quad (17)$$

where S is the supersaturation ratio of the crystallizing component:

$$S = \frac{C_{APA}}{C_{eq,6APA}} \quad (18)$$

with $C_{eq,APA}$ being the solubility of APA.

This solubility depends on the fraction of APA^{\pm} in the solution, which is a function of the pH. The fraction of APA^{+} is given by:

$$F_{APA^{+-}} = \frac{C_{APA^{+-}}}{C_{APA^{+-}} + C_{APA^+} + C_{APA^-}} = \frac{1}{1 + \frac{K_{a,APA^{+-}}}{C_{H^+}} + \frac{C_{H^+}}{K_{a,APA^+}}} \quad (19)$$

These equations can also be obtained for the other fractions. The fractions of the different forms of APA as function of the pH are shown in Figure 5.

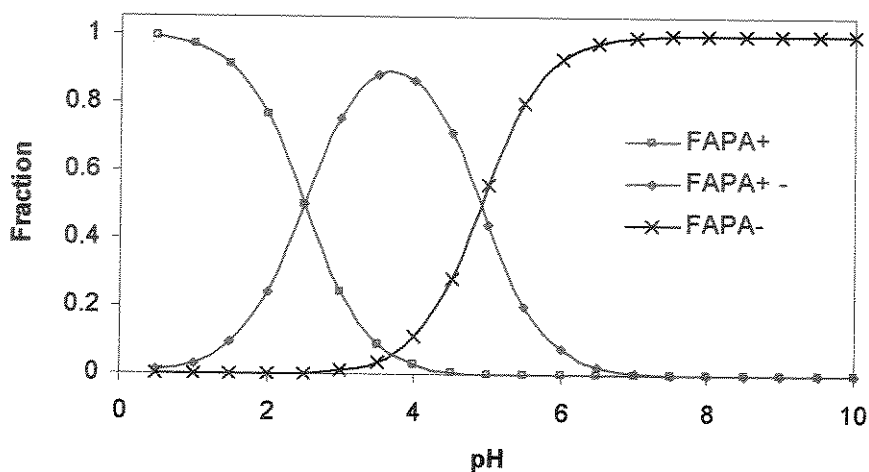


Figure 5: Fractions of different forms of APA as function of pH

When the solubility of APA is plotted against the fraction of APA^{\pm} (as presented in Chapter IV the following figure is obtained.

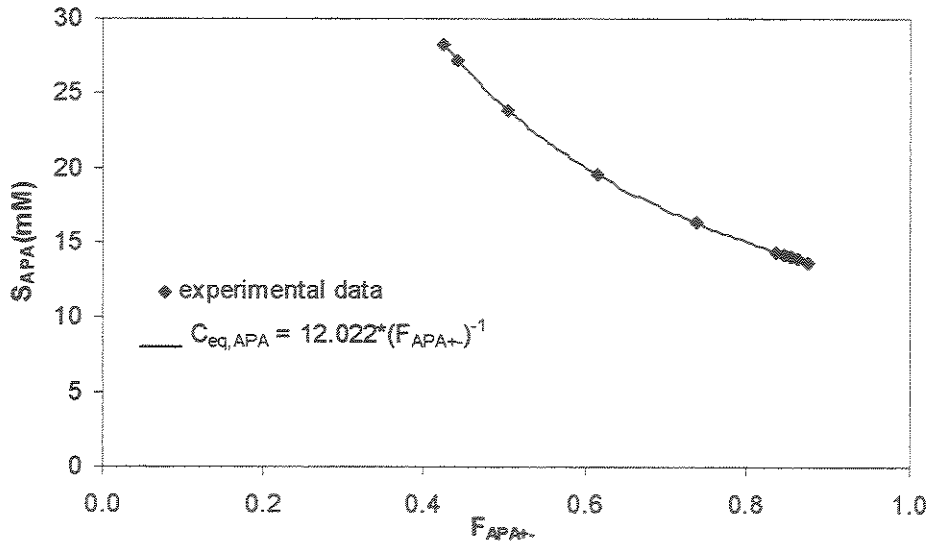


Figure 6: Solubility as function of the APA $^{\pm}$ fraction

The equation for the solubility of APA is:

$$C_{eq,APA} = 12.022 \times (F_{APA\pm})^{-1} \quad (20)$$

By modeling the crystallization as stated before, concentration of APA, amount of crystals and conversion is obtained in a simple manner. Disadvantage is that it is not obtained enough information over the crystal size distribution and over the real amount of supersaturation ratio. The exact way to implement the crystallization kinetics is described here:

The desupersaturation of APA concentration by crystallization is given by (Raphson *et al.*, 2001):

$$\frac{dC_{APA}(t)}{dt} = -\frac{1}{M_w V} \frac{dM(t)}{dt} \quad (21)$$

This term can be considered as the crystallization rate. Where C_{APA} is the concentration of the dissolved APA in mol m^{-3} solvent, M is the mass of APA crystals in kg, M_w is the molar mass in kg mol^{-1} and V is the volume of the reactor in m^3 .

The formation rate of crystals is given by integration over all crystal size classes.

$$\frac{dM(t)}{dt} = \int_0^\infty k_v \rho_v \frac{\partial n(t, x)}{\partial t} x^3 dx \quad (22)$$

where k_v is the crystal shape factor and ρ_v is the crystal density in $\text{kg}\cdot\text{m}^{-3}$. The population balance for crystals in a specific size class is given by:

$$\frac{\partial Vn(t, x)}{\partial t} = -\frac{\partial Vn(t, x)G(t, x)}{\partial x} + Vb(t, x) - Vd(t, x) + \Phi_{in}n_{in}(t, x) - \Phi_{out}n(t, x) \quad (23)$$

where n is the number of particles per volume per size class in $\#\cdot\text{m}^{-4}$, t is time in s, x is the length coordinate in m, G is the growth rate in $\text{m}\cdot\text{s}^{-1}$, V is the reactor volume, b is the birth function in a certain crystal class size in $\#\cdot\text{m}^{-4}\cdot\text{s}^{-1}$, d is the death function in a certain class in $\#\cdot\text{m}^{-4}\cdot\text{s}^{-1}$ and Φ is the flow rate in m^3/s .

Under the assumption of no agglomeration, no breakage, no death, birth only in the lowest particle class, size independent growth and constant volume, the following partial differential equation is obtained for a multi-stage continuous crystallizer:

$$\frac{\partial n(t, x)}{\partial t} = -\frac{\partial [n(t, x)G(t)]}{\partial x} + \frac{\Phi_{in}}{V} n_{in}(t, x) - \frac{\Phi_{out}}{V} n(t, x) \quad (24)$$

This partial differential equation (PDE) can be solved numerically by discretisation. With a first-order single step upward discretisation in space this becomes:

$$\frac{dn_i(t)}{dt} = -\frac{[G(t)(n_i(t) - n_{i-1}(t))]}{\Delta x} + \frac{\Phi_{in}}{V} n_{in,i}(t) - \frac{\Phi_{out}}{V} n_i(t) \quad (25)$$

i indicates the space coordinate. So for every stage, i equations are added being the particle size classes. The crystal size distribution in time can be obtained by integration of the different size classes. The formation rate of crystals, given by integration over all crystal size classes, can then be calculated (eq. 22). The discretised equations can be solved numerically with Matlab.

$$\frac{dM(t)}{dt} = \sum_{i=0}^{i=\infty} k_v \rho_v \frac{dn_i(t)}{dt} i^3 \Delta x^3 \quad (26)$$

The extensive model, which includes particle size distribution, will give better information on the supersaturation. This influences the conversion via a shift in the reaction equilibrium and so will give better information about the real conversion.

A disadvantage is that information is needed on the nucleation rate. In this reactor both primary and secondary nucleation could occur. Another disadvantage is that n (stages) times i (particle classes) differential equations are added to the model. This will slow down the model considerably and can cause instability. For this step of the development of this model, it was decided to use the moments method with constant number of crystals in the model.

2.1.5. Axial dispersion

So far it was assumed that phase separation between stages was complete. But for designing the multi-stage countercurrent reactor it is important to know what the influence of non-ideal phase separation is on the reactor performance and conversion. Backmixing reduces the efficiency of countercurrent mass transfer cascades, owing to its effect on the concentration profiles within the cascades and in decreasing the effective concentration driving forces (Ingham and Dunn, 1994). The back-flow model is incorporated, which

assumes well-mixed non-ideal stages with backflow. The inherent assumptions are as follows (Lo *et al.*, 1991):

1. The content of each stage is well mixed and backmixing occurs by mutual entrainment of the phases between stages.
2. The backmixing is expressed in terms of the ratio α of backmixed to net forward interstage flow and is constant for all stages
3. All mass transfer occurs in the mixer
4. The solvent and raffinate phase are immiscible
5. Fictitious after-settlers 0 and $N+1$ are provided at both ends of the reactor.

The arrangement of the flows is shown in Figure 7. It is possible to have different backmixing coefficients for both organic and aqueous phase.

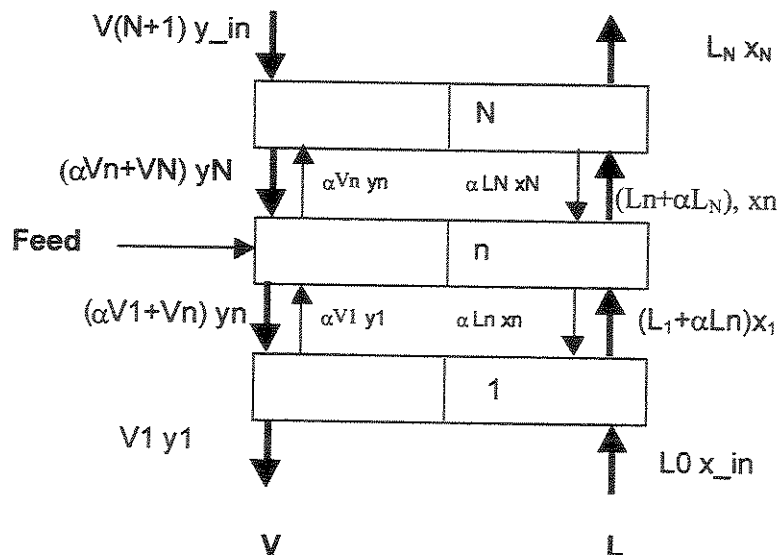


Figure 7: Backflow model: material balance over stage

Here the backmixing flow rates αL or αV act in the reverse direction to the main phase flows, between the stages and along the cascade. One important factor in the modeling process is to realize that, as a consequence of the backmixing flows, that since phase volumes remain constant and then the interstage flow rates along the cascade, in the forward direction, must also be increased by the magnitude of the appropriate backmixing flow contribution. With a backmixing flow αL in the aqueous phase, the resultant forward flow along the cascade must now be $(L+\alpha L)$, since the backmixing does not appear outside the multi-stage countercurrent reactor. Similarly with a backmixed flow αV , the forward flow for the organic phase is also increased to $(V+\alpha V)$. Taking into account the changed flow rates, however, the derivation of the component balance equations follow normal procedures (Ingham and Dunn, 1994)

3. Simulation accuracy and results

3.1. Consistency of the model

To examine if the model values are reliable, different controls are performed. First the extraction yield calculated with the model is compared with the value calculated with the Kremser equation. In the model, the reaction and dissociation constants are set to zero. Then the fraction of PenG that remains in organic phase is simulated.

When the fraction of non-removed PenG was calculated using the Kremser equation the same number was obtained. The conclusion is that in modeling extraction no error occurred.

Furthermore the consistency of the model is guaranteed as both mass balances over the β -lactam nucleus and the phenylacetic acid side chain are closed. These mass balances are respectively:

$$\sum F_j z_{HPenG,j} = V_1 (q_{HPenG,1} + q_{APA,1}) + L_n (C_{HPenG,n} + C_{PenG-,n} + C_{APA,n} + C_{APA-,n} + C_{APA+,n} + C_{APA(s),n}) \quad (27)$$

$$\sum F_j z_{HPenG,j} = V_1 (q_{HPenG,1} + q_{PAAH,1}) + L_n (C_{HPenG,n} + C_{PenG-,n} + C_{PAAH,n} + C_{PAA-,n}) \quad (28)$$

After the simulation, equilibrium is assumed to be achieved when the change in concentration of both side chain and β -lactam nucleus are smaller than 0.1% and all partition and dissociation equilibria are very near to their equilibrium constant.

3.2. The accuracy of the model in predicting experimental results

To study the accuracy of the model, the simulation results are compared with experimental results (Den Hollander *et al.*, 2002). The experimental details and input parameters are shown in Table 4.

Table 4: Experimental details of counter-current PenG hydrolysis

Input variable	Name	Value
V	Organic solvent rate	3.54 g/min
L	Aqueous rate	5.92 g/min
F	Feed rate	3.2 g/min
Z	Concentration HPenG in feed	40.8 mmol/kg
N	Number of stages	3
NF	Feed stage	2
α_V	Fraction of backmixing in organic phase	0
α_L	Fraction of backmixing in aqueous phase	0
	Crystallization	no

The first values for the reaction and mass transfer coefficients were chosen. According to Den Hollander *et al.* (2002), their experiment was at equilibrium. This means that enlarging both constants had no influence on the conversion. The conversion is plotted as function of the reaction and mass transfer constants in Figure 8.

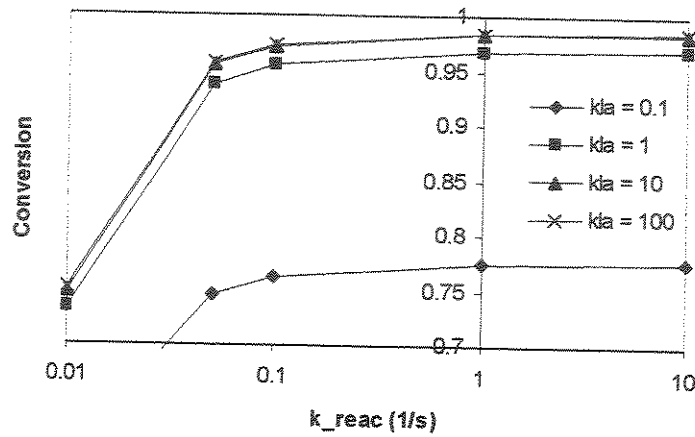


Figure 8: Influence of reaction constant and mass transfer coefficient on the conversion.

As can be seen from Figure 8 for a reaction constant larger than 1 s^{-1} and a mass transfer coefficient larger than 10 s^{-1} the conversion does not increase anymore. Reaction and partition are then also at their equilibrium. These values will be used for designing of a large scale reactor.

In Figures 9 and 10 and Table 5 the experimental and simulation results are shown. This data are obtained from the steady state point of the dynamic simulation.

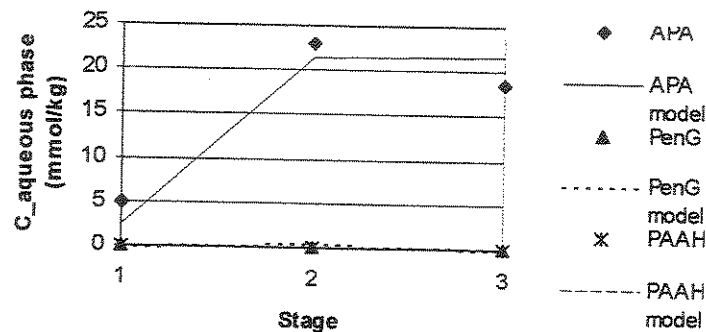


Figure 9: Measured concentrations in aqueous phase (Den Hollander *et al.*, 2002). Model values are indicated with lines

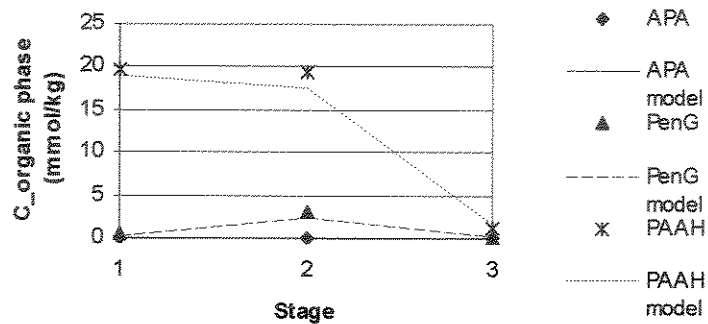


Figure 10: Measured concentrations in organic phase (Den Hollander *et al.*, 2002). Model values are indicated with lines.

Table 5: Theoretical and experimental pH, conversion and purity of components in streams

	Experimental	Model
pH stage 1	3.7	3.68
pH stage 2	3.6	3.63
pH stage 3	3.7	3.72
Conversion	98%	98.3%
Purity APA in aqueous phase	100%	99.4%
Purity PAAH in organic phase	97%	98.5%

The model describes the trend of the experimental results reasonably well.

3.3. Crystallization

If the concentration of APA in the aqueous phase exceeds the solubility, APA will crystallize. The influence of the amount of crystals on the simulation results is examined. Different simulations are tested with different crystal amounts. This assumed amount has direct influence on the supersaturation in the reactor as can be observed from Figure 11.

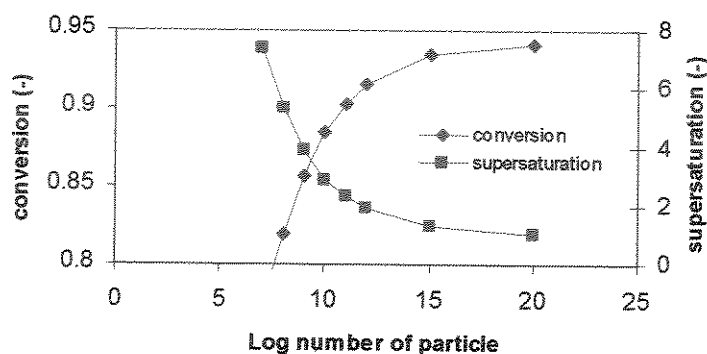


Figure 11: Influence number of particles on the conversion and supersaturation

It is assumed that the supersaturation in the reactor will be low at steady state and according to the Figure 11, the lower the supersaturation the higher the conversion.

3.4. Backmixing

Backmixing interferes with the counter-current flow and causes lower conversion and a decreased separation of the products. With the input parameters shown in Table 4

different simulations are performed by changing the backmixing factor for the aqueous and solvent flow. Resulting conversion and purity of the products are shown in Table 6.

Table 6: Influence of backmixing on conversion and product purity

		Conversion	Purity of PAA	Purity of APA
$\alpha_L = 0$	$\alpha_V = 0$	98.3	98.5	99.4
$\alpha_L = 0$	$\alpha_V = 0.1$	97.9	98.4	98.7
	$\alpha_V = 0.2$	97.5	98.3	98.1
	$\alpha_V = 0.3$	97.3	98.2	97.7
$\alpha_V = 0$	$\alpha_L = 0.1$	97.4	97.7	99.4
	$\alpha_L = 0.2$	96.7	97.7	99.3
	$\alpha_L = 0.3$	96.2	96.4	99.3

The influence of backmixing for this feed concentration is not very high. The influence of backmixing will set the efficiency specifications for the multistage countercurrent reactor.

Analyzing the results of Table 6, it should be pointed out the high level of purity of both products, PAA and APA, proving the viability of the system proposed. In practical applications, the pure APA may be use directly to the semi-synthetic antibiotics and the pure PAA may be recycled to the fermentation process of PenG production.

4. Discussion

In this study different elements that lead to process design of the counter-current reactor are discussed. The process design result has its basis model of counter-current extractive enzymatic reactor that predicts:

- Yield of the process
- Purity of the APA stream
- Stream composition between different stages

The quality of the model predictions depends on the quality of the assumptions that were made in the model. The model describes the experiments performed by Den Hollander *et al.* (2002) reasonably well (Table 5, Figures 9 and 10). But for designing of a large-scale reactor higher feed concentrations of PenG are needed. This leads to crystallization of APA. It is uncertain how good the model is in predicting this situation. The uncertainty of different assumptions is discussed below.

So far, the pH influence on the amidase activity was neglected. As can be seen from the process design results the pH drops below 4. Van der Wielen *et al.* (1996) give an equation for the active fraction of amidase as function of the pH.

$$F_E^0 = \frac{1}{1 + \frac{C_H^+}{K_{aE}}} \quad (27)$$

where F_E^0 is the active fraction of the enzyme, C_H^+ is the concentration of protons in mol L^{-1} and K_{aE} is the kinetic parameter of the enzyme in mol L^{-1} , in this case $8.17 \cdot 10^{-8} \text{ mol L}^{-1}$ (310 K)

When the active fraction is plotted against the pH the following graph is obtained.

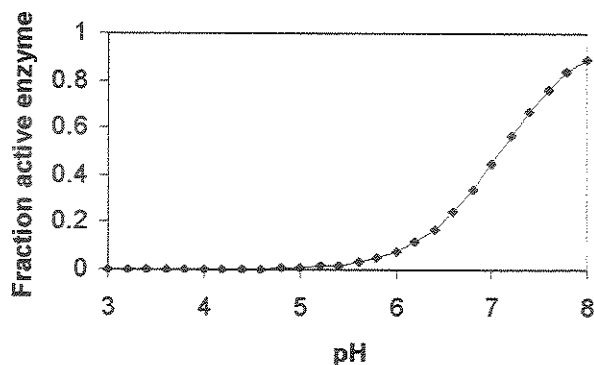


Figure 12: Fraction active enzyme as function of pH.

From Figure 12 can be seen that below a pH of 5 the fraction active enzyme is almost zero. To make the model more accurate, rigorous enzyme kinetics, incorporating enzyme activity, should be. This rigorous kinetics is described by Van der Wielen *et al.* (1996). When this was implemented the model became unstable and it was decided to use the simple description of the enzyme kinetics.

During counter-current experiments performed by Den Hollander *et al.* (2002) the pH in the reactor dropped to 3.7 as shown in Table 5. The enzyme would present very low activity at this pH (Ferreira *et al.*, 2004), but still the conversion of PenG is 98%. The model predictions are in agreement with this. This phenomenon should be further addressed for good model prediction.

The size of the reactor depends to a large extent on the reaction constant k_r of the enzymatic hydrolysis reaction because that is the rate limiting step. It is very important to know this parameter for the process design. It can be seen from Figure 8 that when the reaction constant is larger than 1 s^{-1} this has no effect on the yield. This means that the reaction has run to completeness. Enlarging the residence time, which is related to the reactor volume, will have no effect on the yield. But when this constant is smaller than 1 s^{-1} and, especially smaller than 0.05 s^{-1} , a small deviation will have a large influence on the size of the reactor. So, if the reaction constant of the enzymatic reaction would lie in this range, it is important to measure it very precisely, as it will strongly influence the size of the reactor.

In the partition analysis, the $k_r a$ of the different extraction processes is assumed to be 100 s^{-1} . When it is assumed that the mass transfer coefficient k_t has a value of $10^{-4} \text{ m}\cdot\text{s}^{-1}$ (Van't Riet *et al.*, 1991) the specific surface area per m^3 of reactor volume, a , should be 10^6 m^{-1} . The specific area is calculated from the droplet size by:

$$a = \frac{6\varepsilon}{d_b} \quad (28)$$

With d_b being the droplet size in m and ε being the hold-up of the aqueous phase. When the hold-up is 0.5, the diameter of the droplets in the reactor should be $3 \text{ }\mu\text{m}$. This droplet size seems too small. It can be seen from Figure 8 that decreasing the $k_r a$ by a factor 10 has no effect on the yield and decreasing the $k_r a$ by a factor 100 has only a minor effect on the yield. So a droplet size between 3 and $30 \text{ }\mu\text{m}$ does not influence the process yield and a droplet size up to $300 \text{ }\mu\text{m}$ has only a small effect on the yield. Increasing the droplet size more has a dramatic influence on the yield. It can be concluded that the reactor should be operated at a droplet size smaller than $300 \text{ }\mu\text{m}$ so that the mass transfer is not limiting.

It should be mentioned that crystallization is a very complex phenomenon to measure and to model and in this section it is tried to give an idea which factors concerning crystallization have a large influence on the final design result.

The process yield calculated by the model depends heavily on the assumed supersaturation as can be seen from Figure 11. This again depends on the measured APA solubility and the chosen amount of particles. The best option is to change the model as proposed in item 2.1.4 with particle size distribution. This complicates the model and also information on primary and secondary nucleation is needed. This is not easy to measure accurately.

The simulated crystal size is influenced by the growth rate, the supersaturation and the residence time in the reactor. The growth rate as function of the supersaturation was measured and the results were presented in Chapter IV. The growth rate factor was relatively low.

5. Conclusions

In this work, the process design of a fractionating counter-current enzymatic extractive reactor for the hydrolysis of PenG to APA is presented. This is an alternative process for the existing APA process. The heart of the alternative process design is a series of continuous stirred tank reactors. In these reactors the PenG is extracted from an organic phase to an aqueous phase, where it is hydrolyzed by immobilized amygdase to APA and PAA. The PAA has affinity by the organic phase and is extracted from the aqueous phase. When APA exceeds its solubility it crystallizes. The three-phase system, (aqueous and organic phase and APA crystals) that leaves the reactor is separated in an aqueous crystal phase and an organic phase. The benefit of this new reactor concept over the existing

process lies in: almost complete conversion of substrate by equilibrium limited reaction, separation of products, less unit operation necessary compared to the existing process, less salt produced. The process design results depend strongly on the used assumptions for crystal growth rate, APA solubility and enzyme stability. To increase the validity of the conceptual process design these assumptions should be verified carefully and the model can be adjusted.

6. Reference

DEN HOLLANDER, J.L., ZOMERDIJK, M., STRAATHOF, A.J.J., VAN DER WIELEN, L.A.M.. Continuous enzymatic penicillin G hydrolysis in counter-current water-butyl acetate biphasic systems. *Chem. Eng. Sci.* 2002. 57 (9). 1591-1598.

DIENDER, M.B., STRAATHOF, A.J.J., VAN DER DOES, T., RAS, C., HEIJNEN, J.J.. Equilibrium modeling of extractive enzymatic hydrolysis of penicillin G with concomitant 6-aminopenicillanic acid precipitation. *Biotech. Bioeng.* 2002.78 (4). 395-402.

DIENDER, M.B.. STRAATHOF, A.J.J., VAN DER DOES, T., ZOMERDIJK, M., HEIJNEN, J.J.. Course of pH during the formation of amoxicillin by a suspension-to-suspension reaction. *Enzyme Microb. Technol.* 2000. 27. 576.

FERREIRA, J.S.; STRAATHOF, A.J.J.; L.A.M.; FRANCO, T.T., VAN DER WIELEN, L.A.M.. Activity and stability of immobilized penicillin amidase at low pH values. *Journal of Molecular Catalysis B - Enzymatic.* 2004. 27. 29-35.

INGHAM, J. DUNN, I.J.. HEINZLE, E., PŘENOSIL, J.E. *Chemical Engineering Dynamics. Modeling and Simulation.* Tokyo, VCH. 1994. 701 p.

LI, X.. *Modeling of the crystallization of 6-aminopenicillanic acid*. 2002. Thesis: Master of Science (Doutorado em Engenharia Química) – Department of Biotechnology Delft University of Technology, Delft. The Netherlands.

LO, T.C., BAIRD, M.H.I., HANSON, C.. *Handbook of solvent extraction*, 1991. 980 p.

MINOTTI, M., DOHERTY, M.F., MALONE, M.F.. Design for simultaneous reaction and liquid-liquid extraction, *Industrial and Engineering Chemistry Research*. 1998. 37. 4748-4755.

MULLIN, J.W.. *Crystallization*. Third Edition. Butterworth-Heinemann. 1993. 527 p.

TEWARI, Y.B., GOLDBERG, R.N.. *Thermodynamics of the conversion of penicillin G to phenylacetic acid and 6-aminopenicillanic acid*, *Biophysical Chemistry*. 1988. 29. 245-252.

VAN DER WIELEN, L.A.M., DIEPEN, P.J., HOUWERS, J., LUYBEN, K.CH.A.M.. *A countercurrent adsorptive reactor for acidifying bioconversions*, *Chemical Engineering Science*. 1996. 51. 2315-2325.

VAN ROSMALEN, G.M.. *College dictaat Ontwerpaspecten van apparaten voor de processindustrie, kristallisatie*, TUDelft. 1994

CAPÍTULO VI

A idéia inicial de realizar a hidrólise de PenG em sistema contra-corrente foi a aplicação de colunas de recheio. No entanto, ensaios preliminares demonstraram a baixa eficiência e conversão da coluna de recheio em escala de laboratório para completa conversão da PenG em APA e PAA.

Deste modo, foi necessário buscar um sistema mais adequado de reação e purificação para ser instalado em escala de laboratório. Com as informações disponíveis, foi elaborado um artigo contendo dados necessários para auxiliar na seleção de sistemas específicos de reação e separação empregados na indústria de química fina, em geral.

Este capítulo corresponde a uma revisão bibliográfica que apresenta as diversas configurações de biorreatores extrativos destinados a aplicações específicas, dependendo do tipo do processo e de suas características e limitações. A apresentação dos tipos de equipamentos foi ilustrada com as vantagens de cada configuração, com as restrições dos processos biocatalíticas e com os exemplos práticos de aplicação. As informações dos critérios de seleção e dos tipos de biorreatores foram agrupadas em uma tabela de fácil consulta para a escolha do tipo de configuração desejada. Além disso, foram avaliados dois estudos de caso para demonstração do uso da tabela e das informações apresentadas na revisão. A escolha final de um biorreator extrativo, no entanto, deve ainda ser baseada na combinação da modelagem de processos, experimentos e otimização e avaliação econômica. No entanto, o objetivo desta revisão não abrange estas análise final.

EXTRACTIVE BIOREACTOR TECHNOLOGY

J. S. Ferreira ^{a,b}, A. J. J. Straathof ^a, T. T. Franco ^b, L. A. M. Wielen ^a

^a *Department of Biotechnology, Delft University of Technology, Julianalaan 6., Delft, The Netherlands*

^b *School of Chemical Engineering, State University of Campinas. P.O. Box 6066, 13081-970 Campinas. SP, Brazil*

ABSTRACT

The development of devices that can be used in integrated process represents a fascinating research topic. This integration should allow selectively to remove the product and by-product from the mixture of an enzyme catalyzed reaction, in order to overcome inhibitory or toxic effects. It also shifts unfavorable reaction equilibrium; minimize product losses owing to degradation and reduce the total number of downstream-processing steps. In order to achieve the goal of choosing an appropriate device for integrated production and extraction processes and for use of immobilized biocatalysts, the selection is based on the criteria of each particular system. One of the difficulties of selection of a suitable contactor for extractive bioreaction arises from the wide range of contactor types available for consideration and the large number of design variables involved. Furthermore, it is worth to use a combination of process modeling, experiments, optimization and process economics. Hence, a case-by-case analysis is often necessary before the final choice of a reactor type can be made. The objective of this work is to present a review concerning the selection of various extractive bioreactor equipment for specific process applications based on the respective advantages, limitations and the illustrated applications. The features of extractive bioreactors are compared in a Table based on the criteria for each device that guides the selection for the appropriate set up. Two case studies are evaluated and an appropriate extractive bioreactor is chosen based on the features and criteria presented in this review.

Key words: bioreactor, extractive bioreaction, liquid-liquid extraction, membrane reactors, integrated process.

1- Introduction

Biological conversions are characterized by being performed in aqueous solutions, usually at low temperatures and pressures, and by leading to dilute product solutions and low productivities. These major drawbacks of the biotechnological processes, when compared with the traditional chemical processes, are due to low biocatalysts concentrations in the reactor, inhibition end products, low substrate and/or product solubilities in the aqueous bioconversion media and equilibrium limitation imposed by reversible reaction. The technological approaches to circumvent these problems are based on the increase in the biocatalyst density using immobilized biocatalyst preparations and the integrated production and separation using the *in situ* extraction of bioproducts (Cabral, 1991; Kachasakul *et al.*, 2003). These techniques lead to enhanced rates of mass transfer, decreased level of product inhibition, facilitated product recovery and reduced reaction volume for a given amount of product (Sajc *et al.*, 2000). Moreover, single units that combine reaction and separation operations have received considerable attention, since the reduction in the number of equipment units leads to investment saving (Kachasakul *et al.* 2003).

Concerning on purpose of adapting bioreactor to carry out reactions with immobilized biocatalyst, they are considerably smaller than those for free enzymes and cells due to the higher concentration of the biocatalyst. Techniques have been developed to increase the biocatalyst concentration in the reactor and thus retention for continuous process operation (Hoss, 2000), namely, separation of the biocatalyst at the reactor outlet by sedimentation, flotation, filtration, and centrifugation or by recycling part of the biomass; retention of the biocatalyst by micro or ultrafiltration membranes; and fixation of the biocatalyst on supports or by gel entrapment, encapsulation, adsorption, etc., followed by flocculation and pelletizing.

In order choose a device appropriate for integrated production and extraction processes and for use of immobilized biocatalysts, the selection is based on the criteria of

each particular system. One of the difficulties of selection of a suitable contactor for extractive bioreaction arises from the wide range of contactor types available for consideration and the large number of design variables involved (Pratt and Hanson, 1991). Furthermore, it is worth to use a combination of process modelling, experiments, optimization and process economics. Hence, a case-by-case analysis is often necessary before the final choice of a reactor type can be made (Mills and Chaudhari, 1997).

In the following section (Section 2), we are going to present the different equipment that can be applied in integrated production and separation, showing a wide number of practical examples of medium reactions, biphasic or multiphase systems. The advantages and limitations are discussed for each equipment. The features of extractive bioreactors are compared in a Table based on the criteria for each device that guides the selection for the appropriate set-up (Section 3). In Section 4 of this review, two case studies are evaluated and an appropriated extractive bioreactor is chosen based on the features and criteria presented in this review.

2- Classification of the Extractive-Bioreactor

In this section, a classification of the different types of extractive-bioreactors will be presented, including their general characteristics and a simplified form could be consulted in Table 1.

These devices will be separated in the following sequence:

- 2.1- Mixer-settlers;
- 2.2- Centrifugal extractors;
- 2.3- Columns;
- 2.4- Airlift and loop reactors;

2.5- Raining Bucket or GRAESSER RTL extractor;

2.6- Membrane reactors.

2.7- Reactive Chromatography

2.1- Mixers-Settler

The range of applications of mixer-settlers is now very large, and equipment is available in a wide variety of shapes and sizes (Godfrey and Slater, 1991). Besides many new designs and developments in the field of bioreactors, Hoss (2000) reported that, about 80 % of all biochemical reactions are carried out in stirred-tank reactors. Stirred-tank reactors with different stirrers and mixers are mainly used for immobilized and suspended cells. They are often chosen when the separation requires many equilibrium stages, when extraction kinetics are not rapid and when the separation flow sheet is complex and requires precise location of incoming feed streams with respect to counter-current extraction in multi-solute systems (Pratt and Stevens, 1992). The controllability and flexibility of the stirring tank reactor in terms of independent adjustment of mixing and aeration makes it the most frequent equipment of choice, despite several limitations, such as high power consumptions, high shear, and problems with sealing and stability of shafts in tall bioreactors (Sjac *et al.* 2000).

Industrial gravity settlers are usually horizontal cylindrical or rectangular tanks in which the liquid-liquid dispersion is continuously fed at one end and the separated phases are withdrawn at the other end (Figure 1.a) (Godfrey and Slater, 1994).

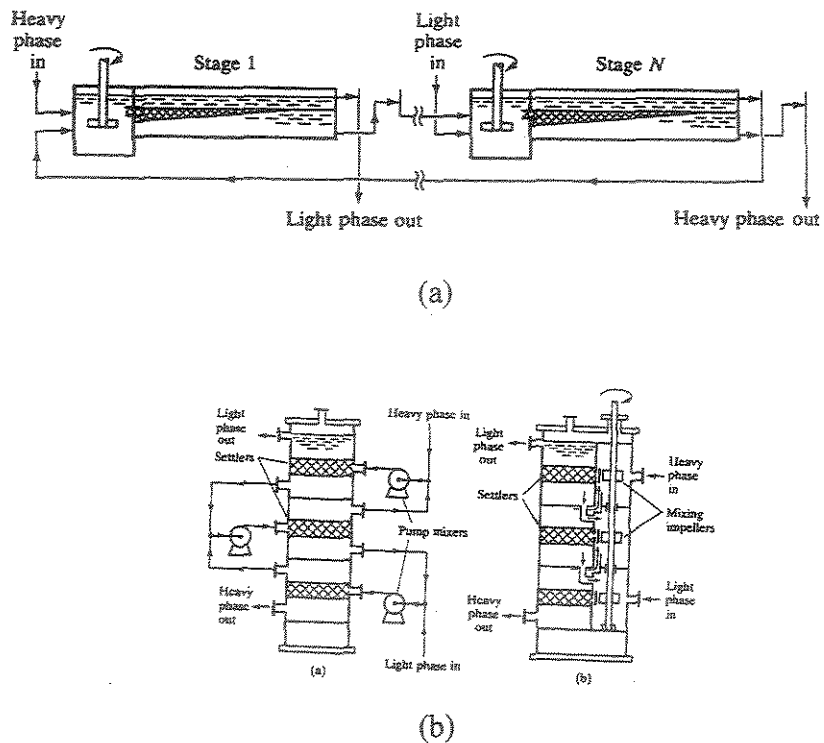


Figure 1: Scheme of a) a two-stage horizontal mixer-settler and b) a vertical settler set-ups (Pratt and Markl, 1992).

A variety of practical examples are presented in the literature. Van Sonsbeek, *et al*, (1993) reported two basic experimental set-ups for extractive fermentation with stirred-tank reactors. The first set-up, shown in Figure 2 (a), is the simpler one, but it can lead to a rather stable emulsion that requires a long settling time. In this case, an external extraction column as shown in Figure 2b is more favourable because emulsion formation is less vigorous. Furthermore, an external extraction column is also more effective because it is a multistage contactor, whereas for direct solvent addition, only one equilibrium stage can be achieved.

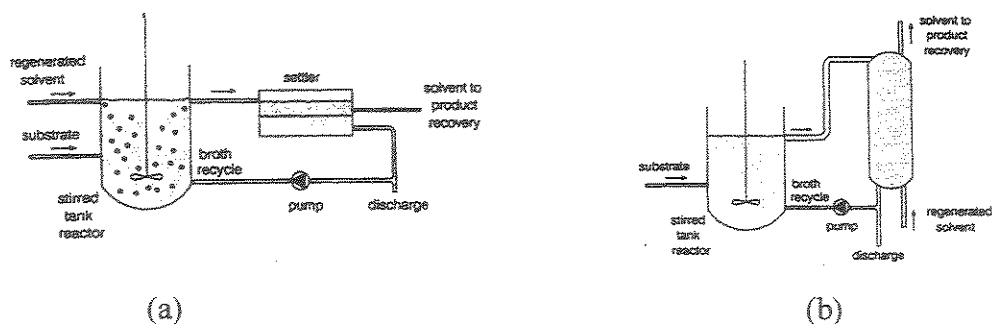


Figure 2: Extraction with (a) direct solvent addition and (b) contacting in an external vessel
(Van Sonsbeek *et al*, 1993)

A different arrangement of mixer settler was proposed by Anwar *et al.* (1998), in order to separate quinoline and iso-quinoline in a multistage countercurrent extraction, and is presented in Figure 3. This unit provides stagewise contacting and complete flexibility in the number of stages used. The design is simple, relatively inexpensive and completely hydraulically independent.

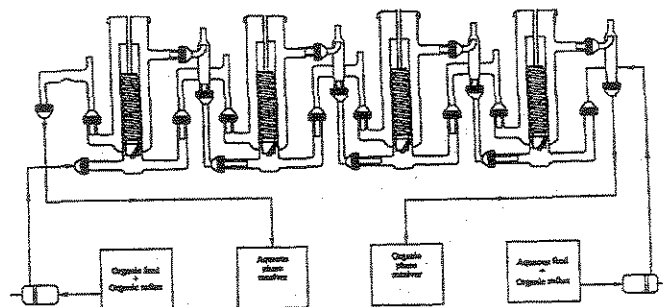


Figure 3: Arrangement of mixer-settler for separation of quinoline and iso-quinoline
(Anwar *et al.* 1998).

2.2- Centrifugal Extractors

The centrifugal extraction equipment was developed for biotechnological practice. This equipment is usually operated in a countercurrent mode. It is especially for systems exhibiting a small density difference, a strong tendency to emulsification or requiring short contact times. Their main advantages are extremely high throughput; very short contact times (few seconds) which is important for the extraction of unstable solutes; low solvent volume in the extractor. On the other hand they present high investment costs; high variable costs; and high pressures (up to 100 bar) can occur locally at the periphery of the rotating cylinder (Schürigel, 1994).

Their performance is evaluated in terms of number of theoretical stages, which varies within the range 2-7, depending upon the particular system used and the required flow ratio (Pratt and Stevens, 1992; Godfrey and Slater, 1994).

Successful applications of centrifugal extractors are reported concerning on the antibiotic production (Kusnetsov *et al.*, 1993). For instance, Podbielniak extractor was a popular industrial version which was first used for penicillin extraction. The stage of extraction in antibiotic production is characterized by a number of problems which are associated with formation of stable emulsions, with considerable losses from decomposition of the antibiotics, and with large volumes of highly volatile, expensive and toxic extractants. These problems can best be solved by the use of multistep centrifugal extractors, in which a high separation factor of the emulsions is achieved with comparatively small volumes. CENTREX centrifugal extractors makes it possible to reach a high efficiency (93-96%) of extraction at every stage due to the intensive stirring of the operation solutions provided by the structure of the extractor (see Figure 4).

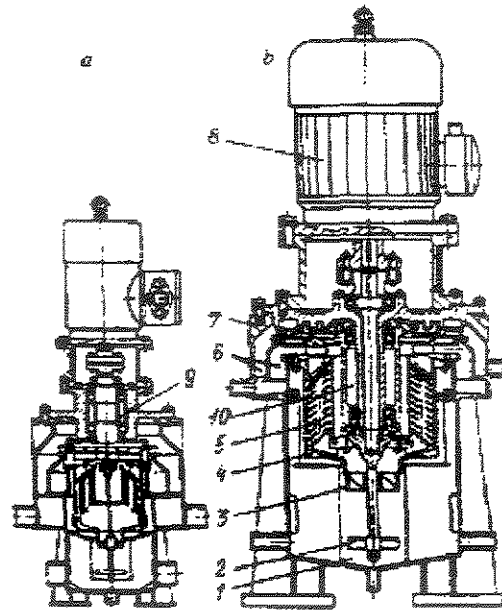


Figure 4: CENTREX centrifugal extractors (Kusnetsov *et al.*, 1993)

Recently Westfalia has developed an Extractor-Decanter (Figure 5), which is used for the direct extraction of antibiotics from fermentation mycelial broths without further separation. It is built with two practical stages and it was obtained with an antibiotics-yield of 97-98% (Schürigel, 1994, Godfrey and Slater, 1994).

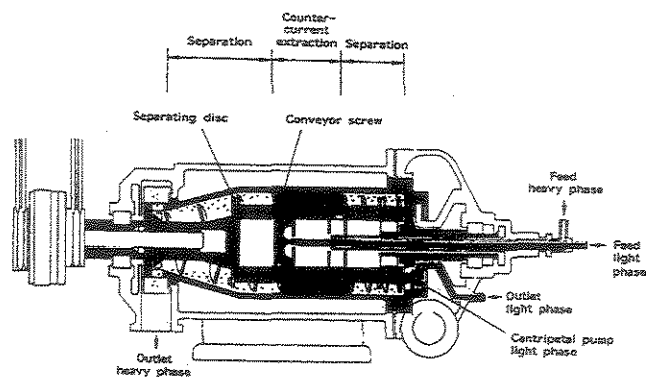


Figure 5: Westfalia axial countercurrent centrifugal extraction decanter (Godfrey and Slater, 1994).

Westfalia overcomes the disadvantages of limited mass transfer performance by employing an axial countercurrent flow of the liquid phases in a rotating drum with special installations. The hydrodynamics conditions remains constant along the extraction path and it is generally possible to increase the mass transfer performance by enlarging the extractor length to a greater degree than in radial machines. The transport of solids is possible without damaging the internals and a very slight difference in height along the tube is sufficient to provide axial countercurrent flow of the two liquid layers (Godfrey and Slater, 1994).

Komives *et al.* (1994) evaluated a continuous centrifugal reactor for the degradation of pesticides in a reversed micellar medium. A continuous-flow centrifugal reactor was demonstrated for carrying out enzyme-catalyzed reactions in two-phase microemulsion systems. Because the enzyme essentially is completely retained in the microemulsion phase due to hydrophilic properties, it is effectively immobilized in the reactor. The conversion in the reactor was limited by partitioning of the substrate between the organic phase and the microemulsion aggregates, but more significantly by the product

inhibition. Mechanical means can be employed. For example, the introduction of channels in the centrifuge tubes would increase the contact time between the phases.

The centrifugal bioreaction-separation principle based on the rate-zonal centrifugation process was applied in order to evaluate the biosynthetic formation and simultaneous sedimentation of native dextran (Setford, 1999). The slowly sedimenting by-product was removed from the more rapidly sedimenting biocatalytic zone by virtue of sedimentation velocity differences. Figure 6 shows a Beckman model J2-MC centrifuge fitted with a JCF-Z Zonal Rotor and Reorienting Gradient core used in the combined centrifugal bioreaction-separation process (Setford and Barker, 1994). Zonal rotors have a number of advantages over conventional centrifuge bucket rotors: larger gradient and sample volumes can be loaded; the samples can be applied to the gradient while rotor is spinning (dynamically), wall effects are minimized, and the contents of the rotor can be unloaded after centrifugation with no appreciable loss in sample resolution.

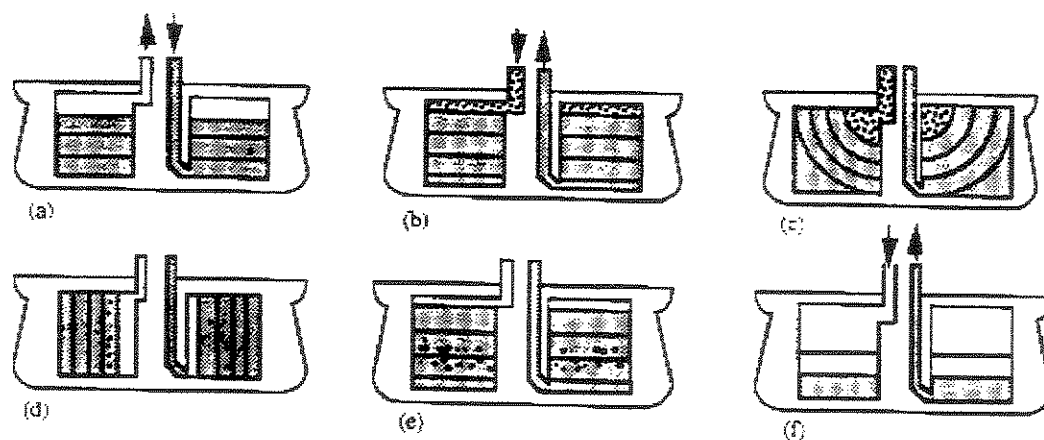


Figure 6: Operating principle of the Beckman JCF-Z Zonal Rotor containing Reorienting Gradient core (Setford and Barker, 1994)

2.3- Columns

The application of columns as extractive bioreactions comprises a wide variety of equipment, with adaptations of agitators or mechanical power input in order to overcome the drawbacks concerning on the mass transfer and low number of stages. Specifically, to design an extraction column, the level of agitation should be taken into account. It must be controlled carefully because the reduction in drop size reduces the capacity of the column for countercurrent flow. Excessive agitation can lead to flooding, foaming, or entrainment of droplets in the continuous phase. Recently, increasing attention is being directed to the non-uniformity in the dispersed phase drop-size distribution. Another disadvantage of excessive agitation is higher axial mixing; and the resulting decrease in the number of equivalent stages may offset the advantage of higher interfacial area (Godfrey and Slater, 1994).

A sequence of the different equipment of columns applied as extractive bioreactor is presented below:

2.3.1- Spray Columns

The spray columns provide a low shear environment very appropriate for the enzyme stability. Roode *et al.* (2001) developed a bioreactor for the semi-continuous production of hexyl glucoside. The half-life time of the enzyme was almost 30 days, whereas the enzyme is totally deactivated in 40 h in a CSTR. The high deactivation rate in a CSTR may be caused by vigorous stirring in combination with the presence of an air-liquid interface and a large polar/apolar liquid interface.

2.3.2- Packed Columns

Fixed beds (Figure 7) are characterized by simple design, operations with minor maintenance, and low backmixing and hence represent the reactor design of choice for continuous operation with immobilized biocatalysts (Huneke and Flaschel, 1998). The packed column is suitable for protein extraction due to moderate mixing and shear stress caused by a stable counter current operation over a wide range of slow rates (Nishi *et al.*, 1999). In liquid-liquid extraction the role of the packing is to reduce large-scale convective mixing or axial dispersion in the continuous phase and to provide surfaces to allow breakage and coalescence of the dispersed phase to enhance mass transfer (Godfrey and Slater, 1994).

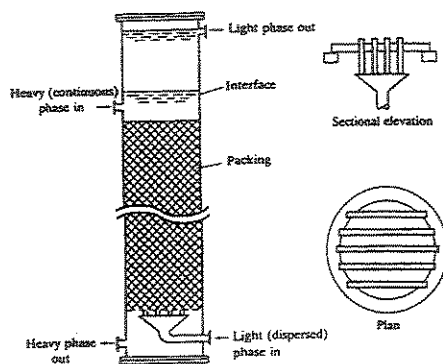


Figure 7: Typical construction of a packed column (Godfrey and Slater, 1994)

Nevertheless, because of the tendency of the phases to flow along the wall, the substrate may be not adequately supplied, thus reducing performance. The substrate limitation, in addition, causes a local decrease of buffer capacity lowering the pH, and, thereby, lowering the enzymatic activity. It has been shown that the choice of the non-polar

phase may be a crucial issue (Huneke and Flaschel, 1998). In order to overcome this drawback, it is common to install redistributors in industrial columns if relatively large packing is being used (Godfrey and Slater, 1994). Moreover, although packed bed reactors are advantageous in that a large amount of cells can be immobilized per unit volume, diffusional limitations of mass transfer to the immobilized cells, as well as the difficulties in supplying and removing gaseous components can limit the use of this equipment for biotransformations (Sjac, *et al.*, 2000).

The performance of packed columns can be improved by mechanical pulsation of the continuous phase, at the expense of a reduced throughput. The columns adapted with this device is named *Pulsed Packed Columns*. The increased performance results from greater shear forces causing a reduction in drop size with an associated increase in interfacial area and mass transfer rate. (Pratt and Stevens, 1992; Godfrey and Slater, 1994).

2.3.2- Pulsed Sieve-Plate Columns

Mass transfer rates could be improved adding mechanical energy in the form of superimposed agitation or pulsation, resulting in higher turbulence at the interface and larger mass transfer area due to smaller drop sizes. In addition, the extra energy input gives greater flexibility in operating the column, but requires a more complex and costly design. If a larger number of theoretical stages is required, agitated or pulsed columns offer an economical solution (Godfrey and Slater, 1994; Pratt and Stevens, 1992). Two different types of pulsed sieve-plate columns have to be distinguished:

2.3.2.1- Liquid pulsed sieve-plate extractors (PSE): (Figure 8) were first applied in the solvent extraction of radioactive materials in the 1940s and although their use was not mentioned yet, these devices present characteristics suitable to bioprocess criteria. Numerous investigations have shown that high throughput, high separation efficiency and insensitivity towards contamination of the interface characterize this type of extractor.

These favourable properties and the simple design of the column have resulted in a widespread application of the type of extraction equipment in industry and although the performance deteriorates as a result of increased backmixing, this can be partially overcome by suitable baffling. However, liquid pulsed sieve-plate extractors should not be used for sticky and greasy liquid and for liquid-liquid systems, which emulsify easily (Godfrey and Slater, 1994).

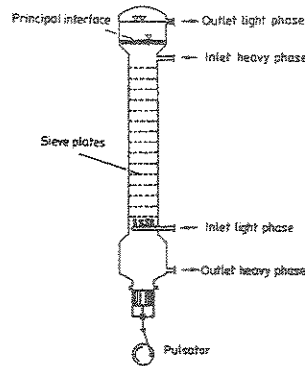


Figure 8: Scheme of pulsed sieve-plate extraction column (Godfrey and Slater, 1994).

2.3.2.2- Reciprocating-plate columns (RPC): They have been widely used in the pharmaceutical, in diameters up to 1.5 m, (Figure 9). They suffer deterioration in performance on scaling up the diameter as a result of increased backmixing and channelling, despite maintaining the plate spacing constant (Pratt and Stevens, 1992).

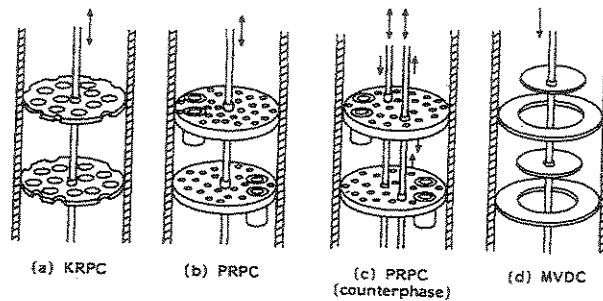


Figure 9: Some types of reciprocating plate column (Godfrey and Slater, 1994).

Two different and most applied RPC designs are:

a) KARR RPC: The KRPC was initially developed for applications in the pharmaceutical industry. The optimum plate spacing relates to the density difference and interfacial tension of the system being used. Increased spacing is recommended for systems with low interfacial tension and low density difference which do not require strong agitation; and vice versa (Godfrey and Slater, 1994).

The advantages of the Karr columns are (Schürigel, 1994):

- High throughput and high mass transfer as well as high volumetric efficiency;
- High degree of versatility and flexibility;
- Easy handling of emulsifiable material and liquids with suspended solids.

b) PROCHASKA RPC: Have downcomers segments for the continuous phases that reduce the hindering effect of continuous phase on the dispersed phase flow through the perforations and thus enhance the column capacity. The alternation of downcomers on neighbouring plates creates a cross-flow of phases in the stages, which improves radial homogeneity and reduces efficiency deterioration in scaling-up of PRPCs.

The mechanical strains in PRPCs are relatively low. The pressure pulsation at the bottom of the column is practically eliminated and a high mechanical stability is reached in columns with counterrotation of plates. In these columns a reduction in axial mixing intensity was also observed (Godfrey and Slater, 1994).

2.3.3- Baffle-Plate Columns

These columns are equipped with side-to-side or ‘disc and doughnut’ baffles, in order to reduce continuous phase backmixing and to induce coalescence and redispersion of dispersed phase (Figure 10). They give a moderate performance, and should be considered for use with ‘dirty’ systems, i.e. those containing solid matters, or with a tendency to emulsify specifically those in the presence of biological materials. They also state that the contact efficiency is of the order of 0.05-0.10 theoretical stages per plate, which although low, leads to a reasonable column height for many purposes with the plate spacings normally used (Pratt and Stevens, 1992).

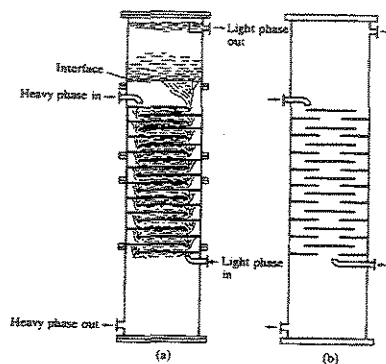


Figure 10: Baffle-plate column: (a) side-to-side; (b) disc-and-doughnut type (Pratt and Stevens, 1992).

2.3.4- Rotary-Agitated Columns

This group comprises the rotary disk, multiturbine (Oldshue-Rushton) and Kuhni columns, all of which give comparable performances (Figures 11a, 11b and 11c,

respectively). These contactors have all been used for non-emulsifying systems in pharmaceutical industries. However, they suffer deterioration in performance on scale-up to large diameters, as a result of increased backmixing and the need to increase compartment height in order to maintain a satisfactory mixing geometry.

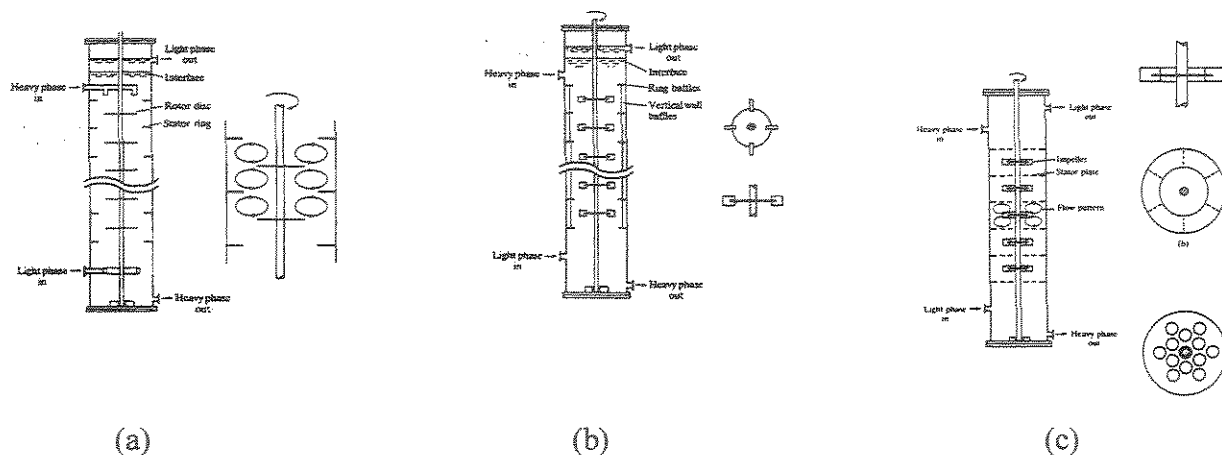


Figure 11: (a) Rotary disc column, (b) Oldshue-Rushton column, (c) Kuhni column (Pratt and Stevens, 1992).

Among of these three devices, Rotary disc column (RDC) presents more flexibility to handle systems containing solids, as in the purification of crystals, the washing of solids, and the extraction of glycerine from soap curd (Figure 11a).

The Kuhni column shown in Figure 11c, consists of an assembly of turbine mixers and the stator plates permit axial flow through the column, but isolate the compartments more thoroughly than is the case with the RDC and Oldshue-Rushton types. This reduces backmixing, especially of dispersed phase. Nevertheless, its structure makes assembly and disassembly for cleaning and maintenance, more difficult (Schürigel, 1994; Pratt and Stevens, 1992).

2.3.5- Scheibel Columns

Besides Scheibel columns present features adequate, so far, no citation of their application in bioprocess was found in the literature. As it can be seen in Figure 12, the function of the packing is twofold; firstly, it isolates the agitator flow patterns between adjacent stages, thus reducing backmixing; and secondly, it induces coalescence of the droplets and separation of the phases. In addition, annular baffles are provided at the column wall to divert the vertical flow of the phases and reduce mixing. The packed sections appear to lead to increased mass-transfer rates, although at the expense of reduced capacity; with systems of high interfacial tension, the packing is sometimes omitted (Pratt and Stevens, 1992).

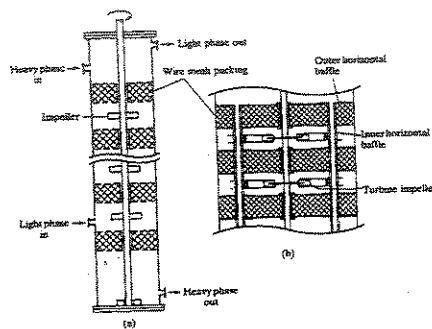


Figure 12: Scheibel column: (a) first type, (b) second type (Pratt and Stevens, 1992).

2.4- Airlift and Loop Bioreactors

Jet loop bioreactors are being widely applied in a number of chemical and biochemical processes which involve gas-liquid reactions (Jamshidi *et al.*, 2001). Airlift bioreactors combine high loading of solid particles and good mass transfer which are inherent for three-phase fluidized beds. Efficient mixing in the liquid phase is generated by

air bubbles, using internal or external recirculation loops. The liquid circulation originates from the difference in the bulk densities of the fluid in the riser and the downcomer. High linear liquid velocities are attainable without recycle and this leads to improved turbulence and good mixing, heat and mass transfer (Sajc *et al.*, .2000).

On the whole, their characteristics are: mechanically simple and robust; gentle, low shear levels (suitable for tissue culture, plant cells, fragile genetically engineered microorganisms flocculating and foaming fermentation systems); high gas throughputs are possible; easy to clean, extended aseptic operation is possible (useful in continuous operation); more uniform distribution of turbulence; limited operational flexibility, low energy requirements and simple design (Sajc *et al.*, .2000, Hoos, 2000; Chisti and Moo-Young, 1991).

An appropriate example of extractive biocatalysis is a type of continuous biological production process that is even improved, by *in situ* recovery of the product is the work developed by Gianetto *et al* (1988). The reactor is an external-loop reactor, in which liquid circulation is induced by a gas flow in one of the vertical tubes and ethanol is extracted by a countercurrent extraction in the other tube (Figure 13).

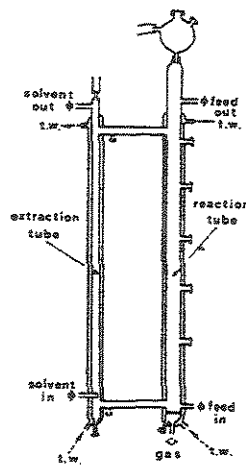


Figure 13: Continuous extraction loop reactor (Gianetto *et al.*, 1988).

Further applications are known such as, the development of an air-lift bioreactor in the use of a low affinity organic phase to selectively extract precursors and end secondary metabolites (Tikhomiroff *et al.*, 2002) and the development and design of an external-loop air-lift bioreactor for continuous production and extraction of plant cells extracellular metabolites. The latter system was regarded as a four-phase system, with dispersed gas, liquid solvent and calcium-alginate-immobilized cells in plant cell medium. In this case, the bioreactor design retained the advantages of using immobilized cells as biocatalysts, but utilizes continuous liquid-liquid extraction of plant cell products in a four-phase flow (Sajc *et al.*, 1995).

2.5- Graesser Extractor

The Graesser raining bucket contactor offers a very promising technology for the treatment of phase systems with low-density difference and low interfacial tension with marked emulsification tendencies (Coimbra *et al.*, 1994). The fact that the drops that are eventually formed by the natural break-up of the stream leaving the buckets are relatively large means they tend to be oscillating, this promoting interfacial renewal and good mass transfer is achieved with comparably less power consumption. In addition, the gentle rotation avoids the formation of emulsions (Jarudilokkul *et al.*, 2000). The droplets are relatively large in comparison to those in other extractor types, but despite this the performance, expressed as number of theoretical stages per meter length, is high. On the other hand, the throughput is relatively small (Figure 14). In general, it requires little headroom, is simple to maintain, and they are suitable to handle aqueous two-phase systems, which are used in the recovery of proteins (e.g. enzymes) from disrupted cells (Schürigel, 1994; Pratt and Stevens, 1992), whey protein (Coimbra *et al.*, 1994) and proteins from fermentation broths using reverse micelles (Jarudilokkul *et al.*, 2000).

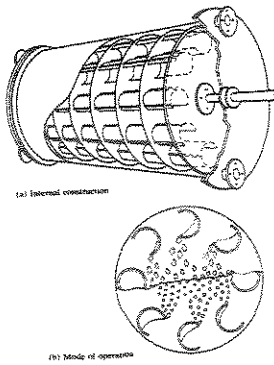


Figure 14: Schematic view of the Graesser contactor (Pratt and Stevens, 1992).

2.6- Membrane Bioreactors

Nowadays, several experts have been performed in order to develop techniques using membrane bioreactors.

The application of membrane reactors is useful to product removal in situ (Dudukovic, 1999). The membrane has the following functions: retention of the biocatalyst; immobilization of the biocatalyst; supply of substrates; removal of products; separation of two fluid phases (perstractive and pervaporative fermentation); modification of selectivity by controlled interaction of reaction and mass transport (HOSS, 2000; Sisak *et al.*, 2000).

Membrane reactors can act as supports for the interface between two liquid immiscible phases provide a high-surface area of contact between both phases, guarantee phase separation during the process, minimize phase toxicity, and make the integration of bioconversion, product recovery and concentration easier (León *et al.*, 2001)

Enzyme membrane reactor, in which and enzyme reactor coupled to ultrafiltration or dialysis membrane with a suitable molecular with cut-off, is capable to keep enzyme and

other larger components, while low-molecular-weight-molecules, e.g., products and/or inhibitor, are allowed to pass freely through the membrane (Wenten and Widiassa, 2002). The biocatalyst can be present free in the retention space, immobilized on a solid support, adsorbed as a membrane boundary layer, or immobilized in the membrane pores. In the latter case, a relatively large surface is used as well as the contacting area between the organic and aqueous phases (Sisak *et al*, 2000).

The number of attempts to utilize membrane reactor has been growing as technology. It is possible to find out different researches in several kinds of process. Van Sonsbeek *et al.* (1993), in their review, reported a membrane bioreactor in which two liquid phases are not in direct contact, but separated by a membrane. The membrane also serves as immobilization support for the biocatalyst, usually an enzyme. Figure 15 presents a schematic process that takes place in such reactor. The reaction is an enzymatic esterification of glycerol and fatty acids with the enzyme lipase immobilized on a hollow-fibre membrane, which keeps the polar and apolar liquid phases separated and this gives the possibility of selective adsorption of monoesters with an adsorption column in the apolar circuit.

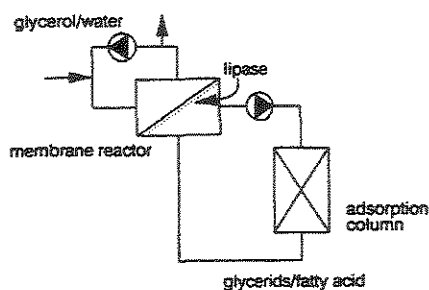


Figure 15: Schematic process design for esterification with a membrane system (Van Sonsbeek *et al*, 1993).

By concerning dialysis, Portner and Markl (1998) reported some examples of extraction, in which product inhibition takes place. The scheme of a laboratory-scale system for suspended cells consists of two reactors, each of which can be stirred separately (Figure 16)

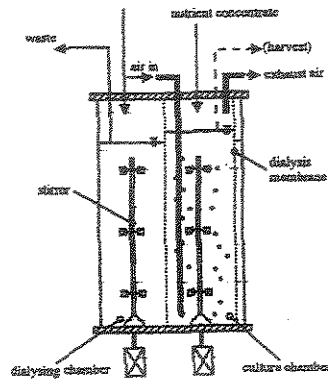


Figure 16: Scheme used in dialysis (Van Sonsbeek *et al.*, 1993)

Hollow fiber membrane is been widely applied in extractive bioreactions, like in extractive fermentation process for butyric acid production form glucose where cells were immobilized in a fibrous-bed bioreactor (Wu and Yang, 2003); in continuous hydrolysis of Penicillin G where penicillin acylase was entrapped within membrane pores and due to the much smaller size of the product, 6-aminopenacillanic acid, compared to the membrane pore, the solute diffuses freely through the membrane (Wenten and Widiase, 2002). Lopez and Matson (1997) evaluated enzyme-catalysed reactions that take place in aqueous solutions, with substrates with very low water solubility. The authors suggested a device which uses the hollow-fibre membrane to immobilize the biocatalyst while placing the enzyme-containing (membrane) phase in direct contact with the substrate-containing (organic) phase, thereby avoiding the intervention of the bulk aqueous phase as occurs in dispersed-phase systems. In addition, the reversible enzyme containment technique (Figure 17) adds to the versatility of multiphase membrane reactors by avoiding covalent enzyme immobilization and facilitating replacement of deactivated enzyme in the field.

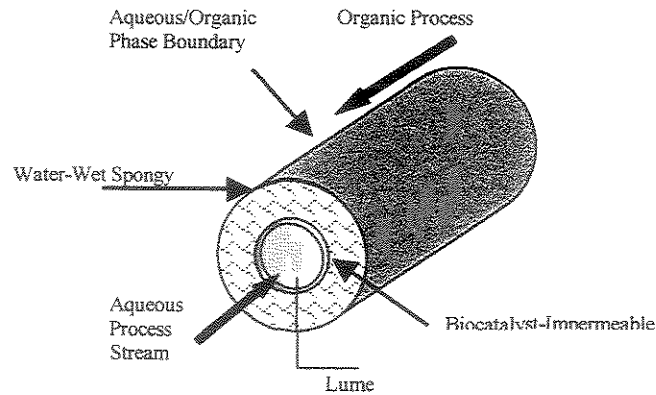


Figure 17: Reversible enzyme containment (Lopez and Matson, 1997)

Finally, the last example is the work by Sahoo *et al.* (1999), The authors studied the non-dispersive reactive extraction of cephalosporin antibiotics using hollow fibre membrane modules. Figure 18 shows the schematic diagram of the experimental set-up. The same membrane module was used for extraction as well as stripping. They concluded that the technique of dispersion free reactive solvent extraction in HF membrane was successfully applied to recover cephalosporins form dilute aqueous solution as well as fermentation broth. There appears to be an appreciable degree of flexibility regarding the flow rates of the phases, the pressure drop may not be a limiting factor for operation of the hollow fibre module.

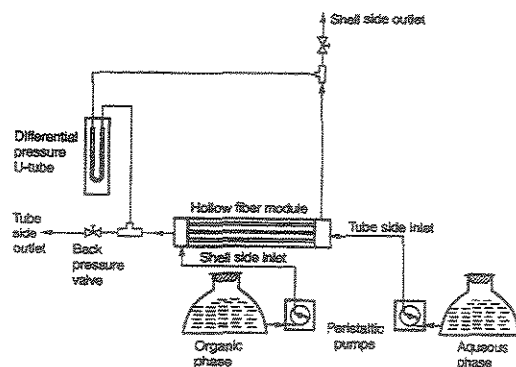


Figure 18: Schematic diagram of the experimental set-up (Sahoo *et al.*, 1999).

2.7- Reactive Chromatography

As a review concerning on the extractive bioreactions, there should be a section reporting the advances provided by chromatographic process.

A chromatographic reactor-separator can be defined as a chromatographic system that is used to convert one or more components partially or totally and to simultaneously separate one or more of the products that are formed. The reaction can take place on the stationary phase, in the mobile phase, or both (Ching and Lu, 1997). It represents an alternative reaction-separation unit which utilizes differences in adsorptivity of the different components involved rather than differences in their volatility. It is, especially, attractive as an alternative to reactive distillation when the species involved are either non-volatile and sensitive to temperature, as is the case, for example, in some fine chemicals or pharmaceutical applications, or exhibit small volatility differences (Lode *et al.*, 2003).

Common to all reactive chromatography processes operated in the classical batch mode are low efficiency in utilizing the stationary phase inventory and large eluent (or desorbent) consumption resulting in an excessive dilution of the final products, in addition

to the usual disadvantages connected with discontinuous operation. This same problem is encountered in the case of purely separative chromatography, but significant improvements have been accomplished recently by transforming these operations into continuous processes. Technically, this has been done in two different ways that is through annular as well as Simulated Moving Bed Reactor (SMBR) (Lode *et al.*, 2001).

Simultaneous bioreaction and separation has been successfully carried out in a Continuous Rotating Annular Chromatography (CRAC) (Sarmidi and Barker, 1993) and in a Simultaneously Countercurrent Chromatographic Bioreactor-Separator (SCCR-S) (Shieh and Barker, 1995) used as bioreactor-separators for the saccharification of modified starch to produce maltose in the presence of enzyme maltogenase.

When compared with other competing technologies, the major advantages of SMBR are the low operating temperature and the adsorptive separation, making it especially attractive for example to applications involving natural products or fine chemicals. The major drawback is the large desorbent requirement, especially when applied to the wide category of water forming reactions, catalyzed for example by sulfonic acid ion-exchange resins. Here, the resulting dilution of the extract and raffinate streams has a substantial negative impact on process economics due to the increased effort required by the subsequent solvent recovery. Therefore, in order to improve the economics of SMBR units the focus should be placed on the development of more suitable solid phases (Lode *et al.* 2001).

3- Selection of Extractive Bioreactor

In this section, the information presented aforementioned is used to create Table 1 based on the criteria of different types of reaction and the features of each device presented in the Section 2. The purpose of Table 1 is to provide enough information to guide the selection a suitable device under some constraints. For a better understanding of the Table,

the plus and minus signs mean that the equipment is or is not appropriate for such criteria. The criteria are listed below:

- Number of stages: important feature for reaction whose mass transfer is a drawback, for instance, in a two-phase system, the reactants and products present low partition coefficient;
- Short residence time: biological medium is sensitive to hard reaction conditions. Usually, the biocatalysts, microorganisms or products undergo degradation under long residence time in the equipment;
- Ability to handle solids: the device must stand solid compounds, i.e., crystals, and biocatalysts in solid form, e.g., immobilized cells or enzymes;
- Tendency to emulsify: generally it is a characteristic of liquid-liquid phase systems, which the density difference is very short;
- Compact: the device should occupy small area;
- Ease of cleaning;
- Low maintenance;
- Equipment cost;
- No moving parts;
- Easy scale-up;
- Simple design;
- Low backmixing: promote good mass transfer and avoid channelling;
- Immobilized enzyme: availability to stand /support immobilized enzyme in different ways: the biocatalysts could be immobilized to the parts of the device, attached to a support or to a membrane inside of the bioreactor;

- pH control: it is necessary to control the pH, in order to keep it constant, when it tends to drop or increase as the reaction takes place;
- Position of feed: the evaluation of different position of the substrate feed is worth, when handling multistage devices.
- Easy control.

Table 1: Selection of types of reactor:

Criteria	Mixer-settlers		Centrifugal Extractors	Columns						Airlift/ Loop	RTL	Membrane Bioreactors
	Horizontal	Vertical		Packed	Pulsed Sieve-Plate		Baffle Plate	Rotary Agitated	Scheibel			
					PSE	RPC						
Number of stages	++	++	--	--	++	++	--	++	++	--	++	++
Short residence time	--	--	++	--	--	--	--	--	--	--	--	--
Ability to handle solids	+/_	+/_	--	--	+/_	++	++	--	--	+/_	+/_	++
Tendency to emulsify	--	--	++	--	--	++	++	--	--	--	++	++
Compact	--	++	++	++	++	++	++	++	++	++	--	++
Ease of cleaning	+/_	+/_	--	++	+/_	++	+/_	++	--	++	+/_	++
Low maintenance	+/_	+/_	--	++	+/_	+/_	++	++	--	++	++	++
Equipment cost	--	+/_	--	++	++	++	++	+/_	+/_	--	+/_	--

4- Case Study

4.1- Synthesis of the aspartame precursor *Z-Asp-Phe-OMe*

Background: There is a rapidly growing market for enantiometrically pure compounds, which are used as active ingredients or as a basis for powerful new drugs. One of the most well-known peptides is aspartame that is 200-fold sweeter than sucrose, and has been used throughout most of the world. The synthesis of the aspartame precursor *Z-Asp-Phe-OMe* is also one of the most widely used model reaction systems in enzymatic dipeptide synthesis (Murakami *et al.*, 2000, Erbeldinger *et al.*, 2001).

Characteristics of the reaction: The yield of synthesis of aspartame precursor in a pure aqueous monophasic system is very low. The optimal pH for thermolysin activity for the synthesis is 6.9 in pure aqueous and in aqueous system saturated with acetic esters, such as, amyl acetate, ethyl acetate and butyl acetate and the enzyme is stable at pH 5.5-9.0. However, the synthesis at low pH provides the suppression of the nonenzymatic decomposition of the substrate L-phenylalanine methyl ester (L-PheOMe) and a lower requirement of NaOH for pH adjustment (Murakami and Hirata, 1997). The extractive bioreaction proposed in the literature (Hirata *et al.*, 1997, Muramaki *et al.*, 2000, Muramaki and Hirata, 1997) is based on the enzymatic synthesis in a biphasic aqueous-organic system where the free enzyme is dissolved in the aqueous phase. The organic solvent is fed to the reactor containing the substrates. These substrates transfer to aqueous phase. After aspartame precursor is synthesized, *Z-Asp-Phe-OMe* is extracted to organic phase. The extractive bioreaction at low pH avoids the decomposition of the substrates, shifts the equilibrium towards product formation, and prevent product inhibition.

Selection of extractive bioreactor: The analysis of the criteria that should be taken into account to select the bioreactor are based on the features of the system: stability of the compounds at low pH, free enzyme, no pH control, no tendency of emulsifying, extremely

low solubility of Z-Asp-Phe-OMe in water and relatively hydrophobic compounds, namely, the substrate the compounds partition selectively into the organic phase and the separation high number of stages is not necessary.

In virtue of the restrictions are not limited to the number of stages, ability to handle solids, short residence time, tendency of emulsifying, pH control and immobilized enzyme, the criteria that should be evaluated in Table 1, show that the more appropriate device in the extractive bioreactor columns without agitation, such as packed bed, pulsed sieve-plate or baffle plate.

In order to have a definite choice among these options selected above, a more rigorous analysis is necessary, such as, the experimental data determined in a pilot-scale, analysis of costs and scale-up. Nevertheless, the scope of this work does not comprehend these analyses.

4.2- Synthesis of the semi-synthetic antibiotic - APA

Background: Enzymatic Penicillin G (PenG) hydrolysis is carried out at industrial scale in order to obtain 6-aminopenicillanic acid (APA). APA is the main precursor for the production of semi-synthetic β -lactam antibiotics, and is produced at an about 10,000 ton/a scale (Van de Sandt and De Vroom, 2000)

Characteristics of the reaction: The conventional enzymatic PenG hydrolysis into APA and Phenylacetic Acid (PAA) carried out in a batch mode and in a pure aqueous phase is characterized by low yield due to limitation of equilibrium reaction and by-product inhibition. The integration of PenG hydrolysis and purification of APA in a continuous aqueous-organic phase allows the shift of equilibrium reaction towards APA production. In the biphasic system, under no pH control, the pH drops as the reaction takes place. At pH lower than 5.0, the partition of PAA to the organic phase and crystallization of APA is favored. These two facts tend to improve the conversion of PenG hydrolysis.

Selection of extractive bioreactor: The analysis of the criteria that should be taken into account to select the bioreactor is based on the features of the system: immobilized enzyme, no pH control, tendency of emulsifying, presence of APA crystals.

In virtue of the features of PenG hydrolysis, the criteria for extractive bioreactor are: number of stages, ability to handle solids, short residence time, tendency of emulsifying, position feed, low backmixing, product and substrate degradation, small difference between partition coefficients and immobilized enzyme. Following these criteria and further information listed in Table 1, the best options of equipment for industrial application are the baffle plate column and Graesser contactor.

Nevertheless, these devices chosen above are appropriate for industrial application. The choice of the equipment can be different in case of laboratory scale. In this case of APA production, a sequence of stirrer tanks and separators, like filter or hydrocyclones or centrifugal extractor can be chosen. In the particular case of PenG hydrolysis, an integrated system of mixers (reactors) and hydrocyclones (separators) is proposed for the development of the counter-current reactor. The adoption of hydrocyclones as separators is due mainly to the stable emulsion formed and, consequently, difficult separation of APA crystals from the interface between water and BuAc.

In order to have a definite choice among these options selected above, a more rigorous analysis is necessary, such as, the experimental data determined in a pilot-scale, analysis of costs and scale-up. Nevertheless, the scope of this work does not comprehend these analyses.

5- Conclusion

Through this review it was possible to recognize the wide variety of equipment that can be used in integrated bioprocesses. The evaluation of the appropriate type of devices should take into account the advantages and the requirements of specific

applications. Studies related to extractive-reactor in biotechnology are recent, and several of them use devices adapted from those found in petrochemical and chemical processes. It means that after some modifications in the design of the reactor, the equipment can become useful for biochemical industries. Recently, lot of effort is focus on the utilization of membrane bioreactors due to the enormous potential of membrane separations and in the application of chromatographic extractive bioreactors to due the advances concerning on the continuous simulated moving bed.

After the selection of the appropriate equipment, it is worth to use a combination of process modeling, experiments, optimization and process economics. Hence, a case-by-case analysis is often necessary before the final choice of a reactor type can be made. Nevertheless, this further evaluations are out of the scope of this review.

6- Reference:

ANWAR, M. M.; ARIF, A. S.; PRITCHARD, D. W.. Multistage separation of quinoline of iso-quinoline by dissociation extraction. *Solvent Extraction and Ion Exchange*. v. 16, n. 4, p. 931-950. 1998.

CABRAL, J.M.S. Extractive removal of product by biocatalysis. In: *Extractive Bioconversions*. Mattiason B, Holst O. *Bioprocess Technology*. v. 11. Marcel Dekker, New York. 328 p. 1991.

CHING, C.B., LU, Z.P. Simulated moving-bed reactor: application in bioreaction and separation. *Industrial Engineering Chemical Research*. v. 36, n 1, 152-159. 1997.

CHISTI, Y.; MOO-YOUNG, M.. Fermentation technology, bioprocessing, scale-up and manufacture. p. 167-206. In *Biotechnology. The Science and the Business* (MOSES, V.; CAPE, R. E.). Harwood Academic Publishers, Switzerland. 596 p., 1991.

COIMBRA, J.R., THÖMMÉS, J., KULA, M.R. Continuous separation of whey proteins with aqueous two-phase systems in a Graesser contactor. *Journal of Chromatography A*. v. 668, n. 1, 85-94. 1994.

DUDUKOVIC, M. P.. Trends in catalytic reaction engineering. *Catalysis Today*. v.48, p. 5-15. 1999.

ERBELDINGER, ME., HALLING, P.J., NI, X. Scale-up of enzymatic solid-to-solid peptide synthesis and enzyme recovery. *AIChE Journal*. v. 47, n, 2, 500-508. 2001.

GIANETTO, A.; RUGGERI, B.; SPECCHIA, V.; SASSI, G.; FORMA, R.. Continuous extraction loop reactor (CELR): Alcoholic fermentation by fluidized entrapped biomass. *Chemical Engineering Science*. v.43, n. 8, p. 1891-1896. 1988.

GODFREY, J. C.; SLATER, M. J. Principles of Mixer-settler design. P. 275-278. In *Handbook of solvent extraction*. (: LO, T. C.; BAIRD, H. J.; HANSON, C.) 2nd edition. Krieger Publishing Company. Malabar, Florida. 980 p. 1991.

GODFREY, J. C.; SLATER, M. J.. *Liquid-liquid Extraction Equipment*. John Wiley and Sons Ltd., 772 p., 1994

HIRATA, M., ISHIMINE, T., HIRATA, A. Development of novel method for enzymatic peptide synthesis utilizing extractive reaction. *Journal of Chemical Engineering of Japan*. v. 30, n. 3, 467-477. 1997.

HOSS, H. Bioreactors. ULLMANN'S ENCYCLOPEDIA OF INDUSTRY CHEMISTRY, Sixth Edition, 2000 Electronic Release

HUNEKE, F. U.; FLASCHEL, E.. Behaviour of liquid/liquid/solid three-phase fixed bed reactors with application in biocatalysis. *Journal of Chemical Technology and Biotechnology*. v.71, p. 213-222. 1998.

JARUDILOKKUL, S. PAULSEN, E., STUCKEY, D.C. The hydrodynamics of a Graesser ("Raining Bucket") contactor with a reverse micellar phase. *Biotechnology Progress*. v. 16, n. 6, 1071-1078. 2000.

KACHASAKUL, P.; ASSABUMRUNGRAT, S.; PRASERTHDAM, P.; PANCHAROEN, U. Extractive reaction for epoxidation of cyclohexene to cyclohexene oxide using dioxirane in ketone/Oxone[®] system. *Chemical Engineering Journal*. v. 92, n. 1-3. 131-139. 2003.

KOMIVES, C., OSBORNE, D., RUSSELL, A.J. Degradation of pesticides in a continuous-flow two-phase microemulsion reactor. *Biotechnology Progress*. v. 10, n. 3, 340-343. 1994.

LEÓN, R., PRAZERES, D.M.F., FERNANDES, P., MOLINARI, F., CABRAL, J.M.S. a multiphase hollow fiber reactor for the whole-cell bioconversion of 2-methyl-1,3-propanediol to (R)- β -hydroxyisobutyric acid. *Biotechnology Progress*. v. 17, n. 3, 468-473. 2001.

LODE, F., HOUMARD, M., MIGLIORINI, C., MAXXOTTI, M., MORBIDELLI, M. Continuous reactive chromatography. *Chemical Engineering Science*. v.56, n. 2, 269-291. 2001.

LODE, F., MAZZOTTI, M., MORBIDELLI, M. Comparing true countercurrent and simulated moving-bed chromatographic reactors. *AIChE Journal*. v. 49, n. 4, 977-990. 2003.

LOPEZ, J. L.; MATSON, S. L.. A multiphase/extractive enzyme membrane reactor for production of diltiazem chiral intermediate. *Journal of Membrane Science*. v. 125, p. 189-211. 1997.

MILLS, P. L.; CHAUDHARI, R. V.. Multiphase catalytic reactor engineering and design for pharmaceuticals and fine chemical. *Catalysis Today*. v.37, p. 367-404. 1997.

MURAKAMI, Y., HIRATA, A. Continuous enzymatic synthesis of aspartame precursor at low pH using an extractive reaction. *Journal of Fermentation and Bioengineering*. v. 84, n. 3, 264-267. 1997.

MURAKAMI, Y., YOSHIDA, T., HAYASHI, S., HIRATA, A. Continuous enzymatic production of peptide precursor in aqueous/organic biphasic medium. *Biotechnology and Bioengineering*. v. 69, n. 1, 57-65. 2000.

NISHI, Y., NII, S., TAKAHASHI, K., TAKEUCHI, H. Extraction of proteins by reversed micellar solution in a packed column. *Journal of Chemical Engineering of Japan*. v. 32. n. 2, 211-216. 1999.

PORTNER, R.; MARKL, H.. Dialysis cultures. *Appl. Microbiol. Biotechnol.* v.50, p. 403-414. 1998.

PRATT, H. R. C.; STEVENS, G. W.. Selection, design, pilot-testing, and scale-up of extraction equipment. p. 492-582. In: *Science and Practice of Liquid-liquid Extraction*.(THORNTON, J. D.). Claredon Press Oxford. v. 1. 603p. 1992.

SAHOO, G. C.; BORTHAKUR, S.; DUTTA, N. N.; DASS, N. N.. Reactive extraction of cephalosporin antibiotics in hollow fiber membrane. *Bioprocess Engineering*. v. 20, p. 117-125. 1999.

SAJC, L. GRUBISIC, D., VUNJAK-NOVAKOVIC, G. Bioreactors for plant engineering: an outlook for further research. *Biochemical Engineering Journal*. v. 4, 89-99. 2000.

SAJC, L., VUNJAK-NOVAKOVIC, G., GRUBISIC, D., KOVAČEVIC, N., VUKOVIĆ, D., BUGARSKI, B. Production of anthraquinones by immobilized *Frangula alnus* Mill. Plant cells in a four-phase air-lift bioreactor. *Applied Microbiology and Biotechnology*. v. 43, n. 3, 416-423. 1995.

SARMIDI, M. R.; BARKER, P. E.. Saccharification of modified starch to maltose in a continuous rotating annular chromatograph (CRAC). *Journal of Chemical Technology and Biotechnology*. v.57, p. 229-235. 1993.

SCHÜRCEL, K. *Solvent extraction in biotechnology: Recovery of primary and secondary metabolites*. Springer-Verlag Berlin Heidelberg. 213 p. 1994.

SETFORD, S.J. Measurement of native dextran synthesis and sedimentation properties by analytical ultracentrifugation. *Journal of Chemical Technology and Biotechnology*. v. 74, n. 1, 17-24. 1999.

SETFORD, S.J., BARKER, P.E. Combined bioreaction and separation in centrifugal fields using zonal rotors. *Journal of Chemical Technology and Biotechnology*. v. 61, n. 1, 19-29. 1994.

SHIEH, M.T., BARKER, P.E. Saccharification of modified starch to maltose in a semi-continuous counter-current chromatographic reactor-separator (SCCR-S). *Journal of Chemical Technology and Biotechnology*. v. 63, n. 2, 125-134. 1995.

SISAK, C.; NAGY, E.; BURFEIND, J.; SCHUGERL, K.. Technical aspects of separation and simultaneous enzymatic reaction in multiphase enzyme membrane reactors. *Bioprocess Engineering*. v. 23, p. 503-512. 2000.

TIKHOMIROFF, C., ALLAIS, S., KLVANA, M., HISIGER, S., JOLICOEUR, M. Continuous selective extraction of secondary metabolites from *Catharantus roseus* hairy roots with silicon oil in a two-liquid-phase bioreactor. *Biotechnology progress*. v. 18, n. 5, 1003-1009. 2002.

Van de SANDT, E.J.A.X., Van De VROOM, E. Innovations in cephalosporin and pencillin production: painting the antibiotics industry green. *Chimica Oggi-Chemistry Today*. v. 18, 72-75. 2000.

Van SONSBECK, H. M.; BEEFTINK, H. H.; TRAMPER, J. Two-liquid phase bioreactors. *Enzyme Microbial Technology*. v. 15, n. 9, p. 722 – 729. 1993.

WENTEN, I.G., WIDIASA, I.N. Enzymatic hollow fiber membrane bioreactor for Penicilin hydrolysis. *Desalination*. v. 149, 279-285. 2002.

WU, Z., YANG, S-T. Extractive fermentation for butyric acid production from glucose by *Clortridium tyrobutyricum*. *Biotechnology and Bioengineering*. v. 82, n. 1, 93-102. 2003.

CAPÍTULO VII

CONCLUSÕES

Este estudo faz parte de um ambicioso projeto envolvendo a empresa DSM e grupos de universidades da Holanda. O intuito deste projeto é o desenvolvimento de um processo biocatalítico de produção de antibióticos semi-sintéticos que seja eficiente, econômico e que produza menos resíduos. Dentre as universidades está a Universidade de Tecnologia de Delft (TUDelft) onde foram desenvolvidas importantes etapas deste trabalho.

Este estudo teve como objetivo dar prosseguimento aos trabalhos realizados anteriormente, possibilitando obter informações necessárias para a instalação de um sistema em escala de laboratório para a hidrólise de PenG em sistema bifásico (acetato de butila e água) e em um reator em contra-corrente, e contribuir com os avanços nos processos de síntese de antibióticos semi-sintéticos.

Nestas condições analisadas, ou seja, hidrólise de PenG no sistema bifásico (água e acetato de butila) em um reator em contra-corrente sem o controle de pH., o pH decresce favorecendo a migração de PAA para a fase orgânica e a cristalização de 6-APA. Ambos fenômenos, separação dos produtos em diferentes fases e cristalização do 6-APA, deslocam o equilíbrio no sentido de conversão do substrato e, conseqüentemente, promovem uma alta

produtividade e alta pureza dos produtos. Esses produtos já purificados são utilizados em etapas subseqüentes. O PAA é reciclado e usado na fermentação de PenG e o 6-APA é usado na síntese de antibióticos semi-sintéticos, como amoxicilina e ampicilina.

As etapas deste trabalho foram a avaliação da atividade e da estabilidade da penicilina amidase imobilizada a ser usada, e a determinação da cinética de cristalização do produto (6-APA), visto que não se tinha o conhecimento de aplicação desta enzima e de cristalização do 6-APA a baixos valores de pH 3-5 e em sistema bifásico água e acetato de butila. Além dos dados cinéticos de atividade enzimática e de cristalização de 6-APA, foi desenvolvido um modelo no intuito de fornecer as melhores condições de operação do sistema contra-corrente em multi-estágio,

Como última etapa, procurou-se selecionar o reator mais adequado para o processo proposto. Ensaios preliminares foram feitos em coluna de recheio e em mixer-settlers. No entanto, os resultados foram insatisfatórios sendo necessário buscar outras alternativas. Diante da ampla variedade de extratores e bioreatores, optou-se por elaborar uma revisão sobre bioreatores extrativos como maneira de auxiliar na seleção da melhor configuração de um reator-separador a ser empregado na hidrólise de PenG nas condições desejadas.

Através da avaliação de atividade e estabilidade enzimática, verificou-se que a máxima atividade enzimática compreendeu a faixa de pH 8.0 a 9.0. A enzima permanece estável mesmo a baixos pH's (3.0 a 6.0). Embora a atividade enzimática sofre um decréscimo de aproximadamente 80%, isto não representa empecilho para sua utilização em processos a baixos pH's, podendo ser perfeitamente viável seu emprego na hidrólise de PenG na processo contínuo bifásico água-acetato de butila.

No estudo de cristalização de APA, produto da hidrólise da PenG e precursor para a síntese de antibióticos semi-sintéticos, os resultados mostraram que as impurezas não exerceram efeito sobre a cristalização de APA, na faixa de pH 4 a 5 e de concentrações de impurezas avaliadas. Além da determinação dos parâmetros cinéticos, foi utilizado um modelo que pode prever as taxas de cristalização de APA nas mesmas condições que serão empregadas na hidrólise de PenG em reator multi-estágio e bifásico, água e acetato de butila.

Na etapa de modelagem, o modelo desenvolvido possibilita o cálculo do pH e das concentrações do substrato e produtos nos estágios do reator contra-corrente. Os dados fornecidos pelo modelo podem ser utilizados para otimizar as condições de operação do reator bifásico multi-estágio (ponto de alimentação, vazão volumétrica das fases e concentração inicial do substrato).

A revisão bibliográfica sobre biorreatores extrativos representa uma importante referência para a seleção de diferentes tipos de configurações dependendo das restrições e características de cada tipo de reação. Através desta revisão, foi verificado que o uso de um sistema, formado por agitadores acoplados a hidrociclones em série, pode representar uma opção adequada de reatores multi-estágio contra-corrente para a hidrólise de PenG em escala de laboratório.

CAPÍTULO VIII

SUGESTÕES PARA TRABALHOS FUTUROS

As informações obtidas durante este trabalho mostraram que o estudo da hidrólise de PenG em um reator contra-corrente e multi-estágio é viável.

Portanto, as próximas etapas a serem desenvolvidas envolvem:

- 1- A implantação de um bioreator extrativo em escala de laboratório. A sugestão inicial seria a instalação de um reator sendo que cada estágio seja formado por agitadores conectados a hidrociclones e ligados em cujo número de estágios correspondem ao número ótimo previamente determinado neste trabalho. A instalação do estágio composto por agitadores e hidrociclones foi sugerida devido às vantagens de: flexibilidade do número de estágios, configuração compacta e pelo fato de o sistema sob agitação (6-APA, água e acetato de butila) formarem uma emulsão estável que exige o uso de separadores mais eficientes como os hidrociclones;
- 2- Execução de ensaios experimentais da hidrólise enzimática de PenG em sistema bifásico (água e acetato de butila) e contra-corrente, realizados em reator multi-estágio de configuração sugerida no item 1;

- 3- Otimização da modelagem ajudando a cinética enzimática e a cinética de cristalização;
- 4- Avaliação da viabilidade econômica do processo em escala industrial;
- 5- Incorporação da síntese de antibióticos semi-sintéticos à hidrólise de PenG, como no caso da Amoxicilina, resultante da síntese entre APA e D-p-hydroxyphenylglycine methyl ester (HPGM);
- 6- Estudo da influência de impurezas na cristalização numa faixa mais ampla de pH, de concentração de impurezas e dos tipos de impurezas.
- 7- Otimização e controle do processo.